VASOPROTECTIVE EFFECTS OF PIOGLITAZONE, AN INSULIN SENSITIZER: MOLECULAR MECHANISMS AND THERAPEUTIC IMPLICATIONS TO PREVENT INTIMAL HYPERPLASIA AFTER ARTERIAL INJURY

by

ISLAM ABDELFATTAH MOHAMED OSMAN

(Under the Direction of Lakshman Segar)

ABSTRACT

Neointimal hyperplasia is a major event in atherosclerosis and restenosis after angioplasty. It is attributable, in part, to exaggerated proliferation of vascular smooth muscle cells (VSMCs). Despite the use of drug-eluting stents to limit intimal hyperplasia, in-stent restenosis still remains a major clinical problem. Several lines of evidence suggest that insulin resistance increases the risk of vascular proliferative disease. In this regard, the contribution of systemic *versus* vessel wall-specific insulin resistance toward dysregulated VSMC phenotype remains unclear. Pioglitazone (PIO), a classical insulin sensitizer that belongs to the family of PPARγ agonists, reduces neointimal hyperplasia after coronary angioplasty in diabetic and nondiabetic subjects. However, the molecular mechanisms by which PIO regulates VSMC phenotype have not been fully elucidated. In particular, the likely intermediary role of AMP-activated protein

kinase (AMPK) toward PIO inhibition of VSMC proliferation remains unclear. The objectives of our study were to examine the role of dysregulated insulin receptor signaling in VSMC proliferation and to identify the molecular mechanisms by which PIO prevents neointima formation after arterial injury. Using human aortic VSMCs *in vitro*, we demonstrated that high fructose treatment dysregulates proximal insulin receptor signaling events. However, high fructose did not affect platelet-derived growth factor (PDGF)-induced proliferative signaling. These findings suggest that systemic rather than VSMC-specific dysregulation of insulin signaling plays a major role in enhancing atherosclerosis and neointimal hyperplasia. Next, we demonstrated that PIO inhibits PDGF-induced key proliferative signaling events in VSMCs through AMPK-dependent and AMPK-independent mechanisms. In particular, PIO activates AMPK to induce raptor phosphorylation, which diminishes PDGF-induced mTOR activity. In addition, PIO inhibits the basal phosphorylation of ERK, independent of AMPK, thereby decreasing cyclin D1 expression and Rb phosphorylation. Furthermore, AMPK-dependent inhibition of mTOR and AMPK-independent inhibition of ERK signaling occur regardless of PPARγ expression/activation in VSMCs. Using arterial injury model *in vivo*, we demonstrated that an AMPK inhibitor (compound C) partially reverses PIO-mediated inhibition of neointima formation. Collectively, our findings suggest that local delivery of PIO at the lesion site may limit restenosis after angioplasty without inducing PPARγ-mediated systemic adverse effects

INDEX WORDS: *Arterial injury*; *vascular smooth muscle cells; fructose; insulin receptor signaling; pioglitazone; AMPK; p70S6K; ERK; PPARγ*

VASOPROTECTIVE EFFECTS OF PIOGLITAZONE, AN INSULIN SENSITIZER: MOLECULAR MECHANISMS AND THERAPEUTIC IMPLICATIONS TO PREVENT INTIMAL HYPERPLASIA AFTER ARTERIAL INJURY

by

ISLAM ABDELFATTAH MOHAMED OSMAN

M.Sc., German University in Cairo, Egypt, 2010

B.Pharm., Cairo University, Egypt, 2004

A Dissertation Submitted to the Graduate Faculty of the University of Georgia

in Partial Fulfillment of the Requirements for the Degree

DOCTOR OF PHILOSOPHY

ATHENS, GEORGIA

2016

VASOPROTECTIVE EFFECTS OF PIOGLITAZONE, AN INSULIN SENSITIZER: MOLECULAR MECHANISMS AND THERAPEUTIC IMPLICATIONS TO PREVENT INTIMAL HYPERPLASIA AFTER ARTERIAL INJURY

by

ISLAM ABDELFATTAH MOHAMED OSMAN

Major Professor: Lakshman Segar

Committee: Susan C. Fagan
Azza B. El-Remessy
Jiliang Zhou
Eric Belin de Chantemele

Electronic Version Approved:

Suzanne Barbour
Dean of the Graduate School
The University of Georgia
August 2016

DEDICATION

I dedicate this thesis to my wife (Sawsan) who spent years of her life away from her home country and family in order for me to achieve this dream. I also dedicate this thesis to my family back home in Egypt; my parents (Abdelfattah and Raafa) and my siblings (Mohamed and Youmna) whose encouragement and support kept me going in times of difficulties throughout my life.

ACKNOWLEDGEMENTS

Working with my mentor, Dr. Lakshman Segar, has been an extreme privilege for me. Under his guidance, I learned to be an independent thinker and believe in my ability to implement my own ideas and make the change I want to see. I am very grateful for the opportunities that Dr. Segar provided to me during my Ph.D. training. I had a successful project, great learning experience and was exposed to major professors and cutting-edge research in our field through attending two international conferences. I was extremely fortunate to work with Dr. Segar's great team. Every single member of the team has helped me in at least one aspect of this work. I would like to thank the previous lab members, Dr. Rajkumar Pyla, Dr. Ninu Pulouse, and Dr. Prahalathan Pichavaram and the current lab members, Arwa Fairaq and Noha Shawky for their time and help. Working with all of them was a pleasure and I really learned how to work efficiently in a successful productive team because of them.

I would like to express my sincere gratitude to my advisory committee members, Dr. Susan C. Fagan, Dr. Azza B. El-Remessy, Dr. Jiliang Zhou, and Dr. Eric Belin de Chantemele for their support and guidance. Their time and effort are greatly appreciated and I have learned a lot from their insightful suggestions, technical support and the study material they provided to me. I also would like to thank Clinical and Experimental Therapeutics (CET) program professor, Dr. Somanath Shenoy for his positive feedback and constructive criticism during the CET journal club meetings. Other CET

postdoctoral fellows, students, and lab technicians have been best coworkers and friends. I could have never wished for a better work environment.

TABLE OF CONTENTS

Page

CHAPTER 1

INTRODUCTION AND LITERATURE REVIEW

Overview of Atherosclerosis and Restenosis after Angioplasty

Cardiovascular disease (CVD) remains the leading cause of death in the United States (U.S.) and worldwide (Mozaffarian et al. 2016). In the U.S., CVD accounted for 30.8% (800,937) of all 2,596,993 deaths, or ~1 of every 3 deaths in the year 2013 (Mozaffarian et al. 2016). On the basis of these data, >2,200 Americans die of CVD every day, an average of 1 death every 40 seconds.

Atherosclerosis is a chronic progressive inflammatory CVD and is a primary risk factor for ischemic heart disease, the leading cause of death worldwide (Ross 1999). Atherosclerotic lesions lead to gradual narrowing of the vessel lumen and hardening of the vessel wall due to excessive build-up of plaque in the vessel wall, often requiring percutaneous coronary interventions (PCI) to open up the occluded vessel and restore blood flow. However, PCI, also known as coronary angioplasty, can trigger a process known as restenosis or renarrowing of the blood vessel requiring target-lesion revascularization.

Annually, ~500,000 patients undergo coronary angioplasty procedures in the U.S. alone (Go et al. 2014). Despite the recent advances in PCI, restenosis still occurs in ~10% of patients (Cassese et al. 2014; Mauri et al. 2008) and thus remains a major complication of coronary angioplasty, especially in diabetic patients (Scheen, Warzee, and Legrand 2004). Since restenosis predominantly occurs due to exaggerated vascular

smooth muscle cell (VSMC) proliferation (as discussed below), systemic therapy with antiproliferative medication have been tested to limit restenosis (Hamon et al. 1998). However, systemic therapy has proven ineffective for this condition because of the lack of feasibility to deliver effective drug concentrations at the injury site without causing serious adverse effects in non-target tissues (Burt and Hunter 2006). As an alternative approach, the insertion of a bare-metal stent (BMS) or drug-eluting stent (DES) during PCI has been employed successfully to prevent elastic recoil and reduce the incidence of restenosis (van der Hoeven et al. 2005). Although DES is considered more effective than BMS in reducing restenosis after angioplasty, their overall safety has been limited by delayed endothelialization and increased risk of in-stent thrombosis (Costa and Simon 2005). Delayed endothelialization is commonly attributed to non-selective antiproliferative effects in both endothelial cells and VSMCs (Costa and Simon 2005). Accordingly, there is an urgent need to develop novel therapeutic alternatives that limit restenosis without serious adverse effects.

Overview of the Role of Vascular Smooth Muscle Cells in Atherosclerosis and Restenosis after Angioplasty

Unlike skeletal muscle cells, VSMCs are not terminally differentiated and they exhibit remarkable phenotypic plasticity (Owens 1995). Accordingly, VSMCs can change their phenotype in response to environmental cues or signals. In adult healthy blood vessels, VSMCs exhibit a differentiated/contractile phenotype where they express a unique repertoire of proteins that are involved in the contractile process such as smooth muscle (SM) α–actin and calponin (Owens, Vernon, and Madsen 1996). These proteins are frequently used as markers for the differentiated/contractile VSMCs. Differentiated

VSMCs are characterized by very low rates of proliferation, migration, and extracellular matrix (ECM) secretion (Owens, Vernon, and Madsen 1996). Thus, in the adult healthy blood vessel, VSMCs are normally confined to the medial layer where they provide the vessel with the ability to withstand high pressure (in large conduit vessels) by means of their secreted ECM proteins; and the contractile process (in resistance vessels) by means of their unique contractile machinery.

In response to vessel injury and the subsequent release of growth factors and cytokines, VSMCs can undergo phenotypic modulation, where the expression of the contractile proteins is downregulated and VSMCs acquire a proliferative/migratory/synthetic phenotype characterized by high rate of proliferation and migration and secrete large amounts of ECM proteins. (Regan et al. 2000). It is important to note however that these two phenotypes are not mutually exclusive. For instance, VSMCs in the fibrous cap in atherosclerotic lesions do not proliferate, but also are not typical differentiated VSMCs (Wilcox 1992).

Phenotypic modulation of VSMCs plays a major role in atherosclerosis and restenosis after angioplasty (Ross 1999; Owens, Kumar, and Wamhoff 2004). In atherosclerosis, dyslipidemia leads to retention of low-density lipoprotein (LDL) in the vascular endothelium, its subsequent modification to oxidized-LDL, initiation of a progressive inflammatory response, accumulation of monocytes/macrophages, foam cell formation and the concomitant release of inflammatory cytokines (e.g. Interleukin-1β and tumor necrosis factor-α) and growth factors (e.g. platelet-derived growth factor; PDGF) that induce phenotypic modulation of medial VSMCs (Bernstein, Antoniades, and Zetter 1982). Accordingly, VSMCs migrate from the medial layer to the sub-intimal space

where they proliferate and secrete large amounts of ECM proteins leading to neointima formation. Notably, this process accounts for much of the mass of the fibrous cap in atherosclerotic lesions and leads to progressive narrowing of the vessel lumen (Ross 1999). However, it is important to note that phenotypic modulation of VSMCs is not always detrimental, as phenotypically modulated VSMCs in the fibrous cap provide stability to the lesion and avoid plaque rupture.

In restenosis after angioplasty, neointima formation occurs as a result of vessel injury due to endothelial denudation/damage that follows balloon inflation and/or stent placement (Clowes, Reidy, and Clowes 1983; Newby and Zaltsman 2000). Loss of endothelial layer renders the vessel thrombogenic and leads to the accumulation of platelets and leukocytes at the injury site. Subsequently, the local production of cytokines/growth factors and the concomitant loss of endothelium-derived anti-atherogenic mediators such as nitric oxide and prostacyclin, ultimately lead to phenotypic modulation of VSMCs and neointima formation (Campbell et al. 1988).

Insulin Resistance, Fructose, and Atherosclerosis

Insulin resistance, characterized by metabolic abnormalities including glucose intolerance and dyslipidemia, is a risk factor for accelerated atherosclerosis (Taegtmeyer 1996; Semenkovich 2006; Bornfeldt and Tabas 2011). While altered metabolic milieu is known to promote proatherogenic phenotype (Semenkovich 2006), the contribution of vascular wall-specific insulin resistance toward atherosclerotic lesion progression remains unclear (Semenkovich 2006; Bornfeldt and Tabas 2011). In particular, VSMCs that play a major role in atherosclerosis have been shown to exhibit proliferative and

proapoptotic phenotypes upon target-specific deletion of insulin receptor signaling components (Lightell, Moss, and Woods 2011; Martinez-Hervas et al. 2014). For instance, insulin receptor gene deficiency in VSMCs leads to a decrease in insulin-induced Akt phosphorylation and an increase in extracellular signal-regulated kinase (ERK) phosphorylation with an accompanying increase in cell proliferation (Lightell, Moss, and Woods 2011). In a different study, small interfering RNA (siRNA)-mediated downregulation of insulin receptor substrate-2 (IRS-2) in VSMCs diminishes insulin-induced phosphorylation of Akt and ERK thereby inducing a proapoptotic phenotype (Martinez-Hervas et al. 2014). Thus, dysregulation of insulin signaling in VSMCs at the level of insulin receptor and IRS-2 may result in proliferative and proapoptotic phenotypes, which would enhance and exacerbate atherosclerosis, respectively.

Although high fructose consumption is known to induce insulin resistance and promote atherosclerosis (D'Angelo et al. 2005; Ning et al. 2015; Lu et al. 2013), it is unknown as to how fructose uptake in VSMCs regulates insulin receptor signaling and proliferative phenotype. Previous studies demonstrate that high fructose diet induces insulin resistance in a rat model, as revealed by hyperinsulinemic-euglycemic clamp technique that shows a significant reduction in glucose infusion rate to maintain euglycemia (D'Angelo et al. 2005). In addition, high fructose diet-induced insulin resistance results in exaggerated atherosclerosis and neointima formation with a significant increase in smooth muscle cell accumulation (Ning et al. 2015; Lu et al. 2013).

Since PDGF is a potent mitogen released at the site of arterial injury (Barrett and Benditt 1987; Rubin et al. 1988; Heldin and Westermark 1999), it is likely that high

fructose-induced increase in neointima formation may occur through enhanced PDGF receptor signaling. Previously, we have shown that PDGF not only increases VSMC proliferation but also attenuates insulin-induced insulin receptor substrate (IRS-1/IRS-2)-associated PI 3-kinase/Akt signaling (Zhao et al. 2011). Accordingly, we tested the hypothesis that high fructose-mediated dysregulation of insulin receptor signaling is associated with enhanced VSMC proliferation. Using human aortic VSMCs, we determined the effects of high fructose on: i) IRS-1 serine phosphorylation and IRS-1/IRS-2 expression; ii) insulin *versus* PDGF-induced changes in the phosphorylation of Akt, S6 ribosomal protein (a downstream target of mammalian target of rapamycin (mTOR)/p70S6K signaling), and ERK; and iii) cell cycle proteins and proliferation.

Protective Effects of Thiazolidinediones against Atherosclerosis and Restenosis after Angioplasty

Thiazolidinediones (TZDs), such as pioglitazone (PIO), are classical insulin sensitizers that belong to the family of peroxisome proliferator-activated receptor-γ (PPARγ) agonists. TZDs have been shown to exhibit beneficial effects in the vessel wall (Yoshimoto et al. 1999; Phillips et al. 2003; Satoh et al. 2003) beyond their insulin-sensitizing action that improves glycemic control in patients with type 2 diabetes (Kahn et al. 2006). Importantly, PIO and other TZDs are reported to reduce intimal hyperplasia both experimentally (Law et al. 1996; Igarashi et al. 1997; Igarashi et al. 2001; Phillips et al. 2003; Yoshimoto et al. 1999; Aizawa et al. 2001; Wang et al. 2006; Desouza, Gerety, and Hamel 2007; Kasai et al. 2008) and clinically in diabetic (Takagi et al. 2003; Nishio et al. 2006; Riche, Valderrama, and Henyan 2007; Geng et al. 2009; Patel et al. 2011) and nondiabetic subjects (Katayama et al. 2005; Marx et al. 2005; Geng et al. 2009).

Moreover, in both experimental animal models and human subjects, TZDs have been shown to stimulate the production of endothelial progenitor cells and promote endothelial repair after vascular injury (Hannan et al. 2003; Makino et al. 2008; Pistrosch et al. 2005; Sorrentino et al. 2007; Werner et al. 2007). All these favorable pleiotropic vasoprotective effects favor the clinical utility of TZDs to mitigate in-stent restenosis. Yet, TZD treatment is associated with several adverse effects, including weight gain, fluid retention, and congestive heart failure, thus raising concerns about their cardiovascular safety (Nesto et al. 2003).

These unfavorable effects are attributed in part to activation of PPARγ. For instance, TZD activation of PPARγ in the renal collecting duct stimulates epithelial sodium channel transcription to promote sodium absorption and fluid accumulation (Guan et al. 2005; Zhang et al. 2005). Notably, PPARγ is also expressed in VSMCs but to a modest extent (Staels et al. 1998; Law et al. 2000; Benson et al. 2000; Benkirane et al. 2006), compared with its abundant expression level in adipose tissue. Although previous studies have reported PPARγ-dependent and PPARγ-independent mechanisms for TZD inhibition of VSMC proliferation (Peuler et al. 1996; Law et al. 1996; Wakino et al. 2000; de Dios et al. 2003; Lee et al. 2009; Subramanian et al. 2010; Zhang et al. 2011), the signaling events associated with TZD action in VSMCs are not fully understood.

TZDs such as rosiglitazone and PIO are currently in clinical use but are prescribed with caution due to the risk of congestive heart failure (Inzucchi et al. 2012; Kaul et al. 2010). Troglitazone has been withdrawn from the market due to hepatotoxicity (Kaul et al. 2010). While commonly being referred to as PPARγ agonists,

PPARγ binding affinity for ROSI is several folds greater than PIO or troglitazone (Young et al. 1998). Despite their differences in PPARγ binding affinities, all three TZDs exhibit comparable inhibitory effects on VSMC proliferation (Law et al. 2000; de Dios et al. 2003) by affecting cell cycle regulatory events critical for G1→S progression (Wakino et al. 2000; de Dios et al. 2003).

The key proliferative signaling components in VSMCs include MEK1/ERK and mTOR/p70S6K that undergo activation upon challenge with mitogens including PDGF or angiotensin II (Braun-Dullaeus et al. 2001; Nagata et al. 2004; Zhao et al. 2011). In this regard, TZDs have been shown to inhibit mitogen-induced activation of ERK signaling in VSMCs (Benkirane et al. 2006; Law et al. 1996; Goetze et al. 1999; Lee et al. 2009). However, the signaling events associated with TZD action in VSMCs are not fully understood.

AMPK as a Therapeutic Target for Atherosclerosis and Restenosis after Angioplasty

AMP-activated protein kinase (AMPK), a cellular energy sensor and regulator, is a heterotrimeric complex with serine/threonine kinase activity (Hardie, Ross, and Hawley 2012). It consists of a catalytic α subunit and regulatory β and γ subunits (Hardie, Carling, and Carlson 1998). AMPK can be phosphorylated at Thr^{172}, and thus activated, by 2 major upstream kinases in response to different stimuli. It can be activated by: 1) Liver Kinase B1 (LKB1) in response to high AMP/ATP ratio (Woods et al. 2003; Hawley et al. 2003); and 2) Ca^{2+}/calmodulin-dependent protein kinase kinase-beta (CaMKKβ) in response to high intracellular Ca^{2+} levels (Hawley et al. 2005; Woods et al. 2005). Activation of AMPK signaling pathway protects the vasculature against CVD by

several mechanisms. By promoting fatty acid (FA) oxidation and inhibiting hormone-sensitive lipase in the adipose tissue, it decreases the levels of circulating FFA (which is detrimental for the vasculature) (Park et al. 2002; Smith et al. 2007). Moreover, by inhibiting gluconeogenesis in the liver, it decreases blood glucose levels and protects the vasculature against the detrimental effects of hyperglycemia (Kahn et al. 2005; Viollet et al. 2009). In addition, activation of AMPK signaling pathway has many direct beneficial effects on the vascular cells including endothelial cells and VSMCs as discussed below.

In Endothelial Cells:

Both AMPKα isoforms are expressed in endothelial cells. However, AMPKα1 is the predominant isoform (Xie et al. 2006). Recently, AMPKα2 was demonstrated to be important for hypoxia-induced angiogenesis (Nagata, Mogi, and Walsh 2003). Activation of AMPK in endothelial cells leads to endothelial nitric oxide synthase (eNOS) phosphorylation (Ser1177) leading to its activation (Morrow et al. 2003). eNOS activation and enhanced NO production have many vasoprotective effects including activation of the soluble guanylate cyclase/cGMP pathway in VSMCs leading to vasorelaxation, antioxidant effect, antiplatelet effect, anti-inflammatory effect, antiproliferative effects in VSMCs (Ewart, Kohlhaas, and Salt 2008; Zhang et al. 2008). In addition, AMPK decreases inflammation by NO-dependent and –independent mechanisms and thus decreases cell adhesion molecule expression/inflammatory cell adhesion/migration (Ewart, Kohlhaas, and Salt 2008).

In VSMCs:

Both AMPKα isoforms are expressed in VSMCs. However, AMPK α1 is the predominant isoform (Goirand et al. 2007; Rubin et al. 2005) Activation of AMPK in VSMCs is associated with endothelium-independent vasorelaxation (Horman et al. 2008; Goirand et al. 2007), anti-inflammatory effects and inhibition of proliferation and migration. Notably, AMPK inhibits VSMC proliferation by multiple mechanisms: 1) inhibition of ERK activation (Nagata et al. 2004; Motobayashi et al. 2009; Uemura et al. 2015); 2) inhibition mTOR/p70S6K signaling leading to cell cycle arrest (Kim et al. 2014); 3) upregulation of cell cycle inhibitors ($p21^{Cip1}$ and $p27^{Kip1}$) that negatively regulate the cell cycle (Igata et al. 2005); and 4) inhibition of the biosynthetic pathways (e.g. protein synthesis, fatty acid synthesis, and cholesterol synthesis) that are required to provide adequate macromolecules before cells can commit to mitotic division (Dandapani and Hardie 2013).

TZDs and the activation of AMPK

TZD treatment results in the activation of AMPK in insulin-responsive tissues/cells (Fryer, Parbu-Patel, and Carling 2002; Saha et al. 2004; Konrad et al. 2005; Coletta et al. 2009) and endothelial cells (Boyle et al. 2008), but such effect has not yet been reported in VSMCs. AMPK activation in VSMCs (e.g., by 5-aminoimidazole-4-carboxamide-1-beta-d-ribofuranoside (AICAR) or adipokines) is associated with inhibition of ERK activation (Nagata et al. 2004; Motobayashi et al. 2009; Uemura et al. 2015). In addition, AMPK activation leads to inhibition of mTOR/p70S6K signaling in different tissues/cell types (Inoki, Kim, and Guan 2012; Saha et al. 2010), including

VSMCs (Kim et al. 2014). Notably, AMPK activation in nonvascular cells promotes raptor phosphorylation to inhibit the activity of mTOR (Gwinn et al. 2008). Hence, it is critically important to examine the likely intermediary role of AMPK toward TZD suppression of key proliferative signaling events in VSMCs.

In skeletal muscle cells and hepatocytes, TZD activation of AMPK has been shown to involve mitochondrial membrane depolarization, a decrease in cellular ATP level, an increase in AMP that binds to AMPKγ subunit to facilitate allosteric activation, and enhanced phosphorylation of Thr^{172} residue in AMPKα unit by LKB1, an upstream kinase for AMPK (Konrad et al. 2005; Fryer, Parbu-Patel, and Carling 2002; Kahn et al. 2005). In addition, AMPK activation leads to phosphorylation and inactivation of acetyl-CoA carboxylase (ACC), a key downstream target of AMPK (Kahn et al. 2005). Nevertheless, it remains unknown as to whether TZD affects cellular energy state to promote AMPK activation in VSMCs.

The objectives of this research project using human aortic VSMCs and CJ57BL/6 mice included the determination of: i) the extent to which PIO regulates the phosphorylation AMPKα^{Thr172} and its downstream target, ACC; ii) PIO regulation of cellular energy state including mitochondrial membrane potential (by tetramethylrhodamine methyl ester (TMRM) fluorescence analysis) and AMP/ATP ratio (by LC-MS/MS MRM analysis); iii) the role of LKB1 *versus* CaMKKβ as likely upstream kinases for PIO-induced AMPK activation; iv) the extent to which PIO activation of AMPK regulates PDGF-induced key proliferative signaling events including mTOR/p70S6K and ERK; v) whether PIO regulation of key proliferative signaling is

dependent on PPARγ expression; and vi) the likely intermediary role of AMPK toward PIO inhibition of neointima formation *in vivo*.

Figure legends

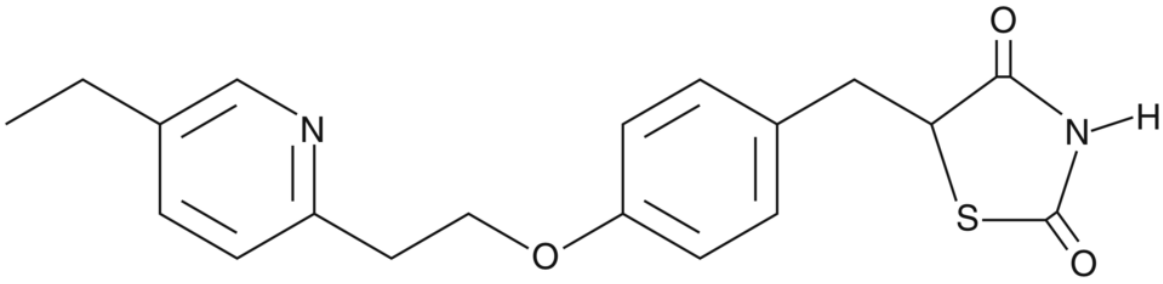

Fig. 1.1. Schematic diagram representing the structure of PIO

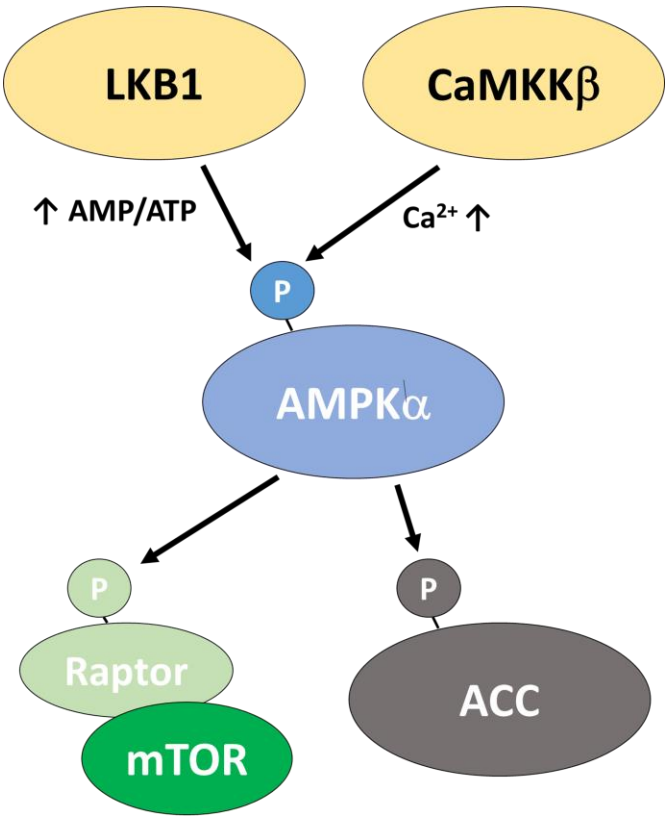

Fig. 1.2. Schematic diagram representing the AMPK signaling pathway. AMPK can be phosphorylated at Thr^{172}, and thus activated, by 2 major upstream kinases in response to different stimuli. It can be activated by: 1) LKB1 in response to high AMP/ATP ratio; and 2) CaMKKβ in response to high intracellular Ca^{2+} levels. Activated AMPK leads to the phosphorylation of many downstream targets including raptor (leading to inactivation of mTOR) and ACC.

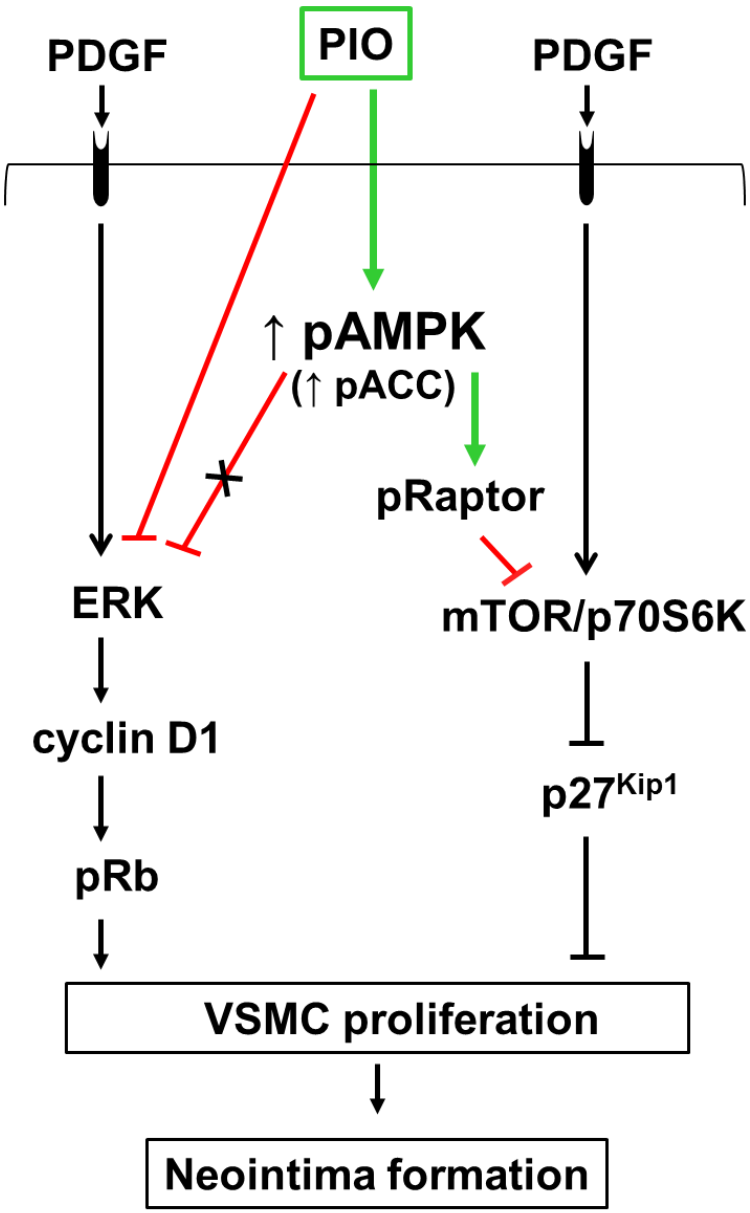

Fig. 1.3. Schematic diagram representing the proposed mechanisms mediating PIO inhibition of PDGF-induced VSMC proliferation *in vitro* and neointima formation *in vivo*

Problem Statement and Specific Aims

Atherosclerosis and restenosis after angioplasty are associated with the phenotypic transition of VSMCs from contractile to the proliferative state. Notably, insulin resistance is associated with increased risk of atherosclerosis and restenosis after angioplasty. However, the exact role of dysregulated VSMC-specific insulin receptor signaling on VSMC proliferation remains unclear. In addition, PIO, a classical insulin sensitizer that belongs to the family of PPARγ agonists, reduces intimal hyperplasia after coronary angioplasty in diabetic and nondiabetic subjects. However, the molecular mechanisms by which PIO regulates VSMC phenotype remain elusive. The objectives of this project were to examine the role of VSMC-specific dysregulated insulin signaling on VSMC proliferation and to identify the key signaling mechanisms by which PIO prevents the phenotypic transition of VSMCs from contractile to the proliferative state.

<u>Aim 1:</u> Examine the effects of high fructose-mediated dysregulation of insulin receptor signaling on PDGF-induced VSMC proliferation

Using human aortic VSMCs, we determined the effects of high fructose on: i) IRS-1 serine phosphorylation and IRS-1/IRS-2 expression; ii) insulin *versus* PDGF-induced changes in the phosphorylation of Akt, S6 ribosomal protein (a downstream target of mTOR/p70S6K signaling), and ERK; and iii) cell cycle proteins and proliferation.

<u>Aim 2:</u> Examine the role of AMPK activation in mediating the vasoprotective effects of PIO against PDGF-induced VSMC proliferation and injury-induced intimal hyperplasia *in vivo*

This aim is further subdivided into 2 sub-aims:

Aim 2A: Examine the role of AMPK activation in mediating the vasoprotective effects of PIO against PDGF-induced VSMC proliferation.

Using human aortic VSMCs we determined: i) the extent to which PIO regulates the phosphorylation AMPKα^{Thr172} and its downstream target, ACC; ii) PIO regulation of cellular energy state including mitochondrial membrane potential (by TMRM fluorescence analysis) and AMP/ATP ratio (by LC-MS/MS MRM analysis); iii) the role of LKB1 *versus* CaMKKβ as likely upstream kinases for PIO-induced AMPK activation; iv) the extent to which PIO activation of AMPK regulates PDGF-induced key proliferative signaling events including mTOR/p70S6K and ERK; and v) whether PIO regulation of key proliferative signaling is dependent on PPARγ expression;

Aim 2B: Examine the role of AMPK activation in mediating the vasoprotective effects of PIO against injury-induced intimal hyperplasia *in vivo*.

Using CJ57BL/6 mice we determined: i) the extent to which PIO regulates the phosphorylation AMPKα^{Thr172} in the vasculature *in vivo*; and ii) whether PIO inhibition of neointima formation is dependent on AMPK activation.

Bibliography

Aizawa, Y., J. Kawabe, N. Hasebe, N. Takehara, and K. Kikuchi. 2001. Pioglitazone enhances cytokine-induced apoptosis in vascular smooth muscle cells and reduces intimal hyperplasia. *Circulation* 104 (4):455-60.

Barrett, T. B., and E. P. Benditt. 1987. sis (platelet-derived growth factor B chain) gene transcript levels are elevated in human atherosclerotic lesions compared to normal artery. *Proc Natl Acad Sci U S A* 84 (4):1099-103.

Benkirane, K., F. Amiri, Q. N. Diep, M. El Mabrouk, and E. L. Schiffrin. 2006. PPAR-gamma inhibits ANG II-induced cell growth via SHIP2 and 4E-BP1. *Am J Physiol Heart Circ Physiol* 290 (1):H390-7.

Benson, S., J. Wu, S. Padmanabhan, T. W. Kurtz, and H. A. Pershadsingh. 2000. Peroxisome proliferator-activated receptor (PPAR)-gamma expression in human vascular smooth muscle cells: inhibition of growth, migration, and c-fos expression by the peroxisome proliferator-activated receptor (PPAR)-gamma activator troglitazone. *Am J Hypertens* 13 (1 Pt 1):74-82.

Bernstein, L. R., H. Antoniades, and B. R. Zetter. 1982. Migration of cultured vascular cells in response to plasma and platelet-derived factors. *J Cell Sci* 56:71-82.

Bornfeldt, K. E., and I. Tabas. 2011. Insulin resistance, hyperglycemia, and atherosclerosis. *Cell Metab* 14 (5):575-85.

Boyle, J. G., P. J. Logan, M. A. Ewart, J. A. Reihill, S. A. Ritchie, J. M. Connell, S. J. Cleland, and I. P. Salt. 2008. Rosiglitazone stimulates nitric oxide synthesis in human aortic endothelial cells via AMP-activated protein kinase. *J Biol Chem* 283 (17):11210-7.

Braun-Dullaeus, R. C., M. J. Mann, U. Seay, L. Zhang, H. E. von Der Leyen, R. E. Morris, and V. J. Dzau. 2001. Cell cycle protein expression in vascular smooth muscle cells in vitro and in vivo is regulated through phosphatidylinositol 3-kinase and mammalian target of rapamycin. *Arterioscler Thromb Vasc Biol* 21 (7):1152-8.

Burt, H. M., and W. L. Hunter. 2006. Drug-eluting stents: a multidisciplinary success story. *Adv Drug Deliv Rev* 58 (3):350-7.

Campbell, G. R., J. H. Campbell, J. A. Manderson, S. Horrigan, and R. E. Rennick. 1988. Arterial smooth muscle. A multifunctional mesenchymal cell. *Arch Pathol Lab Med* 112 (10):977-86.

Cassese, S., R. A. Byrne, T. Tada, S. Pinieck, M. Joner, T. Ibrahim, L. A. King, M. Fusaro, K. L. Laugwitz, and A. Kastrati. 2014. Incidence and predictors of restenosis after coronary stenting in 10 004 patients with surveillance angiography. *Heart* 100 (2):153-9.

Clowes, A. W., M. A. Reidy, and M. M. Clowes. 1983. Mechanisms of stenosis after arterial injury. *Lab Invest* 49 (2):208-15.

Coletta, D. K., A. Sriwijitkamol, E. Wajcberg, P. Tantiwong, M. Li, M. Prentki, M. Madiraju, C. P. Jenkinson, E. Cersosimo, N. Musi, and R. A. Defronzo. 2009. Pioglitazone stimulates AMP-activated protein kinase signalling and increases the expression of genes involved in adiponectin signalling, mitochondrial function and fat oxidation in human skeletal muscle in vivo: a randomised trial. *Diabetologia* 52 (4):723-32.

Costa, M. A., and D. I. Simon. 2005. Molecular basis of restenosis and drug-eluting stents. *Circulation* 111 (17):2257-73.

D'Angelo, G., A. A. Elmarakby, D. M. Pollock, and D. W. Stepp. 2005. Fructose feeding increases insulin resistance but not blood pressure in Sprague-Dawley rats. *Hypertension* 46 (4):806-11.

Dandapani, M., and D. G. Hardie. 2013. AMPK: opposing the metabolic changes in both tumour cells and inflammatory cells? *Biochem Soc Trans* 41 (2):687-93.

de Dios, S. T., D. Bruemmer, R. J. Dilley, M. E. Ivey, G. L. Jennings, R. E. Law, and P. J. Little. 2003. Inhibitory activity of clinical thiazolidinedione peroxisome proliferator activating receptor-gamma ligands toward internal mammary artery, radial artery, and saphenous vein smooth muscle cell proliferation. *Circulation* 107 (20):2548-50.

Desouza, C. V., M. Gerety, and F. G. Hamel. 2007. Long-term effects of a PPAR-gamma agonist, pioglitazone, on neointimal hyperplasia and endothelial regrowth in insulin resistant rats. *Vascul Pharmacol* 46 (3):188-94.

Ewart, M. A., C. F. Kohlhaas, and I. P. Salt. 2008. Inhibition of tumor necrosis factor alpha-stimulated monocyte adhesion to human aortic endothelial cells by AMP-activated protein kinase. *Arterioscler Thromb Vasc Biol* 28 (12):2255-7.

Fryer, L. G., A. Parbu-Patel, and D. Carling. 2002. The Anti-diabetic drugs rosiglitazone and metformin stimulate AMP-activated protein kinase through distinct signaling pathways. *J Biol Chem* 277 (28):25226-32.

Geng, D. F., D. M. Jin, W. Wu, Z. Wang, and J. F. Wang. 2009. Effect of thiazolidinediones on in-stent restenosis in patients after coronary stenting: a meta-analysis of randomized controlled trials. *Atherosclerosis* 202 (2):521-8.

Go, A. S., D. Mozaffarian, V. L. Roger, E. J. Benjamin, J. D. Berry, M. J. Blaha, S. Dai, E. S. Ford, C. S. Fox, S. Franco, H. J. Fullerton, C. Gillespie, S. M. Hailpern, J. A. Heit, V. J. Howard, M. D. Huffman, S. E. Judd, B. M. Kissela, S. J. Kittner, D. T. Lackland, J. H. Lichtman, L. D. Lisabeth, R. H. Mackey, D. J. Magid, G. M. Marcus, A. Marelli, D. B. Matchar, D. K. McGuire, E. R. Mohler, 3rd, C. S. Moy, M. E. Mussolino, R. W. Neumar, G. Nichol, D. K. Pandey, N. P. Paynter, M. J. Reeves, P. D. Sorlie, J. Stein, A. Towfighi, T. N. Turan, S. S. Virani, N. D. Wong, D. Woo, M. B. Turner, Committee American Heart Association Statistics, and Subcommittee Stroke Statistics. 2014. Heart disease and stroke statistics--2014 update: a report from the American Heart Association. *Circulation* 129 (3):e28-e292.

Goetze, S., X. P. Xi, K. Graf, E. Fleck, W. A. Hsueh, and R. E. Law. 1999. Troglitazone inhibits angiotensin II-induced extracellular signal-regulated kinase 1/2 nuclear translocation and activation in vascular smooth muscle cells. *FEBS Lett* 452 (3):277-82.

Goirand, F., M. Solar, Y. Athea, B. Viollet, P. Mateo, D. Fortin, J. Leclerc, J. Hoerter, R. Ventura-Clapier, and A. Garnier. 2007. Activation of AMP kinase alpha1 subunit induces aortic vasorelaxation in mice. *J Physiol* 581 (Pt 3):1163-71.

Guan, Y., C. Hao, D. R. Cha, R. Rao, W. Lu, D. E. Kohan, M. A. Magnuson, R. Redha, Y. Zhang, and M. D. Breyer. 2005. Thiazolidinediones expand body fluid volume

through PPARgamma stimulation of ENaC-mediated renal salt absorption. *Nat Med* 11 (8):861-6.

Gwinn, D. M., D. B. Shackelford, D. F. Egan, M. M. Mihaylova, A. Mery, D. S. Vasquez, B. E. Turk, and R. J. Shaw. 2008. AMPK phosphorylation of raptor mediates a metabolic checkpoint. *Mol Cell* 30 (2):214-26.

Hamon, M., E. Lecluse, J. P. Monassier, G. Grollier, and J. C. Potier. 1998. Pharmacological approaches to the prevention of restenosis after coronary angioplasty. *Drugs Aging* 13 (4):291-301.

Hannan, K. M., R. J. Dilley, S. T. de Dios, and P. J. Little. 2003. Troglitazone stimulates repair of the endothelium and inhibits neointimal formation in denuded rat aorta. *Arterioscler Thromb Vasc Biol* 23 (5):762-8.

Hardie, D. G., D. Carling, and M. Carlson. 1998. The AMP-activated/SNF1 protein kinase subfamily: metabolic sensors of the eukaryotic cell? *Annu Rev Biochem* 67:821-55.

Hardie, D. G., F. A. Ross, and S. A. Hawley. 2012. AMPK: a nutrient and energy sensor that maintains energy homeostasis. *Nat Rev Mol Cell Biol* 13 (4):251-62.

Hawley, S. A., J. Boudeau, J. L. Reid, K. J. Mustard, L. Udd, T. P. Makela, D. R. Alessi, and D. G. Hardie. 2003. Complexes between the LKB1 tumor suppressor, STRAD alpha/beta and MO25 alpha/beta are upstream kinases in the AMP-activated protein kinase cascade. *J Biol* 2 (4):28.

Hawley, S. A., D. A. Pan, K. J. Mustard, L. Ross, J. Bain, A. M. Edelman, B. G. Frenguelli, and D. G. Hardie. 2005. Calmodulin-dependent protein kinase kinase-

beta is an alternative upstream kinase for AMP-activated protein kinase. *Cell Metab* 2 (1):9-19.

Heldin, C. H., and B. Westermark. 1999. Mechanism of action and in vivo role of platelet-derived growth factor. *Physiol Rev* 79 (4):1283-316.

Horman, S., N. Morel, D. Vertommen, N. Hussain, D. Neumann, C. Beauloye, N. El Najjar, C. Forcet, B. Viollet, M. P. Walsh, L. Hue, and M. H. Rider. 2008. AMP-activated protein kinase phosphorylates and desensitizes smooth muscle myosin light chain kinase. *J Biol Chem* 283 (27):18505-12.

Igarashi, M., A. Hirata, H. Yamaguchi, H. Tsuchiya, H. Ohnuma, M. Tominaga, M. Daimon, and T. Kato. 2001. Characterization of an inhibitory effect of pioglitazone on balloon-injured vascular smooth muscle cell growth. *Metabolism-Clinical and Experimental* 50 (8):955-962.

Igarashi, M., Y. Takeda, N. Ishibashi, K. Takahashi, S. Mori, M. Tominaga, and Y. Saito. 1997. Pioglitazone reduces smooth muscle cell density of rat carotid arterial intima induced by balloon catheterization. *Horm Metab Res* 29 (9):444-9.

Igata, M., H. Motoshima, K. Tsuruzoe, K. Kojima, T. Matsumura, T. Kondo, T. Taguchi, K. Nakamaru, M. Yano, D. Kukidome, K. Matsumoto, T. Toyonaga, T. Asano, T. Nishikawa, and E. Araki. 2005. Adenosine monophosphate-activated protein kinase suppresses vascular smooth muscle cell proliferation through the inhibition of cell cycle progression. *Circ Res* 97 (8):837-44.

Inoki, K., J. Kim, and K. L. Guan. 2012. AMPK and mTOR in cellular energy homeostasis and drug targets. *Annu Rev Pharmacol Toxicol* 52:381-400.

Inzucchi, S. E., R. M. Bergenstal, J. B. Buse, M. Diamant, E. Ferrannini, M. Nauck, A. L. Peters, A. Tsapas, R. Wender, and D. R. Matthews. 2012. Management of hyperglycaemia in type 2 diabetes: a patient-centered approach. Position statement of the American Diabetes Association (ADA) and the European Association for the Study of Diabetes (EASD). *Diabetologia* 55 (6):1577-96.

Kahn, B. B., T. Alquier, D. Carling, and D. G. Hardie. 2005. AMP-activated protein kinase: ancient energy gauge provides clues to modern understanding of metabolism. *Cell Metab* 1 (1):15-25.

Kahn, S. E., S. M. Haffner, M. A. Heise, W. H. Herman, R. R. Holman, N. P. Jones, B. G. Kravitz, J. M. Lachin, M. C. O'Neill, B. Zinman, G. Viberti, and Adopt Study Group. 2006. Glycemic durability of rosiglitazone, metformin, or glyburide monotherapy. *N Engl J Med* 355 (23):2427-43.

Kasai, T., K. Miyauchi, T. Yokoyama, K. Kajimoto, K. Sumiyoshi, N. Kubota, E. Ikeda, and H. Daida. 2008. Pioglitazone attenuates neointimal thickening via suppression of the early inflammatory response in a porcine coronary after stenting. *Atherosclerosis* 197 (2):612-9.

Katayama, T., H. Ueba, K. Tsuboi, T. Yasu, N. Kubo, T. Umemoto, M. Kuroki, S. E. Ishikawa, M. Saito, and M. Kawakami. 2005. Reduction of in-stent restenosis by pioglitazone in non-diabetic patients. *Diabetes* 54:A175-A175.

Kaul, S., A. F. Bolger, D. Herrington, R. P. Giugliano, R. H. Eckel, Association American Heart, and Foundation American College Of Cardiology. 2010. Thiazolidinedione drugs and cardiovascular risks: a science advisory from the

American Heart Association and American College Of Cardiology Foundation. *J Am Coll Cardiol* 55 (17):1885-94.

Kim, E. J., Y. K. Choi, Y. H. Han, H. J. Kim, I. K. Lee, and M. O. Lee. 2014. RORalpha suppresses proliferation of vascular smooth muscle cells through activation of AMP-activated protein kinase. *Int J Cardiol* 175 (3):515-21.

Konrad, D., A. Rudich, P. J. Bilan, N. Patel, C. Richardson, L. A. Witters, and A. Klip. 2005. Troglitazone causes acute mitochondrial membrane depolarisation and an AMPK-mediated increase in glucose phosphorylation in muscle cells. *Diabetologia* 48 (5):954-66.

Law, R. E., S. Goetze, X. P. Xi, S. Jackson, Y. Kawano, L. Demer, M. C. Fishbein, W. P. Meehan, and W. A. Hsueh. 2000. Expression and function of PPARgamma in rat and human vascular smooth muscle cells. *Circulation* 101 (11):1311-8.

Law, R. E., W. P. Meehan, X. P. Xi, K. Graf, D. A. Wuthrich, W. Coats, D. Faxon, and W. A. Hsueh. 1996. Troglitazone inhibits vascular smooth muscle cell growth and intimal hyperplasia. *J Clin Invest* 98 (8):1897-905.

Lee, C. S., Y. W. Kwon, H. M. Yang, S. H. Kim, T. Y. Kim, J. Hur, K. W. Park, H. J. Cho, H. J. Kang, Y. B. Park, and H. S. Kim. 2009. New mechanism of rosiglitazone to reduce neointimal hyperplasia: activation of glycogen synthase kinase-3beta followed by inhibition of MMP-9. *Arterioscler Thromb Vasc Biol* 29 (4):472-9.

Lightell, D. J., Jr., S. C. Moss, and T. C. Woods. 2011. Loss of canonical insulin signaling accelerates vascular smooth muscle cell proliferation and migration through changes in p27Kip1 regulation. *Endocrinology* 152 (2):651-8.

Lu, J., J. Ji, H. Meng, D. Wang, B. Jiang, L. Liu, E. Randell, K. Adeli, and Q. H. Meng. 2013. The protective effect and underlying mechanism of metformin on neointima formation in fructose-induced insulin resistant rats. *Cardiovasc Diabetol* 12:58.

Makino, H., S. Okada, A. Nagumo, T. Sugisawa, Y. Miyamoto, I. Kishimoto, T. K. Akie, T. Soma, A. Taguchi, and Y. Yoshimasa. 2008. Pioglitazone treatment stimulates circulating CD34-positive cells in type 2 diabetes patients. *Diabetes Res Clin Pract* 81 (3):327-30.

Martinez-Hervas, S., A. Vinue, L. Nunez, I. Andres-Blasco, L. Piqueras, J. T. Real, J. F. Ascaso, D. J. Burks, M. J. Sanz, and H. Gonzalez-Navarro. 2014. Insulin resistance aggravates atherosclerosis by reducing vascular smooth muscle cell survival and increasing CX3CL1/CX3CR1 axis. *Cardiovasc Res* 103 (2):324-36.

Marx, N., J. Wohrle, T. Nusser, D. Walcher, A. Rinker, V. Hombach, W. Koenig, and M. Hoher. 2005. Pioglitazone reduces neointima volume after coronary stent implantation: a randomized, placebo-controlled, double-blind trial in nondiabetic patients. *Circulation* 112 (18):2792-8.

Mauri, L., T. S. Silbaugh, R. E. Wolf, K. Zelevinsky, A. Lovett, Z. Zhou, F. S. Resnic, and S. L. Normand. 2008. Long-term clinical outcomes after drug-eluting and bare-metal stenting in Massachusetts. *Circulation* 118 (18):1817-27.

Morrow, V. A., F. Foufelle, J. M. Connell, J. R. Petrie, G. W. Gould, and I. P. Salt. 2003. Direct activation of AMP-activated protein kinase stimulates nitric-oxide synthesis in human aortic endothelial cells. *J Biol Chem* 278 (34):31629-39.

Motobayashi, Y., Y. Izawa-Ishizawa, K. Ishizawa, S. Orino, K. Yamaguchi, K. Kawazoe, S. Hamano, K. Tsuchiya, S. Tomita, and T. Tamaki. 2009. Adiponectin inhibits

insulin-like growth factor-1-induced cell migration by the suppression of extracellular signal-regulated kinase 1/2 activation, but not Akt in vascular smooth muscle cells. *Hypertens Res* 32 (3):188-93.

Mozaffarian, D., E. J. Benjamin, A. S. Go, D. K. Arnett, M. J. Blaha, M. Cushman, S. R. Das, S. de Ferranti, J. P. Despres, H. J. Fullerton, V. J. Howard, M. D. Huffman, C. R. Isasi, M. C. Jimenez, S. E. Judd, B. M. Kissela, J. H. Lichtman, L. D. Lisabeth, S. Liu, R. H. Mackey, D. J. Magid, D. K. McGuire, E. R. Mohler, 3rd, C. S. Moy, P. Muntner, M. E. Mussolino, K. Nasir, R. W. Neumar, G. Nichol, L. Palaniappan, D. K. Pandey, M. J. Reeves, C. J. Rodriguez, W. Rosamond, P. D. Sorlie, J. Stein, A. Towfighi, T. N. Turan, S. S. Virani, D. Woo, R. W. Yeh, M. B. Turner, Committee American Heart Association Statistics, and Subcommittee Stroke Statistics. 2016. Heart Disease and Stroke Statistics-2016 Update: A Report From the American Heart Association. *Circulation* 133 (4):e38-e360.

Nagata, D., M. Mogi, and K. Walsh. 2003. AMP-activated protein kinase (AMPK) signaling in endothelial cells is essential for angiogenesis in response to hypoxic stress. *J Biol Chem* 278 (33):31000-6.

Nagata, D., R. Takeda, M. Sata, H. Satonaka, E. Suzuki, T. Nagano, and Y. Hirata. 2004. AMP-activated protein kinase inhibits angiotensin II-stimulated vascular smooth muscle cell proliferation. *Circulation* 110 (4):444-51.

Nesto, R. W., D. Bell, R. O. Bonow, V. Fonseca, S. M. Grundy, E. S. Horton, M. Le Winter, D. Porte, C. F. Semenkovich, S. Smith, L. H. Young, R. Kahn, Association American Heart, and Association American Diabetes. 2003. Thiazolidinedione use, fluid retention, and congestive heart failure: a consensus

statement from the American Heart Association and American Diabetes Association. October 7, 2003. *Circulation* 108 (23):2941-8.

Newby, A. C., and A. B. Zaltsman. 2000. Molecular mechanisms in intimal hyperplasia. *J Pathol* 190 (3):300-9.

Ning, B., X. Wang, Y. Yu, A. B. Waqar, Q. Yu, T. Koike, M. Shiomi, E. Liu, Y. Wang, and J. Fan. 2015. High-fructose and high-fat diet-induced insulin resistance enhances atherosclerosis in Watanabe heritable hyperlipidemic rabbits. *Nutr Metab (Lond)* 12:30.

Nishio, K., M. Sakurai, T. Kusuyama, M. Shigemitsu, T. Fukui, K. Kawamura, S. Itoh, N. Konno, and T. Katagiri. 2006. A randomized comparison of pioglitazone to inhibit restenosis after coronary stenting in patients with type 2 diabetes. *Diabetes Care* 29 (1):101-6.

Owens, G. K. 1995. Regulation of differentiation of vascular smooth muscle cells. *Physiol Rev* 75 (3):487-517.

Owens, G. K., M. S. Kumar, and B. R. Wamhoff. 2004. Molecular regulation of vascular smooth muscle cell differentiation in development and disease. *Physiol Rev* 84 (3):767-801.

Owens, G. K., S. M. Vernon, and C. S. Madsen. 1996. Molecular regulation of smooth muscle cell differentiation. *J Hypertens Suppl* 14 (5):S55-64.

Park, H., V. K. Kaushik, S. Constant, M. Prentki, E. Przybytkowski, N. B. Ruderman, and A. K. Saha. 2002. Coordinate regulation of malonyl-CoA decarboxylase, sn-glycerol-3-phosphate acyltransferase, and acetyl-CoA carboxylase by AMP-

activated protein kinase in rat tissues in response to exercise. *J Biol Chem* 277 (36):32571-7.

Patel, D., B. Walitt, J. Lindsay, and R. L. Wilensky. 2011. Role of pioglitazone in the prevention of restenosis and need for revascularization after bare-metal stent implantation: a meta-analysis. *JACC Cardiovasc Interv* 4 (3):353-60.

Peuler, J. D., S. M. Phare, A. R. Iannucci, and M. J. Hodorek. 1996. Differential inhibitory effects of antidiabetic drugs on arterial smooth muscle cell proliferation. *Am J Hypertens* 9 (2):188-92.

Phillips, J. W., K. G. Barringhaus, J. M. Sanders, Z. Yang, M. Chen, S. Hesselbacher, A. C. Czarnik, K. Ley, J. Nadler, and I. J. Sarembock. 2003. Rosiglitazone reduces the accelerated neointima formation after arterial injury in a mouse injury model of type 2 diabetes. *Circulation* 108 (16):1994-9.

Pistrosch, F., K. Herbrig, U. Oelschlaegel, S. Richter, J. Passauer, S. Fischer, and P. Gross. 2005. PPARgamma-agonist rosiglitazone increases number and migratory activity of cultured endothelial progenitor cells. *Atherosclerosis* 183 (1):163-7.

Regan, C. P., P. J. Adam, C. S. Madsen, and G. K. Owens. 2000. Molecular mechanisms of decreased smooth muscle differentiation marker expression after vascular injury. *J Clin Invest* 106 (9):1139-47.

Riche, D. M., R. Valderrama, and N. N. Henyan. 2007. Thiazolidinediones and risk of repeat target vessel revascularization following percutaneous coronary intervention: a meta-analysis. *Diabetes Care* 30 (2):384-8.

Ross, R. 1999. Atherosclerosis--an inflammatory disease. *N Engl J Med* 340 (2):115-26.

Rubin, K., A. Tingstrom, G. K. Hansson, E. Larsson, L. Ronnstrand, L. Klareskog, L. Claesson-Welsh, C. H. Heldin, B. Fellstrom, and L. Terracio. 1988. Induction of B-type receptors for platelet-derived growth factor in vascular inflammation: possible implications for development of vascular proliferative lesions. *Lancet* 1 (8599):1353-6.

Rubin, L. J., L. Magliola, X. Feng, A. W. Jones, and C. C. Hale. 2005. Metabolic activation of AMP kinase in vascular smooth muscle. *J Appl Physiol (1985)* 98 (1):296-306.

Saha, A. K., P. R. Avilucea, J. M. Ye, M. M. Assifi, E. W. Kraegen, and N. B. Ruderman. 2004. Pioglitazone treatment activates AMP-activated protein kinase in rat liver and adipose tissue in vivo. *Biochem Biophys Res Commun* 314 (2):580-5.

Saha, A. K., X. J. Xu, E. Lawson, R. Deoliveira, A. E. Brandon, E. W. Kraegen, and N. B. Ruderman. 2010. Downregulation of AMPK accompanies leucine- and glucose-induced increases in protein synthesis and insulin resistance in rat skeletal muscle. *Diabetes* 59 (10):2426-34.

Satoh, N., Y. Ogawa, T. Usui, T. Tagami, S. Kono, H. Uesugi, H. Sugiyama, A. Sugawara, K. Yamada, A. Shimatsu, H. Kuzuya, and K. Nakao. 2003. Antiatherogenic effect of pioglitazone in type 2 diabetic patients irrespective of the responsiveness to its antidiabetic effect. *Diabetes Care* 26 (9):2493-9.

Scheen, A. J., F. Warzee, and V. M. Legrand. 2004. Drug-eluting stents: meta-analysis in diabetic patients. *Eur Heart J* 25 (23):2167-8; author reply 2168-9.

Semenkovich, C. F. 2006. Insulin resistance and atherosclerosis. *J Clin Invest* 116 (7):1813-22.

Smith, A. J., B. R. Thompson, M. A. Sanders, and D. A. Bernlohr. 2007. Interaction of the adipocyte fatty acid-binding protein with the hormone-sensitive lipase: regulation by fatty acids and phosphorylation. *J Biol Chem* 282 (44):32424-32.

Sorrentino, S. A., F. H. Bahlmann, C. Besler, M. Muller, S. Schulz, N. Kirchhoff, C. Doerries, T. Horvath, A. Limbourg, F. Limbourg, D. Fliser, H. Haller, H. Drexler, and U. Landmesser. 2007. Oxidant stress impairs in vivo reendothelialization capacity of endothelial progenitor cells from patients with type 2 diabetes mellitus: restoration by the peroxisome proliferator-activated receptor-gamma agonist rosiglitazone. *Circulation* 116 (2):163-73.

Staels, B., W. Koenig, A. Habib, R. Merval, M. Lebret, I. P. Torra, P. Delerive, A. Fadel, G. Chinetti, J. C. Fruchart, J. Najib, J. Maclouf, and A. Tedgui. 1998. Activation of human aortic smooth-muscle cells is inhibited by PPARalpha but not by PPARgamma activators. *Nature* 393 (6687):790-3.

Subramanian, V., J. Golledge, T. Ijaz, D. Bruemmer, and A. Daugherty. 2010. Pioglitazone-induced reductions in atherosclerosis occur via smooth muscle cell-specific interaction with PPAR{gamma}. *Circ Res* 107 (8):953-8.

Taegtmeyer, H. 1996. Insulin resistance and atherosclerosis. Common roots for two common diseases? *Circulation* 93 (10):1777-9.

Takagi, T., A. Yamamuro, K. Tamita, K. Yamabe, M. Katayama, S. Mizoguchi, M. Ibuki, T. Tani, K. Tanabe, K. Nagai, K. Shiratori, S. Morioka, and J. Yoshikawa. 2003. Pioglitazone reduces neointimal tissue proliferation after coronary stent

implantation in patients with type 2 diabetes mellitus: an intravascular ultrasound scanning study. *Am Heart J* 146 (2):E5.

Uemura, Y., R. Shibata, N. Kanemura, K. Ohashi, T. Kambara, M. Hiramatsu-Ito, T. Enomoto, D. Yuasa, Y. Joki, K. Matsuo, M. Ito, S. Hayakawa, H. Ogawa, T. Murohara, and N. Ouchi. 2015. Adipose-derived protein omentin prevents neointimal formation after arterial injury. *Faseb j* 29 (1):141-51.

van der Hoeven, B. L., N. M. Pires, H. M. Warda, P. V. Oemrawsingh, B. J. van Vlijmen, P. H. Quax, M. J. Schalij, E. E. van der Wall, and J. W. Jukema. 2005. Drug-eluting stents: results, promises and problems. *Int J Cardiol* 99 (1):9-17.

Viollet, B., B. Guigas, J. Leclerc, S. Hebrard, L. Lantier, R. Mounier, F. Andreelli, and M. Foretz. 2009. AMP-activated protein kinase in the regulation of hepatic energy metabolism: from physiology to therapeutic perspectives. *Acta Physiol (Oxf)* 196 (1):81-98.

Wakino, S., U. Kintscher, S. Kim, F. Yin, W. A. Hsueh, and R. E. Law. 2000. Peroxisome proliferator-activated receptor gamma ligands inhibit retinoblastoma phosphorylation and G1--> S transition in vascular smooth muscle cells. *J Biol Chem* 275 (29):22435-41.

Wang, K., Z. M. Zhou, M. Zhang, L. M. Fan, F. Forudi, X. R. Zhou, W. Qu, A. M. Lincoff, A. M. Schmidt, E. J. Topol, and M. S. Penn. 2006. Peroxisome proliferator-activated receptor gamma down-regulates receptor for advanced glycation end products and inhibits smooth muscle cell proliferation in a diabetic and nondiabetic rat carotid artery injury model. *Journal of Pharmacology and Experimental Therapeutics* 317 (1):37-43.

Werner, C., C. H. Kamani, C. Gensch, M. Bohm, and U. Laufs. 2007. The peroxisome proliferator-activated receptor-gamma agonist pioglitazone increases number and function of endothelial progenitor cells in patients with coronary artery disease and normal glucose tolerance. *Diabetes* 56 (10):2609-15.

Wilcox, J. N. 1992. Analysis of local gene expression in human atherosclerotic plaques. *J Vasc Surg* 15 (5):913-6.

Woods, A., K. Dickerson, R. Heath, S. P. Hong, M. Momcilovic, S. R. Johnstone, M. Carlson, and D. Carling. 2005. Ca2+/calmodulin-dependent protein kinase kinase-beta acts upstream of AMP-activated protein kinase in mammalian cells. *Cell Metab* 2 (1):21-33.

Woods, A., S. R. Johnstone, K. Dickerson, F. C. Leiper, L. G. Fryer, D. Neumann, U. Schlattner, T. Wallimann, M. Carlson, and D. Carling. 2003. LKB1 is the upstream kinase in the AMP-activated protein kinase cascade. *Curr Biol* 13 (22):2004-8.

Xie, Z., Y. Dong, M. Zhang, M. Z. Cui, R. A. Cohen, U. Riek, D. Neumann, U. Schlattner, and M. H. Zou. 2006. Activation of protein kinase C zeta by peroxynitrite regulates LKB1-dependent AMP-activated protein kinase in cultured endothelial cells. *J Biol Chem* 281 (10):6366-75.

Yoshimoto, T., M. Naruse, H. Shizume, K. Naruse, A. Tanabe, M. Tanaka, K. Tago, K. Irie, T. Muraki, H. Demura, and L. Zardi. 1999. Vasculo-protective effects of insulin sensitizing agent pioglitazone in neointimal thickening and hypertensive vascular hypertrophy. *Atherosclerosis* 145 (2):333-40.

Young, P. W., D. R. Buckle, B. C. Cantello, H. Chapman, J. C. Clapham, P. J. Coyle, D. Haigh, R. M. Hindley, J. C. Holder, H. Kallender, A. J. Latter, K. W. Lawrie, D. Mossakowska, G. J. Murphy, L. Roxbee Cox, and S. A. Smith. 1998. Identification of high-affinity binding sites for the insulin sensitizer rosiglitazone (BRL-49653) in rodent and human adipocytes using a radioiodinated ligand for peroxisomal proliferator-activated receptor gamma. *J Pharmacol Exp Ther* 284 (2):751-9.

Zhang, H., A. Zhang, D. E. Kohan, R. D. Nelson, F. J. Gonzalez, and T. Yang. 2005. Collecting duct-specific deletion of peroxisome proliferator-activated receptor gamma blocks thiazolidinedione-induced fluid retention. *Proc Natl Acad Sci U S A* 102 (26):9406-11.

Zhang, J., Z. Xie, Y. Dong, S. Wang, C. Liu, and M. H. Zou. 2008. Identification of nitric oxide as an endogenous activator of the AMP-activated protein kinase in vascular endothelial cells. *J Biol Chem* 283 (41):27452-61.

Zhang, L. L., C. Y. Gao, C. Q. Fang, Y. J. Wang, D. Gao, G. E. Yao, J. Xiang, J. Z. Wang, and J. C. Li. 2011. PPARgamma attenuates intimal hyperplasia by inhibiting TLR4-mediated inflammation in vascular smooth muscle cells. *Cardiovasc Res* 92 (3):484-93.

Zhao, Y., S. K. Biswas, P. H. McNulty, M. Kozak, J. Y. Jun, and L. Segar. 2011. PDGF-induced vascular smooth muscle cell proliferation is associated with dysregulation of insulin receptor substrates. *Am J Physiol Cell Physiol* 300 (6):C1375-85.

CHAPTER 2

HIGH FRUCTOSE-MEDIATED ATTENUATION OF INSULIN RECEPTOR SIGNALING DOES NOT AFFECT PDGF-INDUCED PROLIFERATIVE SIGNALING IN VASCULAR SMOOTH MUSCLE CELLS (Osman et al 2016)

Islam Osman, Ninu Poulose, Vadivel Ganapathy, Lakshman Segar

Submitted to European Journal of Pharmacology, 05/17/2016

High fructose-mediated attenuation of insulin receptor signaling does not affect PDGF-induced proliferative signaling in vascular smooth muscle cells

Islam Osman [a,b], Ninu Poulose [a,b], Vadivel Ganapathy [c], Lakshman Segar [a,b,d,e,*]

[a] *Center for Pharmacy and Experimental Therapeutics, University of Georgia College of Pharmacy, Augusta, Georgia, USA*

[b] *Charlie Norwood VA Medical Center, Augusta, Georgia, USA*

[c] *Department of Biochemistry and Molecular Biology, Augusta University, Augusta, Georgia, USA*

[d] *Vascular Biology Center, Department of Pharmacology and Toxicology, Augusta University, Augusta, Georgia, USA*

[e] *Department of Medicine, Pennsylvania State University College of Medicine, Hershey, Pennsylvania, USA*

*** Corresponding author:**

Lakshman Segar, Center for Pharmacy and Experimental Therapeutics,

University of Georgia College of Pharmacy, 1120 15th Street, HM-1200

Augusta University Campus, Augusta, Georgia, USA 30912-2450

Tel.: +1 706 721 6491; fax: +1 706 721 3994*; E-mail address:* lsegar@augusta.edu (L. Segar).

ABSTRACT

Insulin resistance is associated with accelerated atherosclerosis. Although high fructose is known to induce insulin resistance, it remains unclear as to how fructose regulates insulin receptor signaling and proliferative phenotype in vascular smooth muscle cells (VSMCs), which play a major role in atherosclerosis. Using human aortic VSMCs, we investigated the effects of high fructose treatment on insulin receptor substrate-1 (IRS-1) serine phosphorylation, insulin *versus* platelet-derived growth factor (PDGF)-induced phosphorylation of Akt, S6 ribosomal protein, and extracellular signal-regulated kinase (ERK), and cell cycle proteins. In comparison with PDGF (a potent mitogen), neither fructose nor insulin enhanced VSMC proliferation and cyclin D1 expression. D-[^{14}C(U)]fructose uptake studies revealed a progressive increase in fructose uptake in a time-dependent manner. Concentration-dependent studies with high fructose (5 to 25 mM) showed marked increases in IRS-1 serine phosphorylation, a key adapter protein in insulin receptor signaling. Accordingly, high fructose treatment led to significant diminutions in insulin-induced phosphorylation of downstream signaling components including Akt and S6. In addition, high fructose significantly diminished insulin-induced ERK phosphorylation. Nevertheless, high fructose did not affect PDGF-induced key proliferative signaling events including phosphorylation of Akt, S6, and ERK and expression of cyclin D1 protein. Together, high fructose dysregulates IRS-1 phosphorylation state and proximal insulin receptor signaling in VSMCs but does not affect PDGF-induced proliferative signaling. In conclusion, although high fructose disrupts VSMC-specific insulin receptor signaling, the metabolic abnormalities (e.g.,

dyslipidemia) associated with high fructose consumption may play a major role in enhanced atherosclerosis and intimal hyperplasia.

Introduction

Insulin resistance, characterized by metabolic abnormalities including glucose intolerance and dyslipidemia, is a risk factor for accelerated atherosclerosis (Taegtmeyer 1996; Semenkovich 2006; Bornfeldt and Tabas 2011). While altered metabolic milieu is known to promote proatherogenic phenotype (Semenkovich 2006), the contribution of vascular wall-specific insulin resistance toward atherosclerotic lesion progression remains unclear (Semenkovich 2006; Bornfeldt and Tabas 2011). In particular, vascular smooth muscle cells (VSMCs) that play a major role in atherosclerosis have been shown to exhibit proliferative and proapoptotic phenotypes upon target-specific deletion of insulin receptor signaling components (Lightell, Moss, and Woods 2011; Martinez-Hervas et al. 2014). For instance, insulin receptor gene deficiency in VSMCs leads to a decrease in insulin-induced Akt phosphorylation and an increase in extracellular signal-regulated kinase (ERK) phosphorylation with an accompanying increase in cell proliferation (Lightell, Moss, and Woods 2011). In a different study, siRNA-mediated downregulation of insulin receptor substrate-2 (IRS-2) in VSMCs diminishes insulin-induced phosphorylation of Akt and ERK thereby inducing a proapoptotic phenotype (Martinez-Hervas et al. 2014). Thus, dysregulation of insulin signaling in VSMCs at the level of insulin receptor and IRS-2 may result in proliferative and proapoptotic phenotypes, which would enhance and exacerbate atherosclerosis, respectively. Although high fructose consumption is known to induce insulin resistance and promote

atherosclerosis (D'Angelo et al. 2005; Ning et al. 2015; Lu et al. 2013), it is unknown as to how fructose uptake in VSMCs regulates insulin receptor signaling and proliferative phenotype.

Previous studies demonstrate that high fructose diet induces insulin resistance in a rat model, as revealed by hyperinsulinemic-euglycemic clamp technique that shows a significant reduction in glucose infusion rate to maintain euglycemia (D'Angelo et al. 2005). In addition, high fructose diet-induced insulin resistance results in exaggerated atherosclerosis and neointima formation with a significant increase in smooth muscle cell accumulation (Ning et al. 2015; Lu et al. 2013). Since platelet-derived growth factor (PDGF) is a potent mitogen released at the site of arterial injury (Barrett and Benditt 1987; Rubin et al. 1988; Heldin and Westermark 1999), it is likely that high fructose-induced increase in neointima formation may occur through enhanced PDGF receptor signaling. Previously, we have shown that PDGF not only increases VSMC proliferation but also attenuates insulin-induced insulin receptor substrate (IRS-1/IRS-2)-associated PI 3-kinase/Akt signaling (Zhao et al. 2011). In the present study, we tested the hypothesis that high fructose-mediated dysregulation of insulin receptor signaling is associated with enhanced VSMC proliferation. Using human aortic VSMCs, we determined the effects of high fructose on: i) IRS-1 serine phosphorylation and IRS-1/IRS-2 expression; ii) insulin *versus* PDGF-induced changes in the phosphorylation of Akt, S6 ribosomal protein (a downstream target of mTOR/p70S6K signaling), and ERK; and iii) cell cycle proteins and proliferation.

Materials and methods

Materials

Recombinant human PDGF-BB was purchased from R&D Systems (Minneapolis, MN). Human insulin (Novolin R) was obtained from a local pharmacy. D-[U-^{14}C]fructose (specific activity: 240-360 mCi/mmol) was purchased from Moravek Biochemicals (Brea, CA). D-fructose was purchased from Sigma Chemical (St. Louis, MO). L-fructose was purchased from Omicron Biochemicals, Inc. (South Bend, IN). The primary antibodies for phospho-IRS1$^{Ser636/639}$ (2388), IRS-1 (3407), IRS-2 (3089), phospho-44/42 MAPK (ERK1/2; 4695), 44/42 MAPK (ERK1/2; 9102), phospho-Akt^{Thr308} (2965), Akt (4691), phospho-S6 ribosomal protein$^{Ser235/236}$ (4857), S6 ribosomal protein (2217), cyclin D1 (2922), phospho-Rb^{Ser795} (9301), and β-actin (8457) were purchased from Cell Signaling Technology (Danvers, MA). All other chemicals were from Fisher Scientific (Fair Lawn, NJ) or Sigma Chemical (St. Louis, MO).

Cell culture and treatments

Human aortic VSMCs, vascular cell basal medium and smooth muscle growth supplement (SMGS) were purchased from ATCC (Manassas, VA). SMGS constituents and their final concentrations after addition to vascular cell basal medium were as follows: 5% FBS (vol/vol), 5 ng/ml human basic fibroblast growth factor, 5 ng/ml human epidermal growth factor, 5 μg/ml insulin, 50 μg/mL ascorbic acid, 10 mM L-glutamine. VSMCs (passages 3–5) were maintained in vascular cell basal medium containing SMGS (complete medium), 5.5 mM D-glucose, and antibiotic/antimycotic solution in a humidified atmosphere of 95% air and 5% CO_2 at 37°C. After the attainment of

confluence (~6–7 days), VSMCs were trypsinized, centrifuged, and seeded onto Petri dishes or multiwell plates. Subconfluent VSMCs were maintained under SMGS (serum)-deprived conditions for 48 hours to achieve quiescence and then subjected to treatments as described in the legends to the respective figures. Equimolar concentrations of L-fructose were used as the vehicle controls for D-fructose in respective experiments.

Cell proliferation

Subconfluent VSMCs were serum-deprived for 48 hr and then treated with insulin (100 nM) or PDGF (30 ng/ml) for 96 hr. Fresh serum-free media containing the respective treatments were replaced every 48 hr. VSMCs were then trypsinized and the changes in cell number were determined using Countess Counter (Life Technologies, Carlsbad, CA), as described (Pyla et al. 2013).

Immunoblot analysis

Immunoblot analysis was performed as described (Osman and Segar 2016). VSMC lysates (20 μg protein per lane) were subjected to electrophoresis using precast 4–12% NuPage mini-gels (Life Technologies). The resolved proteins were then transferred to PVDF membranes (EMD Millipore, Billerica, MA). Subsequently, the membranes were blocked in 5% nonfat milk and probed with the respective primary antibodies. The immunoreactivity was detected using HRP-conjugated horse anti-mouse secondary antibody (7076; Cell Signaling) or goat anti-rabbit secondary antibody (7074; Cell Signaling) followed by enhanced chemiluminescence (ECL; Thermo Scientific,

Wilmington, DE). The protein bands were quantified by densitometric analysis using Image J.

D-[U-^{14}C] fructose uptake studies

Subconfluent VSMCs (100,000 cells/well) were serum-deprived for 48 hr and then washed twice with Krebs-Ringer-phosphate (KRP) buffer containing 130 mM NaCl, 5 mM KCl, 1.3 mM $MgSO_4$, 10 mM Na_2HPO_4, 0.8 mM $CaCl_2$ (pH 7.4). The washing buffer was removed completely and replaced with 500 μl radioactive cocktail (0.5 mM D-fructose and 0.5 μCi D-[U-^{14}C]fructose in KRP buffer). After incubation for different time intervals (2-30 min) at 37°C, the cells were washed twice with ice-cold KRP buffer and then lysed with 500 μl lysis buffer (0.2 N NaOH and 1% SDS) with intermittent shaking for 10 min. The lysates were analyzed using liquid scintillation counter (Beckman Instruments, Inc., Fullerton, CA, Model LS-6500).

Statistical analysis

Results are expressed as the means ± SEM of at least three separate experiments. Statistical analyses of the data were performed using one-way analysis of variance (ANOVA) followed by Bonferroni t-test. Values of $p < 0.05$ were considered statistically significant.

Results

PDGF, but not fructose or insulin, enhances VSMC proliferation

Isolated aortic VSMCs from high fructose-fed rats have been shown to exhibit enhanced proliferation in response to serum trophic factors (Miatello et al. 2001). However, a direct regulatory effect of high fructose on VSMC proliferation has not yet been examined. Insulin has been shown to enhance VSMC proliferation or maintain VSMC quiescence (Pfeifle and Ditschuneit 1981; Wang, Gurevich, and Draznin 2003). PDGF is a potent mitogen and is known to enhance VSMC proliferation (Owens, Kumar, and Wamhoff 2004). In the present study, we determined the effects of high fructose *versus* insulin or PDGF on VSMC proliferation and cell cycle proteins. As shown in **Fig. 2.1A**, fructose or insulin did not show significant effects on VSMC proliferation, whereas PDGF exposure led to an increase in VSMC proliferation by ~2 ± 0.5 fold. Accordingly, fructose or insulin treatment was not associated with an increase in the expression of cyclin D1, a cell cycle protein (**Fig. 2.1B**). In parallel, PDGF treatment led to a significant increase in cyclin D1 expression by ~1.8 ± 0.1-fold. In addition, PDGF enhanced the phosphorylation of retinoblastoma (Rb) protein by ~3.8 ± 0.1 fold (data not shown). Thus, treatment of VSMCs with PDGF, but not fructose or insulin, resulted in the transition to a proliferative phenotype.

Fructose uptake occurs in a time-dependent manner in VSMCs

GLUT5 (fructose transporter) expression and fructose uptake have been demonstrated in several cell types including adipocytes and skeletal muscle cells (Hajduch et al. 2003;

Buchs et al. 1998; Fukuzawa et al. 2013; Hajduch, Darakhshan, and Hundal 1998). Although we and several investigators have reported the expression of GLUT5 in VSMCs (Liu et al. 2011; Pyla et al. 2013), the ability of VSMCs to transport fructose has not been examined. As shown in **Fig. 2.2**, the uptake of D-[U-^{14}C]fructose occurred in a time-dependent manner in VSMCs. A significant increase in fructose uptake was observed within 2 min followed by a progressive increase in fructose transport for up to 30 min.

High fructose treatment enhances IRS-1 serine phosphorylation in VSMCs

Previous studies with hepatic and skeletal muscle tissues have shown that high fructose induces IRS-1 serine phosphorylation, which is reflected by diminished insulin-induced IRS-1 tyrosine phosphorylation and PI 3-kinase activity (Bezerra et al. 2000; Wei, Wang, and Pagliassotti 2005). Hence, we examined the likely regulatory effects of D-fructose on IRS-1 serine phosphorylation state in VSMCs. As shown in **Fig. 2.3,** exposure of VSMCs to D-Fructose at 5.5, 11, and 25 mM concentrations led to a progressive increase in the phosphorylation of IRS-1 by **~2** ± 0.2-, 3 ± 0.2-, and 5 ± 0.5-fold, respectively. Under these conditions, there were no significant changes in the expression levels of IRS-1 and IRS-2 proteins. Thus, high fructose treatment in VSMCs has the potential to dysregulate the phosphorylation state of IRS-1, a key adapter protein in insulin receptor signaling.

High fructose attenuates insulin-induced phosphorylation of Akt, S6 ribosomal protein, and ERK in VSMCs

Previously, we have shown that PDGF-induced IRS-1 serine phosphorylation is associated with diminished insulin-induced PI 3-kinase/Akt signaling in VSMCs (Zhao et al. 2011). In addition, insulin resistance has been shown to suppress PI 3-kinase/Akt signaling with an accompanying activation of ERK signaling in aortic tissues (Jiang et al. 1999). To examine how fructose-induced IRS-1 serine phosphorylation impacts Akt and ERK signaling in VSMCs, we determined the effects of D-fructose pretreatment on acute insulin stimulation. As shown in **Fig. 2.4A**, D-fructose pretreatment at 5.5 mM, 11 mM, and 25 mM concentrations led to progressive decreases in insulin-induced phosphorylation of Akt, S6 ribosomal protein, and ERK1/2. In particular, D-fructose pretreatment at 25 mM concentration resulted in significant diminutions in insulin-induced phosphorylation of Akt, S6, and ERK1/2 by 69 ± 3%, 73 ± 5%, and 50 ± 4%, respectively.

High fructose does not affect PDGF-induced phosphorylation of Akt, S6 ribosomal protein, and ERK in VSMCs

To examine whether high fructose-mediated attenuation of agonist-induced signaling events is specific for insulin, we determined the effects of high fructose on PDGF receptor signaling in parallel. As shown in **Fig. 2.4B**, D-fructose pretreatment at 25 mM concentration did not affect PDGF receptor-β expression and PDGF-induced phosphorylation of key proliferative signaling events such as Akt, S6, and ERK.

High fructose does not affect PDGF-induced cyclin D1 expression in VSMCs

To further confirm whether PDGF-induced signaling events are refractory to high fructose, we examined the changes in cell cycle protein expression. As shown in **Fig. 2.5**, D-fructose pretreatment at 25 mM concentration did not affect PDGF-induced cyclin D1 expression.

Discussion

Previous studies have shown that in rodents fed a 20-40% fructose diet, circulating concentration of fructose increases at a range of 0.2 to 1 mM (Patel et al. 2015). Fructose is known to be transported passively into several tissues including skeletal muscle and adipocytes through plasma membrane-localized fructose transporter (glucose transporter-5, GLUT5) (Douard and Ferraris 2008). The present study provides evidence for fructose uptake in VSMCs for the first time using radiolabeled ^{14}C-fructose. Furthermore, we and several other investigators have demonstrated the expression of GLUT5 mRNA in VSMCs and aortic tissues (Liu et al. 2011; Pyla et al. 2013). In addition to the contribution from GLUT5-mediated fructose uptake, elevation of intracellular fructose concentration can occur through *de novo* synthesis from high glucose. This is achieved through the polyol pathway that involves the activation of aldose reductase (a rate-limiting enzyme) and the intermediary formation of sorbitol (Yasunari et al. 1995; Lanaspa et al. 2013). In this regard, exposure of VSMCs to 25 mM glucose results in the elevation of polyol pathway metabolites including sorbitol and fructose (Liu et al. 2011). Importantly, 25 mM fructose treatment has been shown to enhance intracellular fructose to a similar level with an accompanying induction of GLUT5 mRNA in VSMCs (Liu et al. 2011). The present findings reveal that at 11 to 25 mM concentrations, fructose has

the potential to enhance IRS-1serine phosphorylation in VSMCs, thereby attenuating insulin-induced phosphorylation of downstream signaling components such as Akt and ribosomal protein S6. In addition, high fructose treatment inhibits insulin-induced phosphorylation of ERK. Contrary to our hypothesis, high fructose-mediated disruption of insulin receptor signaling does not affect PDGF-induced key proliferative signaling events as evidenced by sustenance in the phosphorylation state of Akt, S6, and ERK and the expression level of cyclin D1.

Our findings on fructose dysregulation of insulin receptor signaling in VSMCs are in conformity with previous studies, which demonstrate high fructose-induced insulin resistance in hepatic tissue and skeletal muscle (Bezerra et al. 2000; Wei, Wang, and Pagliassotti 2005). For instance, high-fructose diet in rats leads to significant decreases in insulin-induced IRS-1 tyrosine phosphorylation and IRS-1 association with PI 3-kinase in the liver and skeletal muscle (Bezerra et al. 2000). In rat primary hepatocytes treated with high fructose, IRS-1 serine phosphorylation is increased with an accompanying decrease in insulin-induced IRS-1 tyrosine phosphorylation (Wei, Wang, and Pagliassotti 2005). From a mechanistic standpoint, fructose-mediated dysregulation of IRS-1 and the resultant suppression of downstream signaling events may be attributable to several factors including methylglyoxal accumulation and c-jun N-terminal kinase (JNK) activation (Riboulet-Chavey et al. 2006; Liu et al. 2011; Wei, Wang, and Pagliassotti 2005; Dhar et al. 2008). It is noteworthy that, in high-fructose diet-fed rats, a significant accumulation of methylglyoxal has been observed in aortic tissues (Liu et al. 2011). In addition, high fructose treatment (15 to 25 mM) under *in vitro* conditions has been shown to enhance methylglyoxal accumulation in aortic VSMCs (Wang et al. 2006; Liu et al.

2011). Together, these findings suggest that high fructose-mediated accumulation of methylglyoxal may promote IRS-1 serine phosphorylation, thereby disrupting insulin receptor signaling in VSMCs.

Previous studies have shown that in a rat model of obesity, there is a selective resistance to PI 3-kinase/Akt signaling but not ERK pathway in aortic tissues (Jiang et al. 1999). Furthermore, in VSMCs isolated from insulin receptor-deficient mice, a decrease in insulin-induced Akt phosphorylation is associated with an increase in ERK phosphorylation, which may decrease $p27^{Kip1}$ expression to enhance proliferation (Lightell, Moss, and Woods 2011). Such selective insulin resistance in vascular cells would augment the atherogenic potential in insulin-resistant states (Jiang et al. 1999; Gogg, Smith, and Jansson 2009). However, high fructose treatment diminishes insulin-induced activation of Akt, S6 (a downstream target of mTOR), and ERK in VSMCs (present study). Notably, methylglyoxal, an intermediary metabolite of fructose, has been previously shown to inhibit not only IRS-1 tyrosine phosphorylation and Akt signaling but also insulin-induced activation of ERK (Riboulet-Chavey et al. 2006). Thus, high fructose-mediated disruption of insulin receptor signaling including ERK does not result in enhanced VSMC proliferation, as evidenced in the present study.

To further understand the relationship between high fructose exposure and VSMC proliferative phenotype, the present study has also examined whether dysregulated insulin receptor signaling is associated with altered PDGF receptor signaling. Previously, high glucose has been shown to increase aldose reductase activity and fructose formation thereby upregulating PDGF receptor-β expression (Campbell et al. 2003; Kasuya et al. 1999), which in turn results in enhanced PDGF-induced VSMC proliferation. The

present findings reveal that in high fructose-treated VSMCs, PDGF receptor-β expression remains unchanged. In addition, PDGF-induced phosphorylation of key proliferative signaling events (e.g., Akt, S6, and ERK) and the expression of cell cycle protein (e.g., cyclin D1) remain essentially the same with our without high fructose treatment. These findings suggest that, under the conditions of VSMC-specific insulin resistance resulting from high fructose-induced IRS-1 serine phosphorylation, the growth-promoting effects of PDGF will be preserved in the vessel wall.

It is noteworthy that previous observations on insulin resistance and exaggerated neointimal formation in IRS-1-deficient mice have been attributed to altered metabolic milieu (Kubota et al. 2003). High fructose consumption is known to induce metabolic changes in the liver including enhanced *de novo* lipogenesis (Samuel 2011). In addition, high fructose may impair the hepatic clearance of triglyceride-rich lipoproteins (Dekker et al. 2010). Recently, high fructose has been shown to elevate the circulating concentration of proprotein convertase subtilisin/kexin type 9 (PCSK9), which accelerates hepatic LDL receptor degradation to promote hypercholesterolemia (Dong et al. 2015). In conclusion, although high fructose disrupts VSMC-specific insulin receptor signaling, the metabolic abnormalities including dyslipidemia associated with high fructose consumption may play a major role in enhanced atherosclerosis and intimal hyperplasia.

Acknowledgements

This work was supported by the National Heart, Lung, and Blood Institute/National Institutes of Health Grant (R01-HL-097090), University of Georgia Research Foundation Fund, University of Georgia RC Wilson Pharmacy Fund, and University of Georgia College of Pharmacy Graduate Assistantship Award.

Figure legends

Fig. 2.1. Effects of fructose, insulin, *versus* PDGF on VSMC proliferation. Serum-deprived VSMCs were exposed to D-fructose (5.5 or 25 mM), insulin (100 nM) or PDGF (30 ng/ml) for 4 days to determine the changes in cell number using automated counter (**A**) and cyclin D1 expression by immunoblot analysis (**B**). *$p < 0.05$ compared with control; n.s. not significant compared with control. $n = 3$.

FIG. 2.1

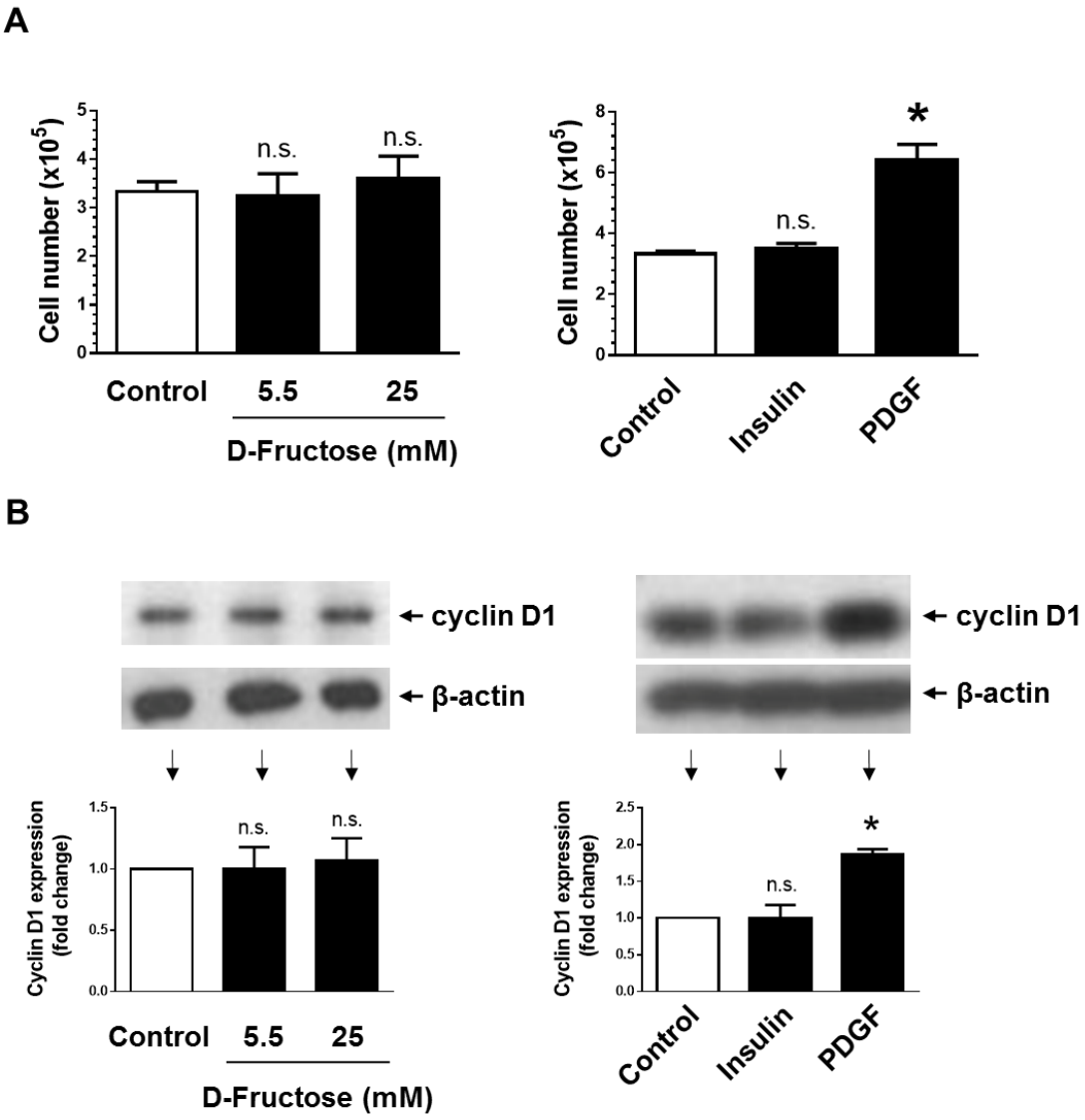
A
Cell number (x10^5)
n.s.
n.s.
Control
5.5
25
D-Fructose (mM)
Cell number (x10^5)
n.s.
*
Control
Insulin
PDGF
B
cyclin D1
β-actin
cyclin D1
β-actin
Cyclin D1 expression (fold change)
n.s.
n.s.
Control
5.5
25
D-Fructose (mM)
Cyclin D1 expression (fold change)
n.s.
*
Control
Insulin
PDGF

Fig. 2.2. Time course of D-fructose uptake in VSMCs. Serum-deprived VSMCs were incubated in Krebs buffer containing 0.5 μCi D-[U-^{14}C] fructose for 2 to 30 min. Cellular uptake of radiolabeled fructose was then determined using liquid scintillation counter. n = 3.

FIG. 2.2

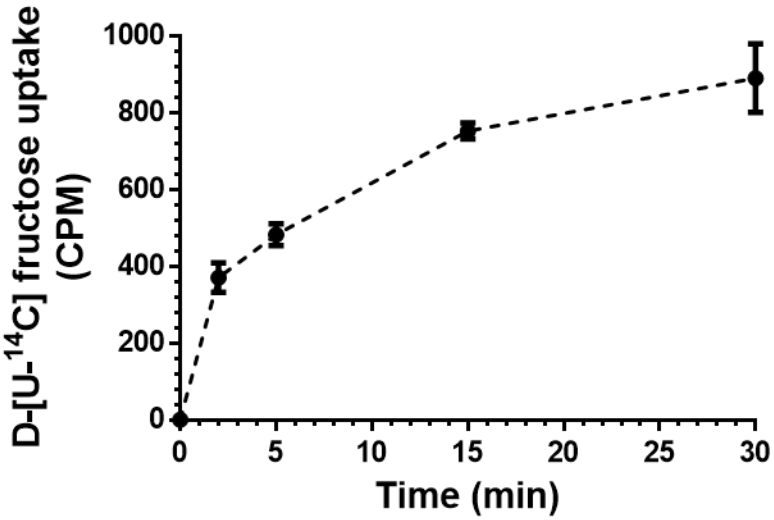
D-[U-14C] fructose uptake (CPM)
1000
800
600
400
200
0
0
5
10
15
20
25
30
Time (min)

Fig. 2.3. Concentration-dependent effects of D-fructose on IRS-1 phosphorylation/expression *versus* IRS-2 expression in VSMCs. Serum-deprived VSMCs were exposed to increasing concentrations of D-fructose for 48 hr. The cell lysates were then subjected to immunoblot analysis using primary antibodies specific for pIRS-1, IRS-1 or IRS-2. *$p < 0.05$ compared with control; n.s. not significant compared with control. $n = 3$.

FIG. 2.3

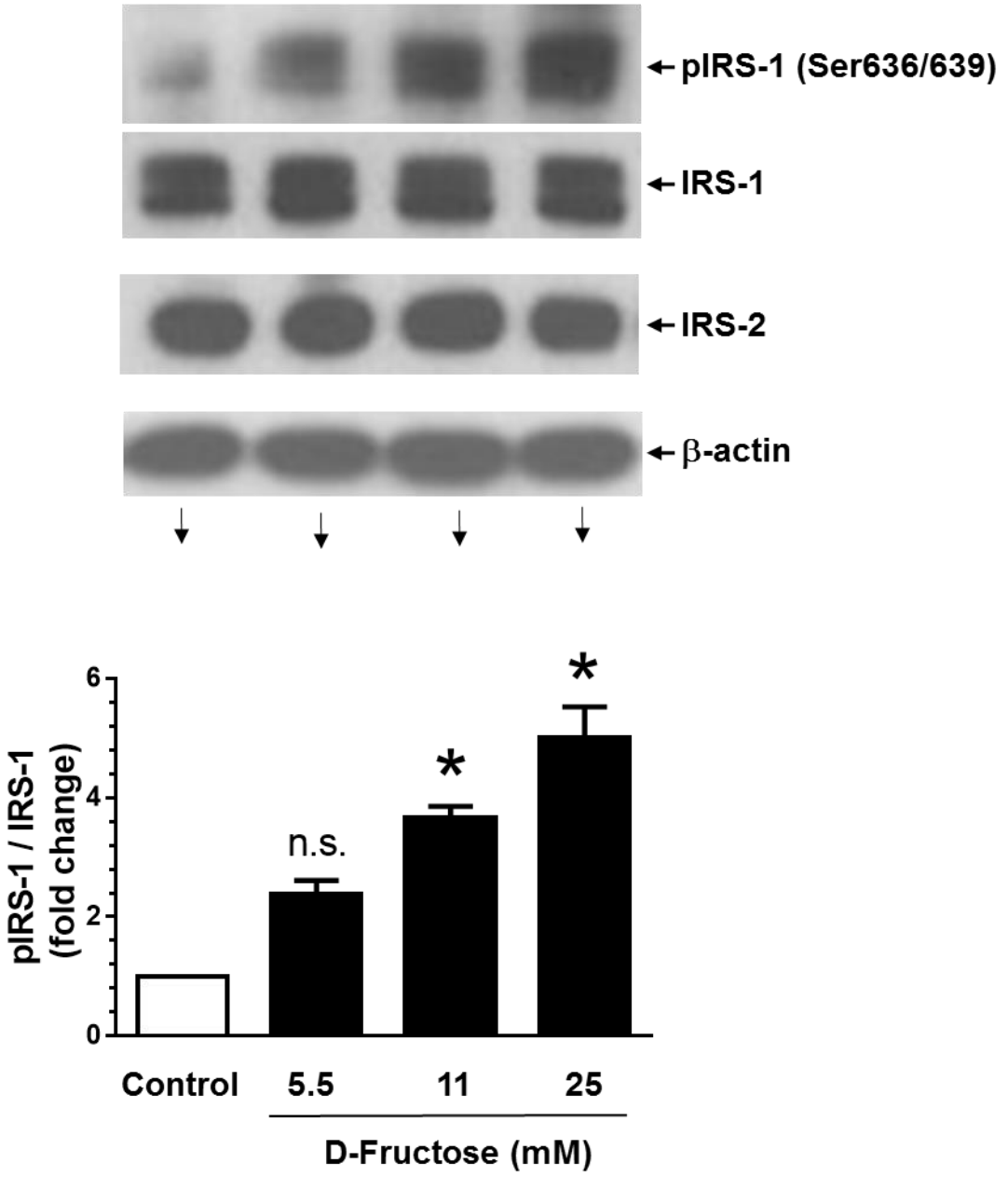
pIRS-1 (Ser636/639)
IRS-1
IRS-2
β-actin
pIRS-1 / IRS-1 (fold change)
0
2
4
6
n.s.
*
*
Control
5.5
11
25
D-Fructose (mM)

Fig. 2.4. Effects of D-fructose pretreatment on insulin- *versus* PDGF-induced phosphorylation of Akt, S6, and ERK in VSMCs. Serum-deprived VSMCs were pretreated with the indicated concentrations of D-fructose for 48 hr followed by acute stimulation with 100 nM insulin (**A**) or 30 ng/ml PDGF (**B**) for 6 min. The cell lysates were then subjected to immunoblot analysis using primary antibodies specific for pAkt, pS6, or pERK1/2. PDGF-treated cells were also probed for PDGFRβ expression. *$p < 0.05$ compared with control; $^{\#}p < 0.05$ compared with insulin alone; n.s. not significant compared with PDGF alone. $n = 3$.

FIG. 2.4A-B

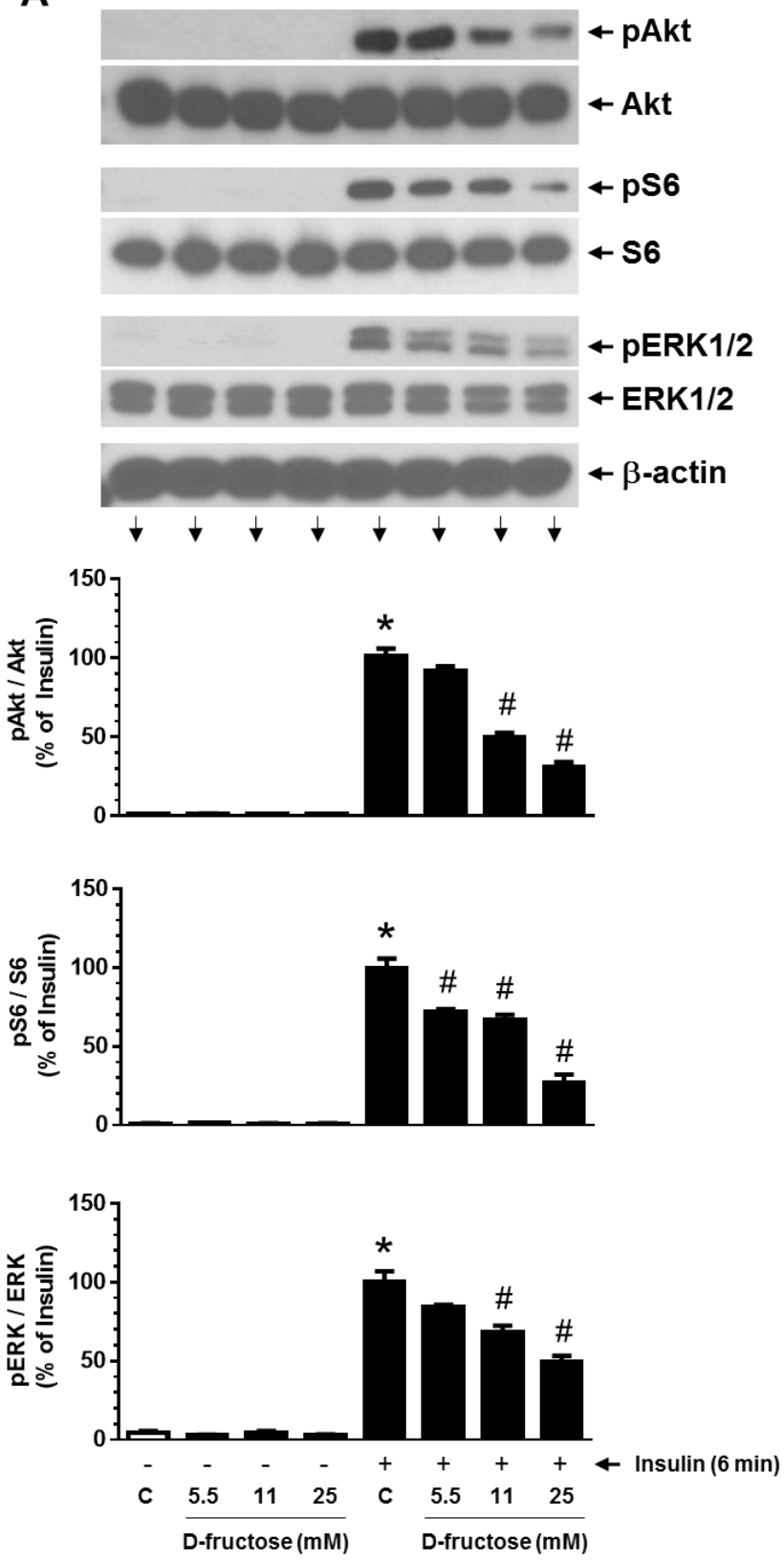
A
pAkt
Akt
pS6
S6
pERK1/2
ERK1/2
β-actin
pAkt / Akt (% of Insulin)
pS6 / S6 (% of Insulin)
pERK / ERK (% of Insulin)
150
100
50
0
*
#
- - - - + + + + Insulin (6 min)
C 5.5 11 25 C 5.5 11 25
D-fructose (mM)
D-fructose (mM)

FIG. 2.4A-B
continued

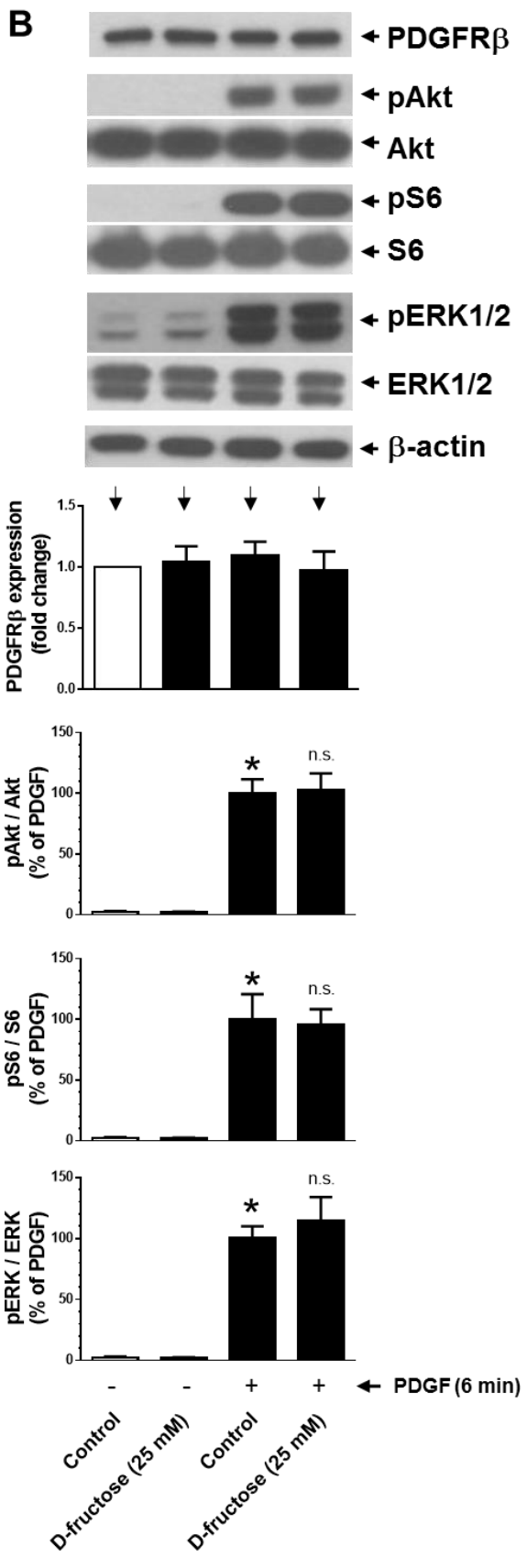

Fig. 2.5. Effects of D-fructose pretreatment on PDGF-induced cell cycle proteins in VSMCs. Serum-deprived VSMCs were pretreated with 25 mM D-fructose for 48 hr followed by exposure to 30 ng/ml PDGF for 48 hr. The cell lysates were then subjected to immunoblot analysis using a primary antibody specific for cyclin D1. *$p < 0.05$ compared with control; n.s. not significant compared with PDGF alone. $n = 3$.

FIG. 2.5

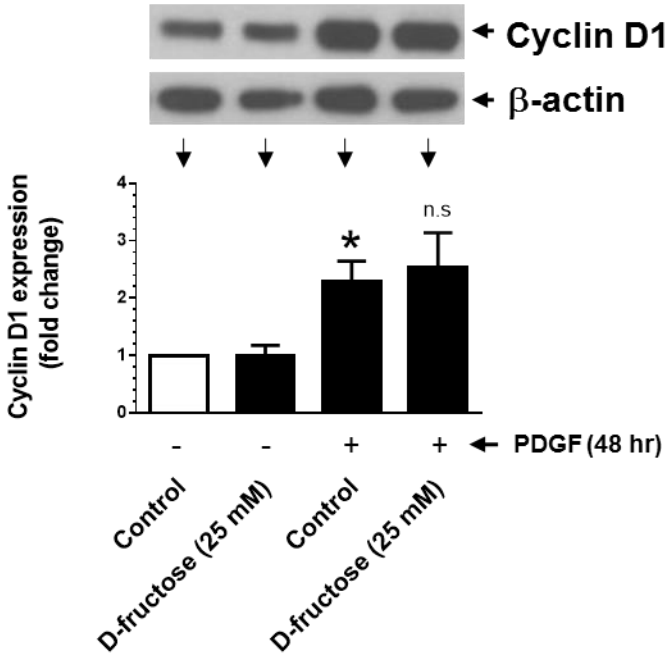
Cyclin D1
β-actin
Cyclin D1 expression (fold change)
0
1
2
3
4
*
n.s
- - + + PDGF (48 hr)
Control
D-fructose (25 mM)
Control
D-fructose (25 mM)

Bibliography

Barrett, T. B., and E. P. Benditt. 1987. sis (platelet-derived growth factor B chain) gene transcript levels are elevated in human atherosclerotic lesions compared to normal artery. *Proc Natl Acad Sci U S A* 84 (4):1099-103.

Bezerra, R. M., M. Ueno, M. S. Silva, D. Q. Tavares, C. R. Carvalho, and M. J. Saad. 2000. A high fructose diet affects the early steps of insulin action in muscle and liver of rats. *J Nutr* 130 (6):1531-5.

Bornfeldt, K. E., and I. Tabas. 2011. Insulin resistance, hyperglycemia, and atherosclerosis. *Cell Metab* 14 (5):575-85.

Buchs, A. E., S. Sasson, H. G. Joost, and E. Cerasi. 1998. Characterization of GLUT5 domains responsible for fructose transport. *Endocrinology* 139 (3):827-31.

Campbell, M., W. E. Allen, J. A. Silversides, and E. R. Trimble. 2003. Glucose-induced phosphatidylinositol 3-kinase and mitogen-activated protein kinase-dependent upregulation of the platelet-derived growth factor-beta receptor potentiates vascular smooth muscle cell chemotaxis. *Diabetes* 52 (2):519-26.

D'Angelo, G., A. A. Elmarakby, D. M. Pollock, and D. W. Stepp. 2005. Fructose feeding increases insulin resistance but not blood pressure in Sprague-Dawley rats. *Hypertension* 46 (4):806-11.

Dekker, M. J., Q. Su, C. Baker, A. C. Rutledge, and K. Adeli. 2010. Fructose: a highly lipogenic nutrient implicated in insulin resistance, hepatic steatosis, and the metabolic syndrome. *Am J Physiol Endocrinol Metab* 299 (5):E685-94.

Dhar, A., K. Desai, M. Kazachmov, P. Yu, and L. Wu. 2008. Methylglyoxal production in vascular smooth muscle cells from different metabolic precursors. *Metabolism* 57 (9):1211-20.

Dong, B., A. B. Singh, S. Azhar, N. G. Seidah, and J. Liu. 2015. High-fructose feeding promotes accelerated degradation of hepatic LDL receptor and hypercholesterolemia in hamsters via elevated circulating PCSK9 levels. *Atherosclerosis* 239 (2):364-74.

Douard, V., and R. P. Ferraris. 2008. Regulation of the fructose transporter GLUT5 in health and disease. *Am J Physiol Endocrinol Metab* 295 (2):E227-37.

Fukuzawa, T., M. Fukazawa, O. Ueda, H. Shimada, A. Kito, M. Kakefuda, Y. Kawase, N. A. Wada, C. Goto, N. Fukushima, K. Jishage, K. Honda, G. L. King, and Y. Kawabe. 2013. SGLT5 reabsorbs fructose in the kidney but its deficiency paradoxically exacerbates hepatic steatosis induced by fructose. *PLoS One* 8 (2):e56681.

Gogg, S., U. Smith, and P. A. Jansson. 2009. Increased MAPK activation and impaired insulin signaling in subcutaneous microvascular endothelial cells in type 2 diabetes: the role of endothelin-1. *Diabetes* 58 (10):2238-45.

Hajduch, E., F. Darakhshan, and H. S. Hundal. 1998. Fructose uptake in rat adipocytes: GLUT5 expression and the effects of streptozotocin-induced diabetes. *Diabetologia* 41 (7):821-8.

Hajduch, E., G. J. Litherland, S. Turban, E. Brot-Laroche, and H. S. Hundal. 2003. Insulin regulates the expression of the GLUT5 transporter in L6 skeletal muscle cells. *FEBS Lett* 549 (1-3):77-82.

Heldin, C. H., and B. Westermark. 1999. Mechanism of action and in vivo role of platelet-derived growth factor. *Physiol Rev* 79 (4):1283-316.

Jiang, Z. Y., Y. W. Lin, A. Clemont, E. P. Feener, K. D. Hein, M. Igarashi, T. Yamauchi, M. F. White, and G. L. King. 1999. Characterization of selective resistance to insulin signaling in the vasculature of obese Zucker (fa/fa) rats. *J Clin Invest* 104 (4):447-57.

Kasuya, Y., J. Nakamura, Y. Hamada, M. Nakayama, H. Sasaki, T. Komori, S. Chaya, G. Watanabe, K. Naruse, E. Nakashima, K. Kato, and N. Hotta. 1999. An aldose reductase inhibitor prevents the glucose-induced increase in PDGF-beta receptor in cultured rat aortic smooth muscle cells. *Biochem Biophys Res Commun* 261 (3):853-8.

Kubota, T., N. Kubota, M. Moroi, Y. Terauchi, T. Kobayashi, K. Kamata, R. Suzuki, K. Tobe, A. Namiki, S. Aizawa, R. Nagai, T. Kadowaki, and T. Yamaguchi. 2003. Lack of insulin receptor substrate-2 causes progressive neointima formation in response to vessel injury. *Circulation* 107 (24):3073-80.

Lanaspa, M. A., T. Ishimoto, N. Li, C. Cicerchi, D. J. Orlicky, P. Ruzycki, C. Rivard, S. Inaba, C. A. Roncal-Jimenez, E. S. Bales, C. P. Diggle, A. Asipu, J. M. Petrash, T. Kosugi, S. Maruyama, L. G. Sanchez-Lozada, J. L. McManaman, D. T. Bonthron, Y. Y. Sautin, and R. J. Johnson. 2013. Endogenous fructose production and metabolism in the liver contributes to the development of metabolic syndrome. *Nat Commun* 4:2434.

Lightell, D. J., Jr., S. C. Moss, and T. C. Woods. 2011. Loss of canonical insulin signaling accelerates vascular smooth muscle cell proliferation and migration through changes in p27Kip1 regulation. *Endocrinology* 152 (2):651-8.

Liu, J., R. Wang, K. Desai, and L. Wu. 2011. Upregulation of aldolase B and overproduction of methylglyoxal in vascular tissues from rats with metabolic syndrome. *Cardiovasc Res* 92 (3):494-503.

Lu, J., J. Ji, H. Meng, D. Wang, B. Jiang, L. Liu, E. Randell, K. Adeli, and Q. H. Meng. 2013. The protective effect and underlying mechanism of metformin on neointima formation in fructose-induced insulin resistant rats. *Cardiovasc Diabetol* 12:58.

Martinez-Hervas, S., A. Vinue, L. Nunez, I. Andres-Blasco, L. Piqueras, J. T. Real, J. F. Ascaso, D. J. Burks, M. J. Sanz, and H. Gonzalez-Navarro. 2014. Insulin resistance aggravates atherosclerosis by reducing vascular smooth muscle cell survival and increasing CX3CL1/CX3CR1 axis. *Cardiovasc Res* 103 (2):324-36.

Miatello, R., N. Risler, C. Castro, S. Gonzalez, M. Ruttler, and M. Cruzado. 2001. Aortic smooth muscle cell proliferation and endothelial nitric oxide synthase activity in fructose-fed rats. *Am J Hypertens* 14 (11 Pt 1):1135-41.

Ning, B., X. Wang, Y. Yu, A. B. Waqar, Q. Yu, T. Koike, M. Shiomi, E. Liu, Y. Wang, and J. Fan. 2015. High-fructose and high-fat diet-induced insulin resistance enhances atherosclerosis in Watanabe heritable hyperlipidemic rabbits. *Nutr Metab (Lond)* 12:30.

Osman, I., and L. Segar. 2016. Pioglitazone, a PPARgamma agonist, attenuates PDGF-induced vascular smooth muscle cell proliferation through AMPK-dependent and

AMPK-independent inhibition of mTOR/p70S6K and ERK signaling. *Biochem Pharmacol* 101:54-70.

Owens, G. K., M. S. Kumar, and B. R. Wamhoff. 2004. Molecular regulation of vascular smooth muscle cell differentiation in development and disease. *Physiol Rev* 84 (3):767-801.

Patel, C., K. Sugimoto, V. Douard, A. Shah, H. Inui, T. Yamanouchi, and R. P. Ferraris. 2015. Effect of dietary fructose on portal and systemic serum fructose levels in rats and in KHK-/- and GLUT5-/- mice. *Am J Physiol Gastrointest Liver Physiol* 309 (9):G779-90.

Pfeifle, B., and H. Ditschuneit. 1981. Effect of insulin on growth of cultured human arterial smooth muscle cells. *Diabetologia* 20 (2):155-8.

Pyla, R., N. Poulose, J. Y. Jun, and L. Segar. 2013. Expression of conventional and novel glucose transporters, GLUT1, -9, -10, and -12, in vascular smooth muscle cells. *Am J Physiol Cell Physiol* 304 (6):C574-89.

Riboulet-Chavey, A., A. Pierron, I. Durand, J. Murdaca, J. Giudicelli, and E. Van Obberghen. 2006. Methylglyoxal impairs the insulin signaling pathways independently of the formation of intracellular reactive oxygen species. *Diabetes* 55 (5):1289-99.

Rubin, K., A. Tingstrom, G. K. Hansson, E. Larsson, L. Ronnstrand, L. Klareskog, L. Claesson-Welsh, C. H. Heldin, B. Fellstrom, and L. Terracio. 1988. Induction of B-type receptors for platelet-derived growth factor in vascular inflammation: possible implications for development of vascular proliferative lesions. *Lancet* 1 (8599):1353-6.

Samuel, V. T. 2011. Fructose induced lipogenesis: from sugar to fat to insulin resistance. *Trends Endocrinol Metab* 22 (2):60-5.

Semenkovich, C. F. 2006. Insulin resistance and atherosclerosis. *J Clin Invest* 116 (7):1813-22.

Taegtmeyer, H. 1996. Insulin resistance and atherosclerosis. Common roots for two common diseases? *Circulation* 93 (10):1777-9.

Wang, C. C., I. Gurevich, and B. Draznin. 2003. Insulin affects vascular smooth muscle cell phenotype and migration via distinct signaling pathways. *Diabetes* 52 (10):2562-9.

Wang, H., Q. H. Meng, T. Chang, and L. Wu. 2006. Fructose-induced peroxynitrite production is mediated by methylglyoxal in vascular smooth muscle cells. *Life Sci* 79 (26):2448-54.

Wei, Y., D. Wang, and M. J. Pagliassotti. 2005. Fructose selectively modulates c-jun N-terminal kinase activity and insulin signaling in rat primary hepatocytes. *J Nutr* 135 (7):1642-6.

Yasunari, K., M. Kohno, H. Kano, K. Yokokawa, T. Horio, and J. Yoshikawa. 1995. Aldose reductase inhibitor prevents hyperproliferation and hypertrophy of cultured rat vascular smooth muscle cells induced by high glucose. *Arterioscler Thromb Vasc Biol* 15 (12):2207-12.

Zhao, Y., S. K. Biswas, P. H. McNulty, M. Kozak, J. Y. Jun, and L. Segar. 2011. PDGF-induced vascular smooth muscle cell proliferation is associated with dysregulation of insulin receptor substrates. *Am J Physiol Cell Physiol* 300 (6):C1375-85.

CHAPTER 3

PIOGLITAZONE, A PPARγ AGONIST, ATTENUATES PDGF-INDUCED VASCULAR SMOOTH MUSCLE CELL PROLIFERATION THROUGH AMPK-DEPENDENT AND AMPK-INDEPENDENT INHIBITION OF mTOR/p70S6K AND ERK SIGNALING (Osman and Segar, 2016)

Islam Osman and Lakshman Segar. 2016, Biochemical Pharmacology, 101:54-70,

Reprinted here with permission of the publisher

Pioglitazone, a PPARγ agonist, attenuates PDGF-induced vascular smooth muscle cell proliferation through AMPK-dependent and AMPK-independent inhibition of mTOR/p70S6K and ERK signaling

Islam Osman [a,b] and Lakshman Segar [a,b,c,d,*]

[a]*Center for Pharmacy and Experimental Therapeutics, University of Georgia College of Pharmacy, Augusta, Georgia, USA*

[b]*Charlie Norwood VA Medical Center, Augusta, Georgia, USA*

[c]*Vascular Biology Center, Department of Pharmacology and Toxicology, Georgia Regents University, Augusta, Georgia, USA*

[d]*Department of Medicine, Pennsylvania State University College of Medicine, Hershey, Pennsylvania, USA*

*** Corresponding author:**

Lakshman Segar, Center for Pharmacy and Experimental Therapeutics,

University of Georgia College of Pharmacy, 1120 15th Street, HM-1200

Georgia Regents University Campus, Augusta, Georgia, USA 30912-2450

Tel.: +1 706 721 6491; fax: +1 706 721 3994*; E-mail address:* lsegar@gru.edu (L. Segar).

Abstract

Pioglitazone (PIO), a PPARγ agonist that improves glycemic control in type 2 diabetes through its insulin-sensitizing action, has been shown to exhibit beneficial effects in the vessel wall. For instance, it inhibits vascular smooth muscle cell (VSMC) proliferation, a major event in atherosclerosis and restenosis after angioplasty. Although PPARγ-dependent and PPARγ-independent mechanisms have been attributed to its vasoprotective effects, the signaling events associated with PIO action in VSMCs are not fully understood. To date, the likely intermediary role of AMP-activated protein kinase (AMPK) toward PIO inhibition of VSMC proliferation has not been examined. Using human aortic VSMCs, the present study demonstrates that PIO activates AMPK in a sustained manner thereby contributing in part to inhibition of key proliferative signaling events. In particular, PIO at 30 μM concentration activates AMPK to induce raptor phosphorylation, which diminishes PDGF-induced mTOR activity as evidenced by decreased phosphorylation of p70S6K, 4E-BP1, and S6 and increased accumulation of $p27^{kip1}$, a cell cycle inhibitor. In addition, PIO inhibits the basal phosphorylation of ERK in VSMCs. Downregulation of endogenous AMPK by target-specific siRNA reveals an AMPK-independent effect for PIO inhibition of ERK, which contributes in part to diminutions in cyclin D1 expression and Rb phosphorylation and the suppression of VSMC proliferation. Furthermore, AMPK-dependent inhibition of mTOR/p70S6K and AMPK-independent inhibition of ERK signaling occur regardless of PPARγ expression/activation in VSMCs as evidenced by gene silencing and pharmacological inhibition of PPARγ. Strategies that utilize nanoparticle-mediated PIO delivery at the

lesion site may limit restenosis after angioplasty without inducing PPARγ-mediated systemic adverse effects.

Keywords: vascular smooth muscle cells; pioglitazone; AMPK; p70S6K; ERK

Introduction

Vascular smooth muscle cell (VSMC) proliferation is a major event in the development of atherosclerosis and restenosis after angioplasty (Ross 1999; Owens, Kumar, and Wamhoff 2004). Thiazolidinediones (TZDs) have been shown to exhibit beneficial effects in the vessel wall (Yoshimoto et al. 1999; Phillips et al. 2003; Satoh et al. 2003) beyond their insulin-sensitizing action that improves glycemic control in patients with type 2 diabetes (Kahn et al. 2006). Yet, TZD treatment is associated with several adverse effects, including weight gain, fluid retention, and congestive heart failure, thus raising concerns about their cardiovascular safety (Nesto et al. 2003). These unfavorable effects are attributed in part to activation of peroxisome proliferator-activated receptor-γ (PPARγ). For instance, TZD activation of PPARγ in the renal collecting duct stimulates epithelial sodium channel transcription to promote sodium absorption and fluid accumulation (Guan et al. 2005; Zhang et al. 2005). Notably, PPARγ is also expressed in VSMCs but to a modest extent (Staels et al. 1998; Law et al. 2000; Benson et al. 2000; Benkirane et al. 2006), compared with its abundant expression level in adipose tissue (Staels et al. 1998). Although previous studies have reported PPARγ-dependent and PPARγ-independent mechanisms for TZD inhibition of VSMC proliferation (Peuler et al. 1996; Law et al. 1996; Wakino et al. 2000; de Dios et al. 2003;

Lee et al. 2009; Subramanian et al. 2010; Zhang et al. 2011), the signaling events associated with TZD action in VSMCs are not fully understood.

TZDs such as rosiglitazone (ROSI) and pioglitazone (PIO) are currently in clinical use but are prescribed with caution due to the risk of congestive heart failure (Kaul et al. 2010; Inzucchi et al. 2012). Troglitazone (TRO) has been withdrawn from the market due to hepatotoxicity (Kaul et al. 2010). While commonly being referred to as PPARγ agonists, PPARγ binding affinity for ROSI is several folds greater than PIO or TRO (Young et al. 1998). Despite their differences in PPARγ binding affinities, all three TZDs exhibit comparable inhibitory effects on VSMC proliferation (Law et al. 2000; de Dios et al. 2003) by affecting cell cycle regulatory events critical for G1→S progression (Wakino et al. 2000; de Dios et al. 2003). The key proliferative signaling components in VSMCs include MEK1/ERK and mTOR/p70S6K that undergo activation upon challenge with mitogens including platelet-derived growth factor (PDGF) or angiotensin II (Braun-Dullaeus et al. 2001; Nagata et al. 2004; Zhao et al. 2011). In this regard, TZDs have been shown to inhibit mitogen-induced activation of ERK signaling in VSMCs (Benkirane et al. 2006; Law et al. 1996; Goetze et al. 1999; Lee et al. 2009). Importantly, TZD treatment results in the activation of AMP-activated protein kinase (AMPK) in insulin-responsive tissues/cells (Fryer, Parbu-Patel, and Carling 2002; Saha et al. 2004; Konrad et al. 2005; Coletta et al. 2009) and endothelial cells (Boyle et al. 2008), but such effect has not yet been reported in VSMCs. AMPK activation in VSMCs (e.g., by AICAR or adipokines) is associated with inhibition of ERK activation (Nagata et al. 2004; Motobayashi et al. 2009; Uemura et al. 2015). In addition, AMPK activation leads to inhibition of mTOR/p70S6K signaling in different tissues/cell types (Inoki, Kim, and

Guan 2012; Saha et al. 2010), including VSMCs (Kim et al. 2014). Notably, AMPK activation in nonvascular cells promotes raptor phosphorylation to inhibit the activity of mTOR (Gwinn et al. 2008). Hence, it is critically important to examine the likely intermediary role of AMPK toward TZD suppression of key proliferative signaling events in VSMCs.

In skeletal muscle cells and hepatocytes, TZD activation of AMPK has been shown to involve mitochondrial membrane depolarization, a decrease in cellular ATP level, an increase in AMP that binds to AMPKγ subunit to facilitate allosteric activation, and enhanced phosphorylation of Thr^{172} residue in AMPKα unit by LKB1, an upstream kinase for AMPK (Konrad et al. 2005; Fryer, Parbu-Patel, and Carling 2002; Kahn et al. 2005). In addition, AMPK activation leads to phosphorylation and inactivation of acetyl-CoA carboxylase (ACC), a key downstream target of AMPK (Kahn et al. 2005). Nevertheless, it remains unknown as to whether TZD affects cellular energy state to promote AMPK activation in VSMCs.

The objectives of the present study using human aortic VSMCs are to determine: i) the extent to which PIO regulates the phosphorylation $AMPK\alpha^{Thr172}$ and its downstream target, ACC; ii) PIO regulation of cellular energy state including mitochondrial membrane potential (by TMRM fluorescence analysis) and AMP/ATP ratio (by LC-MS/MS MRM analysis); iii) the role of LKB1 as a likely upstream kinase; iv) the extent to which PIO activation of AMPK regulates PDGF-induced key proliferative signaling events including mTOR/p70S6K and ERK; and v) whether PIO regulation of key proliferative signaling is dependent on PPARγ expression.

Materials and methods

Materials

Pioglitazone, rosiglitazone, and GW-9622 were purchased from Cayman Chemical Company (Ann Arbor, MI). Recombinant human PDGF-BB was purchased from R&D Systems (Minneapolis, MN). The primary antibodies for phospho-AMPKα^{Thr172} (2535), pan-AMPKα (2532), AMPKα1 (2795), AMPKα2 (2757), phospho-ACC^{Ser79} (11818), ACC (3676), phospho-LKB1^{Ser428} (3482), LKB1 (3047), phospho-44/42 MAPK (ERK1/2; 4695), 44/42 MAPK (ERK1/2; 9102), phospho-Akt^{Thr308} (2965), Akt (4691), phospho-GSK3β^{Ser9} (9323), GSK3β (12456), phospho-p70S6K^{Thr389} (9234), p70S6K (2708), phsopho-4E-BP1^{Ser65} (9451), 4E-BP1 (9644), phospho-S6 ribosomal protein$^{Ser235/236}$ (4857), S6 ribosomal protein (2217), phospho-Raptor^{Ser792} (2083), Raptor (2280), PPARγ (2435), p27^{Kip1} (3686), cyclin D1 (2922), phospho-Rb^{Ser795} (9301), phospho-p53^{Ser15} (9286), p53 (2524), p21^{Cip1} (2947), CD36 (14347), and β-actin (8457) were purchased from Cell Signaling Technology (Danvers, MA). The primary antibody for SM α-actin (ab5694) was purchased from Abcam (Cambridge, MA). The primary antibody for calponin (C2687) was purchased from Sigma Chemical (St. Louis, MO). LKB1, AMPKα1, AMPKα2, PPARγ silencer select siRNAs and scrambled siRNA were purchased from Life Technologies (Carlsbad, CA). Adenosine 5'-triphosphate disodium (ATP), adenosine 5'-diphosphate monosodium (ADP), and adenosine 5'-monophosphate disodium (AMP) were purchased from EMD Millipore Chemicals (Billerica, MA). All other chemicals were from Fisher Scientific (Fair Lawn, NJ) or Sigma Chemical (St. Louis, MO).

Cell culture and treatments

Human aortic VSMCs, vascular cell basal medium and smooth muscle growth supplement (SMGS) were purchased from ATCC (Manassas, VA). SMGS constituents and their final concentrations after addition to vascular cell basal medium were as follows: 5% FBS (vol/vol), 5 ng/ml human basic fibroblast growth factor, 5 ng/ml human epidermal growth factor, 5 μg/ml insulin, 50 μg/mL ascorbic acid, 10 mM L-Glutamine. VSMCs (passages 3–5) were incubated in vascular cell basal medium containing SMGS (complete medium) and 5.5 mM D-glucose along with antibiotic/antimycotic solution in a humidified atmosphere of 95% air and 5% CO_2 at 37°C. After the attainment of confluence (~6–7 days), VSMCs were trypsinized, centrifuged, and seeded onto Petri dishes or multiwell plates. Subconfluent VSMCs were maintained under SMGS (serum)-deprived conditions for 48 hours to achieve quiescence and then subjected to treatments as described in the legends to the respective figures. DMSO (0.1%) was used as the vehicle control for PIO or ROSI treatment.

Cell counts

Subconfluent VSMCs were serum-deprived for 48 hr and then pretreated with PIO (3, 10 or 30 μM, 30 min) or vehicle control followed by exposure to PDGF (30 ng/ml, 96 hr). We replaced the medium with fresh serum-free medium containing the indicated concentrations of PIO and/or PDGF every 48 hr. VSMCs were then trypsinized and the changes in cell number were determined using Countess Counter (Life Technologies), as described (Pyla et al. 2013).

DNA synthesis assay

Serum-deprived VSMCs were treated with PIO (30 μM) or vehicle control for 24 hr and then exposed to PDGF (30 ng/ml) for another 24 hr. DNA synthesis was measured using click iT® EdU microplate assay according to the manufacturer's instructions (Life technologies). In brief, VSMCs were incubated with 5-ethynyl-2'-deoxyuridine (EdU; a nucleoside analog) during the last 18 hr of respective treatments. Subsequently, cells were exposed to the supplied fixative reagent followed by labeling of EdU with green-fluorescent Oregon Green® azide. Signal amplification was then achieved by incubation with HRP-conjugated anti-Oregon Green® antibody followed by reaction with Amplex® UltraRed substrate that produces a brightly red fluorescent product (excitation/emission: 568/585 nm).

Immunoblot analysis

VSMC lysates (20 μg protein per lane) were subjected to electrophoresis using precast 4–12% NuPage mini-gels (Life Technologies). The resolved proteins were then transferred to PVDF membranes (EMD Millipore). Subsequently, the membranes were blocked in 5% nonfat milk and probed with the respective primary antibodies. The immunoreactivity was detected using HRP-conjugated horse anti-mouse secondary antibody (7076; Cell Signaling) or goat anti-rabbit secondary antibody (7074; Cell Signaling) followed by enhanced chemiluminescence (ECL; Thermo Scientific, Wilmington, DE). Immunoblots for ECL detection of a given protein target and its phosphorylated form were run in parallel. β-actin was used as an internal control. The displayed β-actin in the respective figures is representative of β-actin immunoreactivity

for all blots. The protein bands shown in respective figures represent the results obtained from at least three separate independent experiments. The protein bands were quantified using Image J.

Assessment of mitochondrial membrane potential

Mitochondrial membrane potential ($\Delta\psi$) was determined using a MitoPT TMRM assay kit according to manufacturer's instructions (ImmunoChemistry Technologies, Bloomington, MN). Briefly, serum-deprived VSMCs were exposed to PIO (30 μM) for 1 or 3 hr, or vehicle control. Subsequently, VSMCs were stained with tetramethylrhodamine methyl ester (TMRM, 200 nM, 20 min at 37°C in the dark), washed with 1 ml wash buffer, and then visualized by fluorescence microscopy (Zeiss, Thornwood, NY). In intact cells, the cationic nature of TMRM allows it to accumulate within the inner membrane region of polarized mitochondria, resulting in a marked increase in TMRM-associated orange fluorescence. When mitochondrial membrane depolarizes, TMRM gets dispersed throughout the cytosol at a concentration that yields minimal fluorescence upon excitation. Thus, mitochondrial membrane potential was assessed by examination of TMRM-associated orange fluorescence (Excitation/Emission: 548 nm/573 nm). Carbonylcyanide m-chlorophenylhydrazone (CCCP, 50 μM, 1 hr) a generic mitochondrial membrane depolarizer, was used as a positive control.

Quantification of adenine nucleotides (ATP, ADP, and AMP) using LC-MS/MS MRM

Quantification of adenine nucleotides in VSMCs was done as previously described (Pyla et al. 2014). Briefly, serum-deprived VSMCs were exposed to PIO (30 μM, 3hr) or

vehicle control. VSMCs were collected in ice-cold PBS, lysed in ice-cold 5% perchloric acid, and then centrifuged at 10,000 x g for 5 min at 4°C to remove the acid-insoluble material. The perchloric acid in the collected supernatant was extracted by three washes with 10% excess volume of a 1:1 mixture of tri-n-octylamine and 1,1,2-trichlorotrifluroethane. Adenine nucleotides in the aqueous phase were analyzed using liquid chromatography/tandem mass spectrometry (LC-MS/MS) with multiple reaction monitoring (MRM) on a 4000 QTRAP LC/MS/MS system (Applied Biosystems, Carlsbad, CA). The samples and standards were run on a Amide XBridge HPLC column (Cat # 186004860; 3.5 µM particle size; 2.1 mm inner diameter x 100 mm length, Waters, Milford, MA) using buffer A (20 mM ammonium hydroxide and 20 mM ammonium acetate in 5% acetonitrile, pH 9.0) and buffer B (100% acetonitrile) at a flow rate of 0.3 ml/min for 10 min. The mobile phase consists of isocratic elution with 20% buffer B. The concentrations of AMP, ADP and ATP were calculated from standard curves of a serial dilution of a standard consisting of known concentrations of AMP, ADP, and ATP that were run in parallel with the samples in the same session.

Nucleofection of VSMCs with target-specific siRNAs

Subconfluent VSMCs were transfected with 500 pmoles of target-specific Silencer® Select Pre-Designed siRNA (Life technologies, Carlsbad, CA) using the Amaxa nucleofector-II device U-025 program (Lonza, Germany). The scrambled siRNA- and target-specific siRNA-transfected VSMCs were incubated in complete medium for 48 hr. Subsequently, VSMCs were serum-deprived for 24 hr and then subjected to treatments as described in the legends to the respective figures.

Nascent protein synthesis assay

Serum-deprived VSMCs were exposed to PIO (30 μM) or vehicle control for 24 hr in the absence or presence of PDGF (30 ng/ml). Nascent protein synthesis was determined using click-iT® Plus OPP Alexa Fluor® 488 protein synthesis assay kit according to the manufacturers' instructions (Life Technologies). Briefly, VSMCs were incubated with 20 μM Click-iT® OPP working solution for 30 min, fixed with 4% paraformaldehyde in PBS, permeabilized with 0.5% Triton X-100 in PBS. VSMCs were then incubated with Click-iT® Plus OPP reaction cocktail for 30 min at room temperature, protected from light, and incubated with NuclearMask™ Blue Stain to label nuclei. Nascent protein synthesis was assessed by determination of signal intensity in the green fluorescent channel as determined by confocal microscopy (Zeiss, Thornwood, NY).

RNA extraction, cDNA synthesis and real-time quantitative RT-PCR (qRT-PCR)

RNA extraction, cDNA synthesis, and qRT-PCR were performed as previously described (Pyla et al. 2013). Briefly, total RNA was extracted from VSMCs by RNeasy mini-kit (Qiagen, Valencia, CA) and then treated with RNase-free DNase I (Qiagen) to remove contamination due to genomic DNA. RNA quantification and purity assessment were performed spectroscopically using NanoDrop 2000 spectrophotometer (Thermo Scientific). 500 ng of total RNA was reverse transcribed to cDNA by Superscript First Strand RT-PCR system (Life Technologies) using oligo(dT) primers. qRT-PCR analysis was performed using Applied Biosystems 7900HT Fast Real-Time PCR system and QuantiTect SYBR Green PCR kit (Qiagen). Relative mRNA expression values were determined by the comparative threshold cycle (C_T) method. C_T values were normalized

with internal control gene β2 microglobulin (β2M). Cyclin D1 primer sequences were as follows: Forward primer (5'-TGTCCTACTACCGCCTCACA-3') and reverse primer (5'-TCCTCCTCTTCCTCCTCCTC-3'). β2M primer sequences were as follows: Forward primer (5'-TGGTCTTTCTGGTGCTTGTCT-3') and reverse primer (5'-TATGTTCGGCTTCCCATTCT-3').

Nuclear and cytoplasmic protein extraction

Nuclear and cytoplasmic protein fractions were obtained using a nuclear and cytoplasmic extraction kit according to manufacturer's instructions (Thermo Scientific). Briefly, serum-deprived VSMCs were exposed to PIO (30 μM) or vehicle control for 48 hr. Cells were harvested with trypsin-EDTA and then centrifuged at 500 × g for 5 min. The cell pellet was washed with ice-cold PBS. Subsequently, ice-cold cytoplasmic extraction reagents (CER I and CER II) were mixed with protease/phosphatase inhibitor cocktail (Thermo Scientific) and added to the cell pellet to cause cell membrane disruption and the release of cytoplasmic contents. After recovering the nuclear pellet from the cytoplasmic extract by centrifugation (16,000 × g for 5 min), the nuclear proteins were extracted with the nuclear extraction reagent (NER) plus protease/phosphatase inhibitor cocktail.

Statistical analysis

Results are expressed as the means ± SEM of at least three separate experiments. Statistical analyses of the data were performed using one-way analysis of variance (ANOVA) followed by Bonferroni t-test for data involving more than two groups, or

unpaired two-tailed t-test for data involving two groups only. Values of $p < 0.05$ were considered statistically significant.

Results

PIO inhibits PDGF-induced VSMC proliferation

Previous studies have shown that TZDs suppress mitogen-induced VSMC proliferation (Peuler et al. 1996; Law et al. 1996; Wakino et al. 2000; Igarashi et al. 2001; de Dios et al. 2003), by affecting the cell cycle regulatory events critical for G1→S progression (Wakino et al. 2000; de Dios et al. 2003). In the present study, we examined the effects of PIO on PDGF-induced VSMC proliferation, DNA synthesis, and the associated changes in cell cycle proteins. Prior to treatments, VSMCs were maintained under serum-deprived conditions to promote the transition to a contractile phenotype. As shown in **Fig. 3.1A**, serum deprivation led to an increase in the expression of SM α-actin and calponin by ~7 ± 0.3- and 6 ± 0.2-fold, respectively. **Fig. 3.1B** shows that PIO treatment, by itself, did not affect basal VSMC proliferation at 3 to 30 μM concentrations. However, it diminished PDGF-induced VSMC proliferation by 18 ± 10% ($p = 0.9$), 42 ± 14% ($p = 0.4$), and 84 ± 6% ($p < 0.05$) at 3, 10, and 30 μM concentrations, respectively. In addition, PIO at 30 μM concentration did not affect basal DNA synthesis but significantly decreased PDGF-induced DNA synthesis by 96 ± 3% ($p < 0.05$) (**Fig. 3.1C**). Together, PIO treatment shows a trend toward a decrease in PDGF-induced VSMC proliferation at 10 μM concentration with a more pronounced inhibition at 30 μM concentration.

Furthermore, PIO treatment led to significant inhibition of PDGF-induced increase in cyclin D1 expression by 32 ± 10% ($p < 0.05$) and 97 ± 8% ($p < 0.05$) at 10 and 30 μM concentrations, respectively (**Fig. 3.1D**). It also inhibited PDGF-induced increase in Rb phosphorylation by 42 ± 4% ($p < 0.05$) and 93 ± 11% ($p < 0.05$) at 10 and 30 μM concentrations, respectively. Importantly, PIO, by itself, enhanced the accumulation of $p27^{Kip1}$ (a cell cycle inhibitor) (Tanner et al. 2000) by 35 ± 7% ($p < 0.05$) and 43 ± 9% ($p < 0.05$) at 10 μM and 30 μM concentrations, respectively. In addition, PIO prevented PDGF-induced degradation of $p27^{Kip1}$ by ~83 ± 13%. At all three concentrations used in this study, PIO did not affect the viability of VSMCs as determined by trypan blue exclusion test.

Since TRO and ROSI have previously been shown to attenuate mitogen-induced $p21^{Cip1}$ expression in VSMCs (Wakino et al. 2000), we examined the effects of PIO on $p21^{Cip1}$ expression in PDGF-exposed VSMCs. As shown in **Fig. 3.1E**, PIO at 30 μM concentration significantly diminished the basal expression of $p21^{Cip1}$ by 47 ± 4 %. In addition, PIO treatment led to a significant decrease in PDGF-induced $p21^{Cip1}$ expression, compared with PDGF alone. Since p53 activation and its accumulation have been shown to inhibit VSMC proliferation (Igata et al. 2005), we also examined the effects of PIO on p53 in VSMCs. Neither PIO treatment nor PDGF stimulation affected the phosphorylation or expression level of p53 in VSMCs.

Thus, PIO inhibition of PDGF-induced VSMC proliferation was associated with accumulation of $p27^{Kip1}$ and diminutions in $p21^{Cip1}$ expression, cyclin D1 expression, and Rb phosphorylation.

PIO enhances the phosphorylation of AMPK and ACC as a function of concentration and time in VSMCs

TZD activation of AMPK has been demonstrated in insulin-responsive tissues/cells (e.g., skeletal muscle, adipose tissue, and liver) (Fryer, Parbu-Patel, and Carling 2002; Saha et al. 2004; Konrad et al. 2005; Coletta et al. 2009) and endothelial cells (Boyle et al. 2008) but not in VSMCs. Since AMPK activation has been shown to regulate key proliferative signaling events such as MEK1/ERK (Nagata et al. 2004; Motobayashi et al. 2009; Uemura et al. 2015) and mTOR/p70S6K (Kim et al. 2014) in VSMCs, we examined the likely regulatory effects of TZDs on AMPK and its downstream target, ACC. As shown in **Fig. 3.2A,** exposure of VSMCs to PIO at 3, 10, and 30 μM concentrations led to a progressive increase in the phosphorylation of $AMPK^{Thr172}$ by ~1.9 ± 0.2-, 2.3 ± 0.1-, and 3.6 ± 0.1-fold, respectively. This increase in $AMPK^{Thr172}$ phosphorylation by PIO was accompanied by significant increases in ACC phosphorylation. In addition, PIO treatment at 30 μM concentration resulted in a time-dependent increase in $AMPK^{Thr172}$ phosphorylation between 3 hr and 48 hr (**Fig. 3.2B)**. Furthermore, PIO induced a sustained increase in ACC phosphorylation between 1 hr and 48 hr. Under the same treatment conditions, PIO did not induce any changes in the phosphorylation of LKB1, an upstream kinase for AMPK (Kahn et al. 2005). To determine whether a different TZD derivative could activate AMPK in VSMCs, select studies examined the effects of rosiglitazone (ROSI) *versus* PIO. As shown in **Fig. 3.2C**, exposure of VSMCs to ROSI (30 μM) led to an increase in the phosphorylation of $AMPK^{Thr172}$ and ACC at 24 hr, much greater than that observed at 48 hr time point. In parallel, PIO enhanced the phosphorylation of $AMPK^{Thr172}$ and ACC at 24 hr (to an

extent similar to ROSI) but induced a further increase in the phosphorylation of $AMPK^{Thr172}$ and ACC at 48 hr time point (unlike ROSI). Thus, PIO activation of AMPK occurred in a more sustained manner compared with rosiglitazone.

PIO activates AMPK independent of LKB1 in VSMCs

Although PIO did not affect LKB1 phosphorylation (as shown in Fig. 2A-B), we further verified whether LKB1 expression is required for PIO activation of AMPK. This is because previous studies have shown that injury-induced neointima formation is associated with suppression of LKB1 and AMPK activity (Yu et al. 2012). As shown in **Fig. 3.3A-B**, transfection of VSMCs with target-specific siRNA led to downregulation of LKB1 by ~86 ± 4%. In addition, LKB1 downregulation did not result in significant changes in basal or PIO-induced phosphorylation of AMPK and ACC.

PIO does not affect mitochondrial membrane potential or AMP/ATP ratio in VSMCs

TZD activation of AMPK in skeletal muscle cells is mediated by a reduction in mitochondrial membrane potential and/or an increase in AMP/ATP ratio (Fryer, Parbu-Patel, and Carling 2002; Konrad et al. 2005; Brunmair et al. 2004). Hence, we also examined whether the observed activation of AMPK by PIO is due to changes in cellular energy state. As shown in **Fig. 3.4A**, exposure of VSMCs to 30 μM PIO did not affect mitochondrial membrane potential at 1 hr or 3 hr time points. The effect of CCCP (50 μM, 1 hr), a generic mitochondrial membrane depolarizer, was examined in parallel and thus served as a positive control. In addition, the effects of PIO (30 μM) on adenine nucleotides levels (AMP, ADP, and ATP) were examined at the 3 hr time point, using

LC-MS/MS MRM analysis. PIO treatment resulted in a marginal but insignificant increase in AMP/ATP ratio (**Fig. 3.4B**). Collectively, these data suggest that PIO-induced AMPK activation in VSMCs occurs independently of changes in mitochondrial membrane potential or AMP/ATP ratio.

PIO inhibits basal ERK phosphorylation, and PDGF-induced mTOR/p70S6K signaling and protein synthesis

Previously, we and several other investigators have shown that mitogen-induced VSMC proliferation is mediated by activation of different signaling pathways, including MEK/ERK, PI3K/Akt, and mTOR/p70S6K (Braun-Dullaeus et al. 2001; Nagata et al. 2004; Zhao et al. 2011). In the present study, we examined whether PIO suppression of PDGF-induced VSMC proliferation occurs through inhibition of these key signaling components. As shown in **Fig. 3.5A,** pretreatment with PIO alone led to a significant diminution in basal ERK1/2 phosphorylation by ~80%. Exposure of control and PIO-treated VSMCs to PDGF resulted in a significant increase in ERK1/2 phosphorylation by ~4.2-fold and ~9.3-fold, respectively. Thus, PIO treatment reduced basal ERK1/2 phosphorylation but not PDGF-induced ERK phosphorylation. **Fig. 3.5B** shows that PIO did not affect PDGF-induced phosphorylation of Akt (Thr^{308}) or its downstream effector GSK-3β (Ser^{9}). With regard to mTOR/p70S6K signaling, PIO diminished both basal and PDGF-induced phosphorylation of $p70S6K^{Thr389}$, and its downstream effectors, 4E-BP1 (Ser^{65}) and S6 ribosomal protein (S6, $Ser^{235/236}$) (**Fig. 3.5C**). Since mTOR activation is associated with cell growth *via* enhanced protein synthesis (Ma and Blenis 2009), we also studied the effects of PIO on PDGF-induced protein synthesis. As shown in **Fig. 3.5D-E,**

pretreatment with PIO (30 μM, 30 min) inhibited PDGF (30 ng/ml, 24 hr)-induced protein synthesis by ~63 ± 15 %. Together, these data suggest that PIO attenuates VSMC proliferation by inhibiting ERK and p70S6K signaling pathways.

AMPK mediates PIO-induced inhibition of S6 phosphorylation and accumulation of p27^{kip1}

Recently, regulatory associated protein of mTOR (Raptor), a scaffolding protein that provides a bridge between mTOR and its downstream targets, has been identified as a direct substrate of AMPK that undergoes phosphorylation (Ser^{792}) to facilitate allosteric inhibition of mTOR activity (Gwinn et al. 2008; Hardie 2008). In conformity with these reports, the present findings reveal that PIO treatment (30 μM) was associated with enhanced raptor phosphorylation (Ser^{792}) in VSMCs, suggesting an intermediary role of AMPK toward inhibition of mTOR/p70S6K signaling (**Fig. 3.6D).** Next, we examined whether AMPKα1 or AMPK α2 isoform contributes to this effect. As shown in **Fig. 3.6A-C**, transfection of VSMCs with target-specific siRNA led to downregulation of AMPKα1 and AMPKα2 isoforms by ~75 ± 2% and ~50 ± 6 %, respectively. Downregulation of AMPKα1, but not AMPKα2, markedly inhibited PIO (30 μM, 48 hr)-induced AMPK and ACC phosphorylation, indicating that AMPKα1 mediates PIO-induced AMPK activation (**Fig. 3.6A**). Importantly**,** AMPKα1 downregulation prevented PIO-mediated increase in raptor phosphorylation and the concomitant decrease in PDGF-induced S6 phosphorylation, thus providing direct evidence for the intermediary role of AMPK in PIO-mediated inhibition of mTOR/p70S6K signaling in VSMCs (**Fig. 3.6D**).

In addition, AMPKα1 downregulation prevented PIO-mediated accumulation of $p27^{kip1}$ (**Fig. 3.6D**).

Since we observed PIO inhibition of ERK1/2 phosphorylation and cyclin D1 expression (sections *3.5* and *3.1*, respectively), the intermediary role of AMPK in these effects was also examined. AMPKα1 downregulation did not alter PIO-mediated inhibitory effects on ERK1/2 phosphorylation or cyclin D1 expression, indicating that these effects were independent of AMPK activation (**Fig. 3.6E).** Collectively, these data suggest that PIO inhibits VSMC proliferation by at least two independent mechanisms: activation of AMPK/mTOR/$p27^{kip1}$ and inhibition of ERK signaling pathways.

PIO downregulates cyclin D1 mRNA in VSMCs

MEK/ERK signaling pathway is the well-characterized pathway controlling the transcription of cyclin D1. Accordingly, we examined if PIO-mediated inhibition of basal ERK1/2 phosphorylation was associated with transcriptional repression of cyclin D1. Quantitative RT-PCR analysis revealed that exposure of serum-deprived VSMCs to PIO (30 μM, 48 hr) resulted in ~65 ± 3% decrease in cyclin D1 mRNA, compared with vehicle control ($p < 0.05$; $n = 3$). These data suggest that PIO inhibition of basal ERK1/2 phosphorylation is likely responsible for the observed transcriptional repression of cyclin D1.

PIO activates AMPK and inhibits S6 phosphorylation, ERK1/2 phosphorylation and cyclin D1 expression independent of PPARγ

TZDs, including PIO, are potent activators of PPARγ and thus have robust insulin-sensitizing activities. Although PPARγ is abundantly expressed in adipose tissue, it is expressed to a modest extent in several other tissues/cells, including VSMCs (Staels et al. 1998; Law et al. 2000). Thus, we examined whether PIO-mediated AMPK activation and the associated changes in signaling components are mediated through the activation of PPARγ. Using differentiated 3T3-L1 cells as a positive control that expresses both PPARγ1 and PPARγ2, we confirmed previous reports that PPARγ1 protein is expressed in human aortic VSMCs and was localized predominantly in the nuclear fraction (**Fig. 3.7A**). Exposure of VSMCs to PIO (30 μM, 48 hr) led to a marked increase in PPARγ expression in the nuclear fraction (**Fig. 3.7A)** and in whole cell lysate (**Fig. 3.7B)**. In mock-transfected VSMCs (using scrambled siRNA), PIO treatment led to a significant increase in the expression of PPARγ (by ~3 ± 0.6-fold) and its target gene (Bishop-Bailey, Hla, and Warner 2002), CD36 (by ~2 ± 0.5-fold) (**Fig. 3.7B)**. Importantly, downregulation of PPARγ expression (~87 ± 3%) by target-specific siRNA prevented PIO-induced CD36 expression (**Fig. 3.7B-C)**. However, it did not alter PIO-mediated AMPK phosphorylation or PIO inhibition of PDGF-induced S6 phosphorylation (**Fig. 3.7D)**. Moreover, PPARγ downregulation did not alter PIO-mediated inhibition of basal ERK1/2 phosphorylation or PDGF (30 ng/ml, 48 hr)-induced cyclin D1 expression. To confirm these results, we pretreated VSMCs with GW-9662 (10 μM, 30 min), an inhibitor of PPARγ, before PIO treatment. As shown in **Fig. 3.7E**, GW-9662 did not affect any of the aforementioned signaling events in VSMCs.

Discussion

The present study demonstrates that the antidiabetic drug, pioglitazone (PIO), activates AMPK in a sustained manner thereby contributing in part to inhibition of key proliferative signaling events in VSMCs (**Fig. 3.8**). In particular, PIO at 30 μM concentration activates AMPK to induce raptor phosphorylation, which diminishes PDGF-induced mTOR activity as evidenced by decreased phosphorylation of p70S6K, 4E-BP1, and S6 and increased accumulation of $p27^{kip1}$, a cell cycle inhibitor. In addition, PIO inhibits the basal phosphorylation of ERK in VSMCs. Downregulation of endogenous AMPK by target-specific siRNA reveals an AMPK-independent effect for PIO inhibition of ERK, which contributes in part to diminutions in cyclin D1 expression and Rb phosphorylation and the suppression of VSMC proliferation. Furthermore, AMPK-dependent inhibition of mTOR/p70S6K and AMPK-independent inhibition of ERK signaling occur regardless of PPARγ expression/activation in VSMCs as evidenced by gene silencing and pharmacological inhibition of PPARγ. Strategies that utilize nanoparticle-mediated PIO delivery at the lesion site may limit restenosis after angioplasty without inducing PPARγ-mediated systemic adverse effects (Nagahama et al. 2012; Joner et al. 2008).

Previous studies demonstrate that AMPK activation suppresses VSMC proliferation (Nagata et al. 2004; Igata et al. 2005; Stone et al. 2013; Uemura et al. 2015), whereas genetic and pharmacological strategies to inactivate AMPK restore VSMC proliferative response (Nagata et al. 2004; Igata et al. 2005; Uemura et al. 2015). Unlike these earlier observations with an AMPK activator (e.g., AICAR) (Nagata et al. 2004; Igata et al. 2005; Stone et al. 2013), the present findings with a TZD derivative (e.g., PIO) highlight

its role in AMPK activation that mediates the suppression of VSMC proliferative signaling in a partial manner. Notably, ectopic expression of dominant-negative AMPK to inhibit AMPK activity (Nagata et al. 2004; Igata et al. 2005) prevents AICAR inhibition of serum-induced VSMC proliferation and the associated phosphorylation of Rb (Igata et al. 2005). In the present study, downregulation of endogenous AMPK by target-specific siRNA abolishes PIO-mediated accumulation of $p27^{Kip1}$ (a cell cycle inhibitor) (Tanner et al. 2000) but does not prevent PIO inhibition of PDGF-induced cyclin D1 expression. Together, these findings reveal that PIO has the potential to inhibit VSMC proliferation through AMPK-dependent and AMPK-independent mechanisms beyond its role as a PPARγ agonist. Furthermore, AMPK activation by AICAR results in increased p53 phosphorylation/expression and $p21^{Cip1}$ expression, which in turn inhibits Rb phosphorylation to suppress VSMC proliferation (Igata et al. 2005). The present findings reveal that PIO does not affect p53 phosphorylation/expression but it decreases $p21^{Cip1}$ expression, suggesting that p53-p21 axis may not play an intermediary role in PIO inhibition of VSMC proliferation.

Studies with AICAR and adipokines have shown that AMPK activation is associated with diminished ERK activation (Nagata et al. 2004; Motobayashi et al. 2009; Uemura et al. 2015), which in turn is attributable to the suppression of VSMC proliferation (Nagata et al. 2004; Uemura et al. 2015). However, there is no apparent causal link between the observed AMPK activation and diminished ERK phosphorylation toward PIO inhibition of VSMC proliferation (present study). For instance, while AICAR activates AMPK and inhibits agonist-induced ERK phosphorylation (Nagata et al. 2004; Motobayashi et al. 2009), overexpression of dominant-negative AMPK abrogates the downstream signal

(e.g., ACC phosphorylation) and augments agonist-induced ERK phosphorylation to promote VSMC proliferation (Nagata et al. 2004). In addition, adipokines such as omentin and adiponectin activate AMPK to inhibit ERK phosphorylation in VSMCs (Uemura et al. 2015; Motobayashi et al. 2009). In particular, genetic blockade of AMPK activation prevents omentin inhibition of PDGF-induced ERK phosphorylation to restore VSMC proliferation (Uemura et al. 2015). In contrast to AICAR and the aforementioned adipokines, the present findings show that PIO inhibition of basal ERK phosphorylation remains essentially the same after AMPK downregulation and the associated abrogation of ACC phosphorylation. This is further supported by the persistent decrease in PDGF-induced cyclin D1 expression by PIO after AMPK downregulation, thereby suggesting that PIO inhibition of VSMC proliferation occurs in part through mechanisms independent of AMPK activation.

Several lines of evidence suggest that AMPK activation results in the inhibition of mTOR/p70S6K signaling (and *vice versa*) in different tissues/cell types (Inoki, Kim, and Guan 2012; Saha et al. 2010), including VSMCs (Kim et al. 2014). In particular, AMPK activation in nonvascular cells promotes raptor phosphorylation to inhibit the activity of mTOR (Gwinn et al. 2008), a key signaling component that regulates protein synthesis (Sengupta, Peterson, and Sabatini 2010; Ning and Clemmons 2010), cell cycle progression and cell proliferation (Martinet, De Loof, and De Meyer 2014). Recent studies with VSMCs demonstrate that ectopic expression of retinoic acid receptor-related orphan receptor-α (RORα) enhances AMPK phosphorylation to inhibit mTOR/p70S6K phosphorylation, thereby suppressing VSMC proliferation (Kim et al. 2014). The present findings reveal that PIO not only activates AMPK but also promotes raptor

phosphorylation to inhibit mTOR signaling (e.g., ↓ phosphorylation of p70S6K, 4E-BP1, and S6) and protein synthesis in VSMCs. This novel observation is supported by AMPK downregulation studies using target-specific siRNA. Importantly, downregulation of AMPK diminishes PIO-mediated phosphorylation of ACC and raptor, thereby restoring S6 phosphorylation with an accompanying blockade in the accumulation of $p27^{Kip1}$ (a cell cycle inhibitor) (Tanner et al. 2000). Together, these findings suggest that in addition to strategies that overexpress RORα in VSMCs (Kim et al. 2014), treatment with PIO may provide another promising approach to attenuate exaggerated VSMC growth through ↑AMPK → ↓mTOR axis.

While the present findings with PIO point toward AMPK-independent (*via* ↓ ERK) and AMPK-dependent (*via* ↓ mTOR/p70S6K) mechanisms to suppress VSMC proliferation, it is critically important to know whether PPARγ regulates these signaling events. Previously, loss-of-function studies (e.g., dominant-negative PPARγ mutation that suppresses endogenous PPARγ function) have revealed exaggerated neointima formation in mice but without any changes in growth factor-induced ERK phosphorylation, suggesting that endogenous PPARγ does not regulate ERK activation during VSMC proliferation (Meredith et al. 2009). In a different study, rosiglitazone inhibits PDGF- or arterial injury-induced ERK activation in a PPARγ-independent manner, as evidenced by the use of dominant-negative PPARγ mutant (Lee et al. 2009). In conformity with these earlier findings, the present study demonstrates that PIO, while upregulating PPARγ expression in the nucleus, exerts an inhibitory effect on ERK phosphorylation and cyclin D1 expression. Importantly, PIO inhibition of ERK phosphorylation and cyclin D1 expression is unaffected after PPARγ downregulation

(~87%) by target-specific siRNA. Since the contribution of ~13% residual PPARγ expression (in PPARγ siRNA-treated VSMCs) cannot be fully excluded, we employed an additional approach involving VSMC treatment with GW-9662. Pharmacological inhibition of PPARγ by GW-9662 yielded results similar to that observed in PPARγ siRNA-treated VSMCs. Together, these studies suggest that PIO inhibition of key proliferative signaling events (e.g., pERK and cyclin D1) occurs by mechanisms independent of PPARγ in VSMCs. It is noteworthy that the basal ERK phosphorylation in vascular cells is mediated in part by reactive oxygen species (ROS), including superoxide (O_2^-) (Li et al. 2004; Lee et al. 2015). In addition, PIO has been shown to inhibit NADPH oxidase-mediated generation of ROS in aortic tissues and VSMCs (Martin et al. 2012; Perez-Giron et al. 2014). Thus, it is likely that PIO inhibits the basal ERK activation by suppressing ROS production in VSMCs.

It is widely accepted that TZD activation of PPARγ in adipocytes results in the synthesis and release of adiponectin (Kadowaki et al. 2006). Recent studies demonstrate that exposure of VSMCs to rosiglitazone for 24 hours enhances the expression of adiponectin (Ding et al. 2012), which in turn can act in an autocrine/paracrine manner to activate AMPK in VSMCs (Ding et al. 2012; Ding et al. 2011). From the present findings that reveal PIO activation of AMPK, it may, therefore, be argued that PPARγ-mediated adiponectin synthesis/release is a critical transcriptional event for such an effect. However, our experimental approaches involving siRNA-mediated PPARγ downregulation, chemical inhibition of PPARγ by GW-9662, and time course studies do not support the likely intermediary role of adiponectin toward PIO activation of AMPK in VSMCs. First, neither PPARγ downregulation nor GW-9662 affects PIO activation of

AMPK or PIO inhibition of PDGF-induced S6 phosphorylation. Second, PIO activation of AMPK occurs as early as 1 to 3 hours (present study) in contrast to a much longer time frame (≥ 24 hr) that is required for adiponectin upregulation and subsequent AMPK activation (Ding et al. 2012; Ding et al. 2011) in VSMCs. Third, PIO is several folds less potent than rosiglitazone as a PPARγ activator (Young et al. 1998). Together, these studies suggest that PIO activation of AMPK occurs by PPARγ- and adiponectin-independent mechanisms in VSMCs.

TZD derivative(s) have been shown to activate AMPK through ↓ mitochondrial respiratory chain complex I (Brunmair et al. 2004), ↓ mitochondrial membrane potential (Konrad et al. 2005), ↑AMP/ATP ratio (Fryer, Parbu-Patel, and Carling 2002; Saha et al. 2004), and/or LKB1 (Boyle et al. 2008) in insulin-responsive tissues and HeLa cells. In particular, ROSI but not PIO at 10 μM and 30 μM concentrations significantly inhibits respiratory complex I enzyme activity in rat skeletal muscle and liver (Brunmair et al. 2004), suggesting that PIO activation of AMPK in VSMCs may not involve inhibition of respiratory complex I. Although TRO has been shown to activate AMPK by acutely reducing mitochondrial membrane potential in skeletal muscle cells (Konrad et al. 2005), the present findings from TMRM fluorescence studies do not support the possibility for mitochondrial membrane depolarization by PIO as a likely intermediary event in VSMCs *at least* under the chosen time intervals. In view of the critical link between ↑AMP/ATP ratio and AMPK activation (Fryer, Parbu-Patel, and Carling 2002; Saha et al. 2004), we have also analyzed adenine nucleotide levels in PIO-treated VSMCs. While ROSI at 200 μM concentration increases AMP/ATP ratio in skeletal muscle cells (Fryer, Parbu-Patel, and Carling 2002), PIO treatment in VSMCs shows a trend toward ↑AMP/ATP ratio but

without statistical significance. Given that LKB1 is a catalytic enzyme, the contribution of ~14% residual LKB1 protein (in LKB1 siRNA-treated VSMCs) cannot be fully excluded with regard to AMPK activation. Furthermore, PIO treatment enhances the phosphorylation of ACC, a key downstream target of AMPK (Kahn et al. 2005) prior to AMPKα^{Thr172} phosphorylation in VSMCs as revealed in our time course study. This may be attributed to an apparent allosteric activation of AMPK without AMPKα^{Thr172} phosphorylation as has been evidenced previously in human melanoma cells upon treatment with A769662, a direct AMPK activator that does not increase intracellular AMP or ADP levels (Gowans et al. 2013). Future studies are clearly warranted that should compare the role of PIO *versus* ROSI/TRO toward inducing temporal changes in mitochondrial function, including the potential inhibitory effects on mitochondrial pyruvate carrier (Divakaruni et al. 2013), to identify the upstream signaling events critical for PIO activation of AMPK in VSMCs.

From a clinical standpoint, the findings from the meta-analysis of randomized trials suggest that, in comparison with rosiglitazone that may increase the risk of ischemic events, PIO has a more favorable effect on ischemic vascular complications (Lincoff et al. 2007). PROactive study (PROspective pioglitAzone Clinical Trial In macroVascular Events) reveals that PIO treatment is associated with improved cardiovascular outcomes in patients with type 2 diabetes and macrovascular disease (Dormandy et al. 2005). Nevertheless, the precise mechanisms for such vasoprotective effects remain largely unknown due to the pleiotropic actions of PIO. Notably, PIO has been shown to lower blood pressure (Hsueh and Law 2001) and improve endothelial function (Hsueh and Law 2001). It also exhibits anti-inflammatory (Ishibashi et al. 2002), anti-migratory (Game et

al. 2005), and anti-proliferative (Yoshimoto et al. 1999) effects in VSMCs. The concentration of PIO used in the present *in vitro* study with VSMCs is nearly one order of magnitude higher than the peak plasma concentration (~3 μM) observed in human subjects on PIO treatment (Hanefeld 2001). At this juncture, it is important to note that in comparison with the inhibitory effects of 10-30 μM PIO added directly to VSMCs in culture (present findings and previous studies) (Hong et al. 2010), a pronounced inhibition of VSMC proliferation occurs upon *in vitro* addition of serum samples obtained from PIO-treated type 2 diabetic subjects (Hong et al. 2010). These data suggest that, under *in vivo* conditions, circulating PIO has the potential to exert direct and indirect inhibitory effects on VSMC proliferation. The indirect inhibitory effects of PIO may be attributable to its role in anti-inflammatory action and enhanced adiponectin release. It is well accepted that PIO activation of PPARγ in adipose tissue would enhance circulatory levels of adiponectin (Kadowaki et al. 2006), which in turn would suppress neointima formation (Arita et al. 2002) through AMPK activation in VSMCs (Ding et al. 2012; Ding et al. 2011). The present findings suggest a yet another mechanism for PIO inhibition of VSMC proliferation through AMPK-dependent and AMPK-independent signaling mechanisms regardless of PPARγ expression. Notably, AMPK activation by AICAR has been shown to inhibit neointimal formation in balloon-injured rat carotid artery (Stone et al. 2013). Recent studies demonstrate that AICAR and metformin inhibit the differentiation of monocytes to macrophages through AMPKα1 activation *in vitro* (Vasamsetti et al. 2015). In addition, oral administration of metformin attenuates atherosclerotic lesion by inhibiting macrophage accumulation in apoE-deficient mouse aorta (Vasamsetti et al. 2015). Future studies should compare the effects of the

therapeutically relevant concentration of PIO *versus* metformin/AICAR on neointima formation after arterial injury in AMPKα1-deficient mice.

In conclusion, PIO has the potential to inhibit VSMC proliferation through indirect effects involving adiponectin/AMPK (Kadowaki et al. 2006; Ding et al. 2012; Ding et al. 2011; Arita et al. 2002), and in part through direct effects involving AMPK-dependent and AMPK-independent regulation of cell cycle regulatory proteins.

Acknowledgements

This work was supported by the National Heart, Lung, and Blood Institute/National Institutes of Health Grant (R01-HL-097090), University of Georgia Research Foundation Fund, and University of Georgia College of Pharmacy Graduate Assistantship Award.

Figure legends

Fig. 3.1. Effects of PIO on VSMC proliferation, DNA synthesis, and cell cycle proteins in the absence or presence of PDGF. (**A**) Subconfluent VSMCs were maintained in complete medium (CM) or serum-deprived conditions (SF) for 48 hr. VSMC lysates were then subjected to immunoblot analysis using primary antibodies specific for SM α-actin or calponin. The immunoblots shown are representative of n = 3. (**B**) Serum-deprived VSMCs were pretreated with PIO (3, 10, or 30 μM) or vehicle control for 30 min. This was followed by exposure to PDGF (30 ng/ml) for 96 hr to determine the changes in cell number. (**C**) Serum-deprived VSMCs were pretreated with PIO (30 μM) or vehicle control for 24 hr and then exposed to PDGF (30 ng/ml) for 24 hr to determine the changes in DNA synthesis. Serum-deprived VSMCs were pretreated with PIO at the indicated concentrations or vehicle control for 30 min. This was followed by exposure to PDGF (30 ng/ml) for 48 hr to determine the changes in: (**D**) cyclin D1, pRb, and $p27^{Kip1}$; and (**E**) pp53, p53, and $p21^{Cip1}$ by immunoblot analysis. *$p < 0.05$ compared with vehicle control; $^{\#}p < 0.05$ compared with PDGF alone; n = 3.

FIG. 3.1A-E

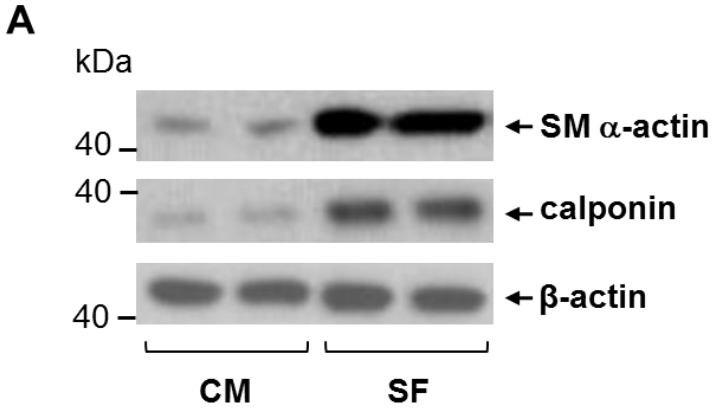
A
kDa
40
40
40
SM α-actin
calponin
β-actin
CM
SF

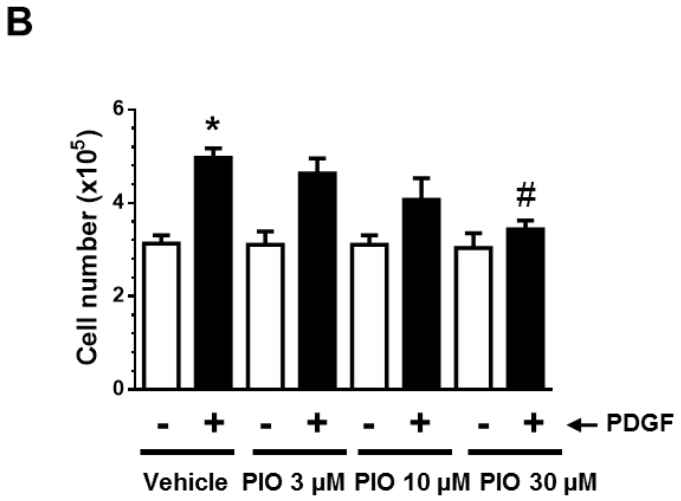
B
Cell number (x10^5)
6
4
2
0
*
#
- + - + - + - +
PDGF
Vehicle
PIO 3 μM
PIO 10 μM
PIO 30 μM

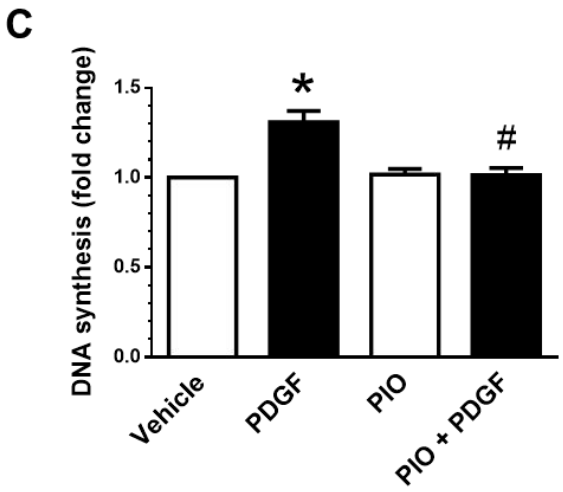
C
DNA synthesis (fold change)
1.5
1.0
0.5
0.0
*
#
Vehicle
PDGF
PIO
PIO + PDGF

FIG. 3.1A-E continued

D

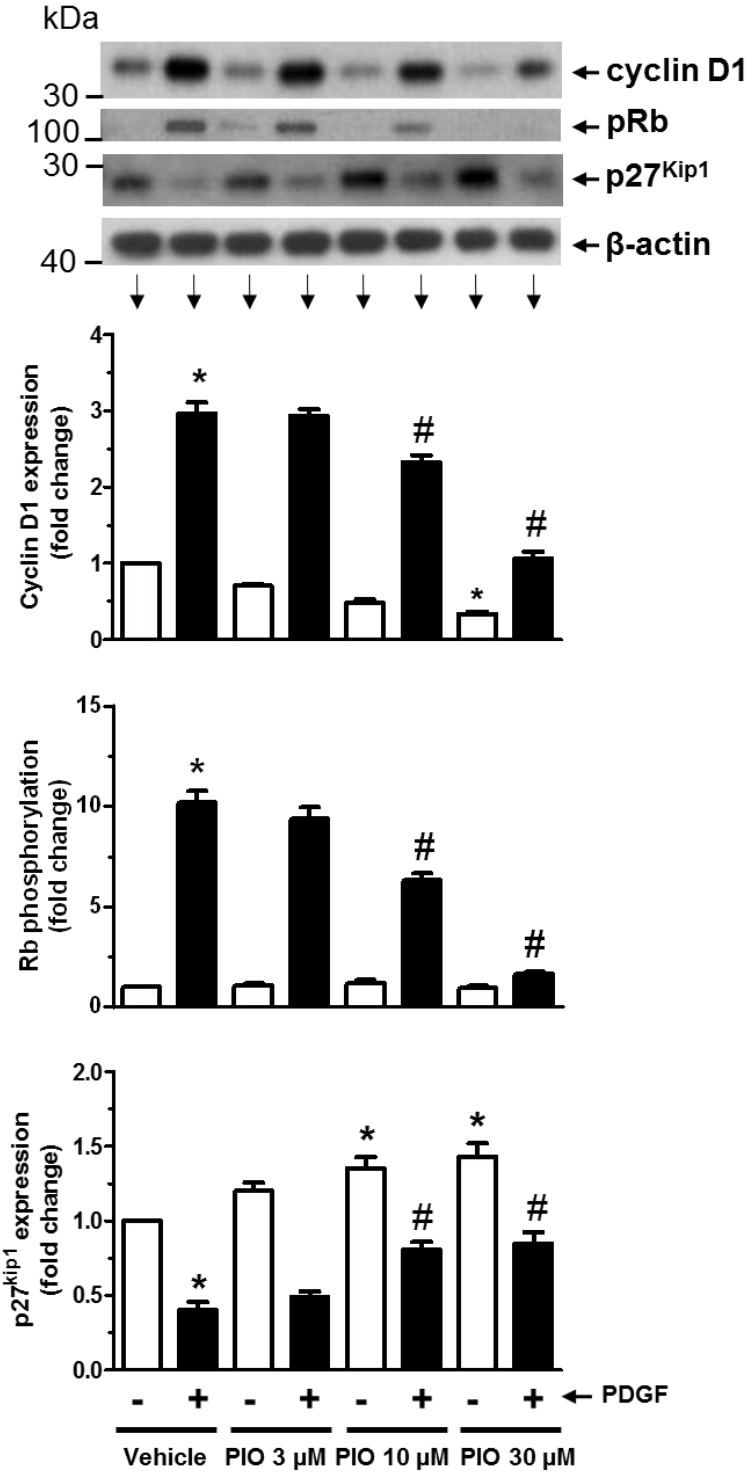

FIG. 3.1A-E continued

E

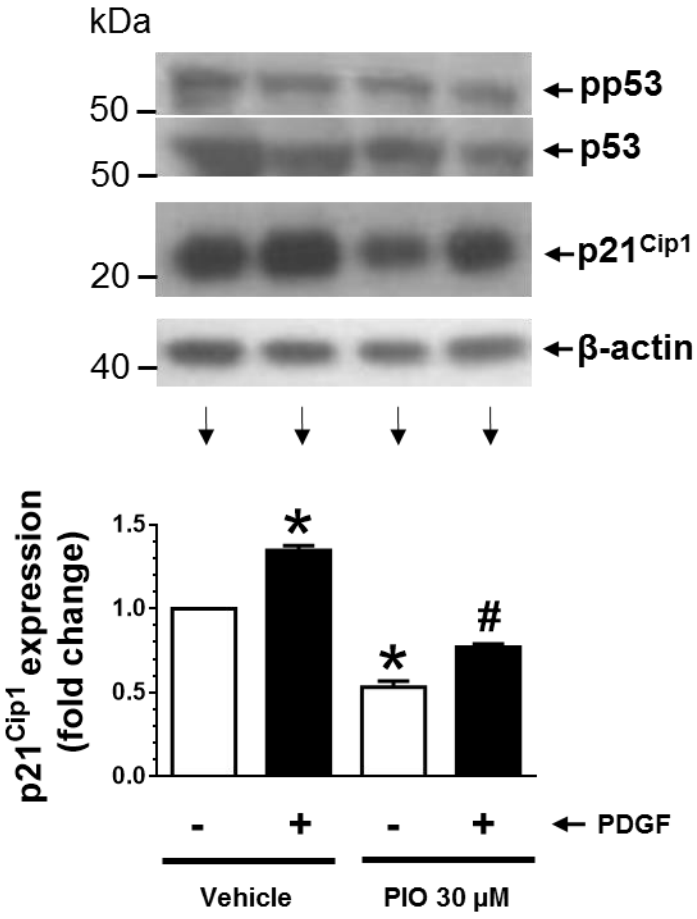

Fig. 3.2. Effects of PIO on AMPK and ACC phosphorylation as a function of concentration and time. Serum-deprived VSMCs were treated with increasing concentrations of PIO (3 to 30 μM) or vehicle control for 48 hr (**A**) or a fixed concentration of PIO (30 μM) for 1 to 48 hr (**B**). In addition, serum-deprived VSMCs were exposed to ROSI (30 μM) *versus* PIO (30 μM) for 24 or 48 hr (**C**). VSMC lysates were then subjected to immunoblot analysis using primary antibodies specific for pAMPK, pACC, or pLKB1. *$p < 0.05$ compared with vehicle control; $n = 3$.

FIG. 3.2A-C

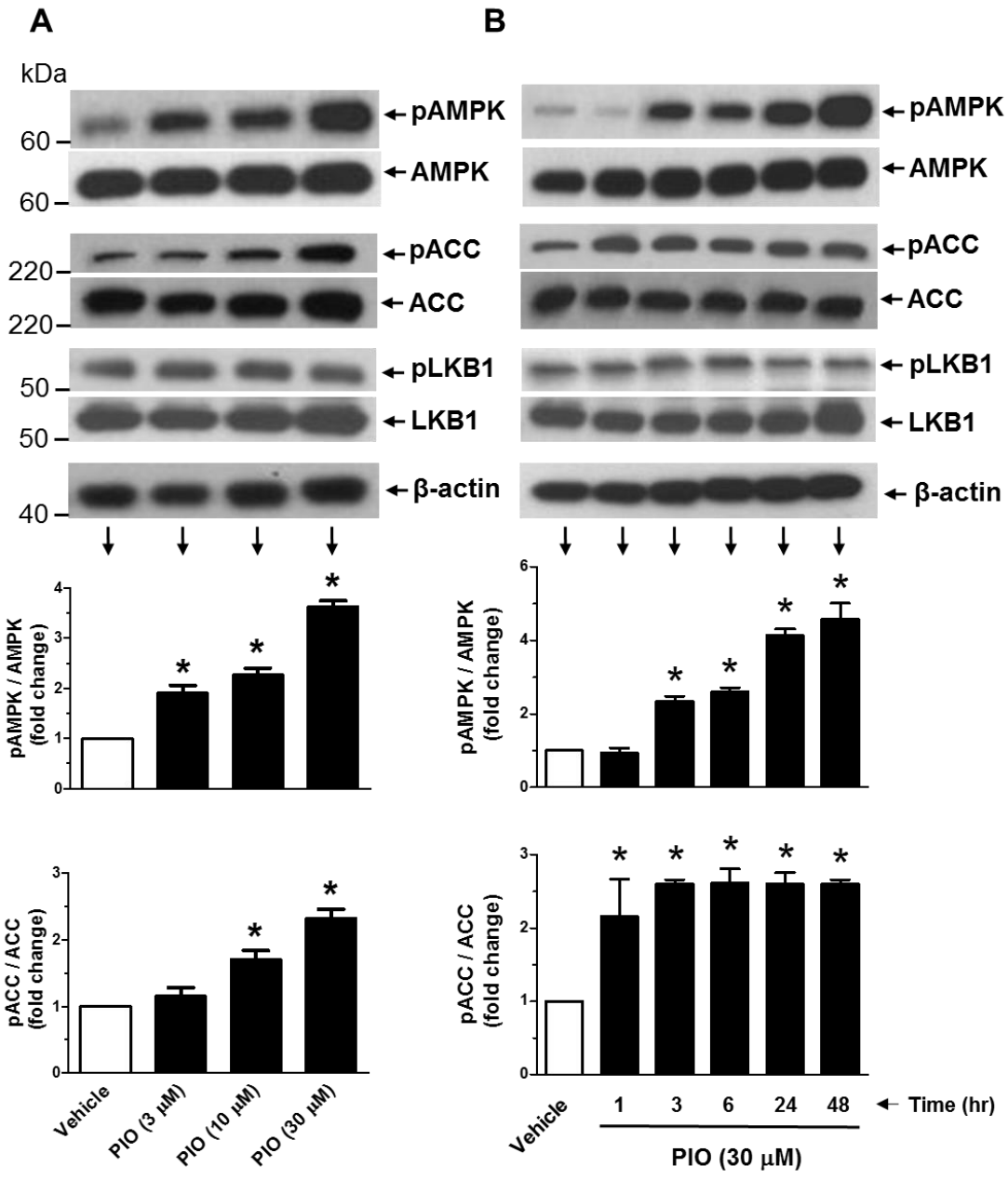
A
B
kDa
60
60
220
220
50
50
40
pAMPK
AMPK
pACC
ACC
pLKB1
LKB1
β-actin
pAMPK / AMPK (fold change)
pACC / ACC (fold change)
Vehicle
PIO (3 μM)
PIO (10 μM)
PIO (30 μM)
1
3
6
24
48
Time (hr)
PIO (30 μM)

FIG. 3.2A-C
continued

C

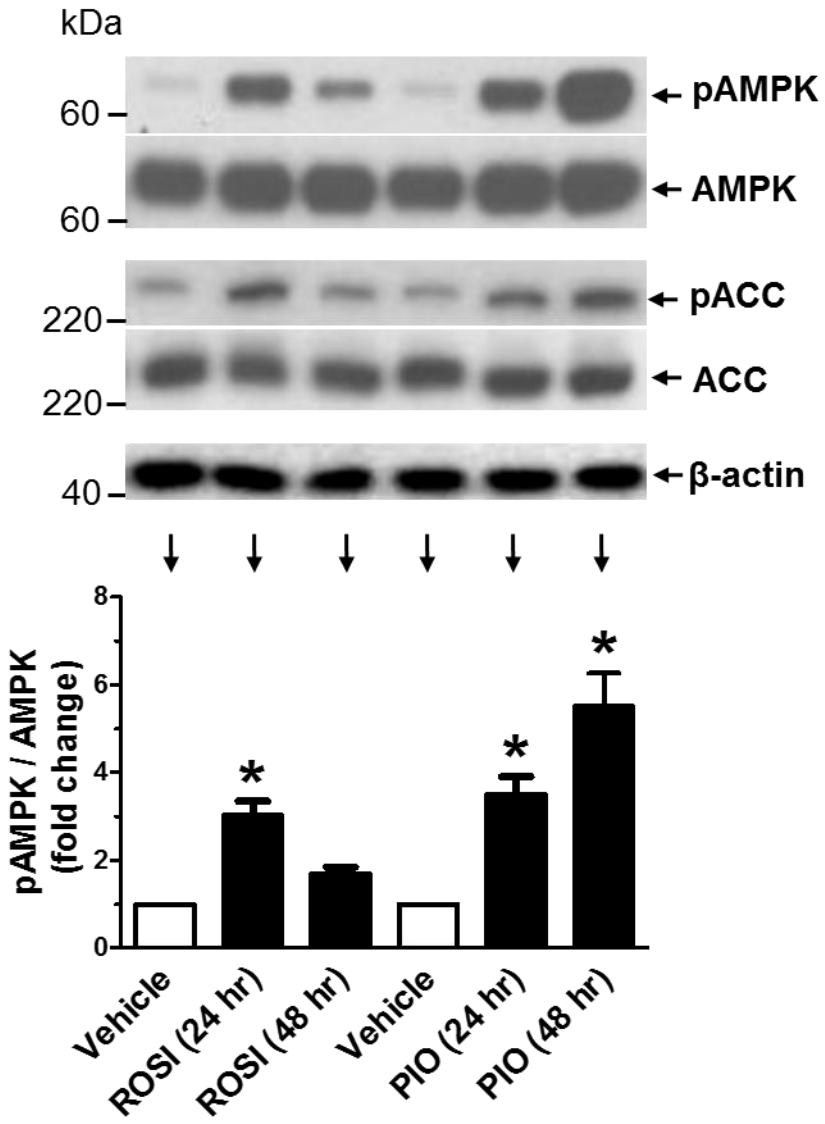

Fig. 3.3. Effects of LKB1 downregulation on PIO activation of AMPK in VSMCs. (**A-B**) VSMCs were transfected with scrambled (Scr.) or LKB1 siRNA followed by maintenance in culture for 48 hr. Subsequently, VSMCs were treated with PIO (30 μM, 48 hr) or vehicle control under serum-deprived conditions. VSMC lysates were then subjected to immunoblot analysis using primary antibodies specific for LKB1, pAMPK, and pACC. *$p < 0.05$ compared with scr. siRNA; immunoblots shown are representative of $n = 3$.

FIG. 3.3A-B

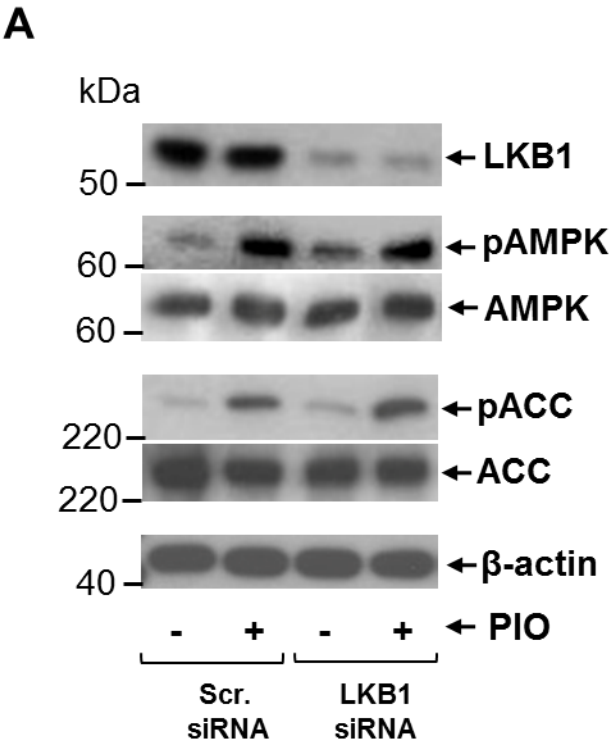
A
kDa
50
LKB1
60
pAMPK
60
AMPK
220
pACC
220
ACC
40
β-actin
- + - +
PIO
Scr. siRNA
LKB1 siRNA

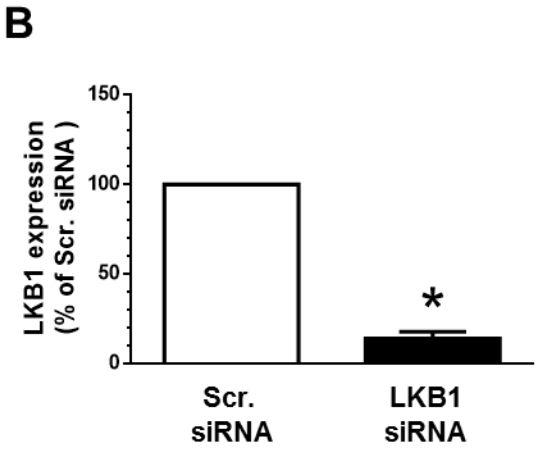
B
LKB1 expression (% of Scr. siRNA)
150
100
50
0
*
Scr. siRNA
LKB1 siRNA

Fig. 3.4. Effects of PIO on mitochondrial membrane potential and AMP/ATP ratio in VSMCs. Serum-deprived VSMCs were treated with: (**A**) PIO (30 μM, 1 or 3 hr), CCCP (50 μM, 1 hr), or vehicle control followed by fluorescence microscopy analysis of mitochondrial membrane potential; or (**B**) PIO (30 μM, 3 hr) or vehicle control followed by LC-MS/MS MRM analysis of AMP/ATP ratio. n.s. not significant compared with vehicle control; n = 4.

FIG. 3.4A-B

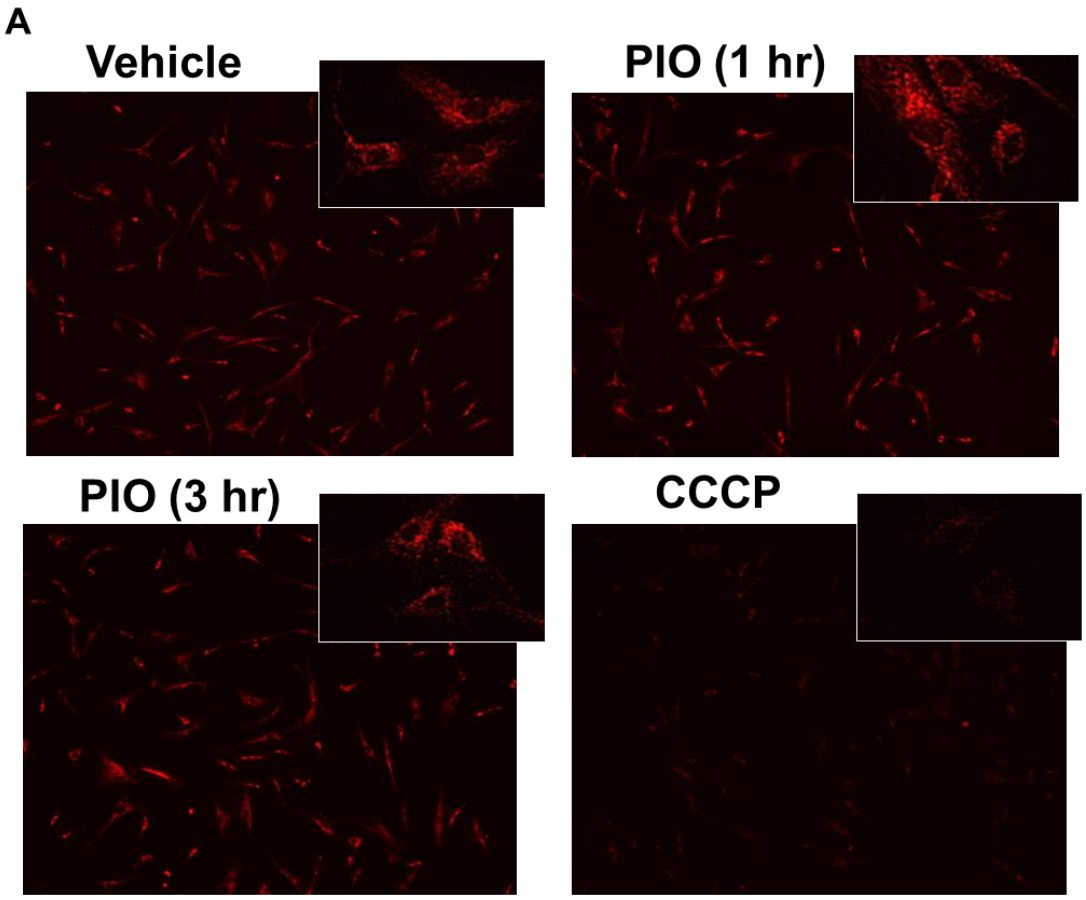
A
Vehicle
PIO (1 hr)
PIO (3 hr)
CCCP

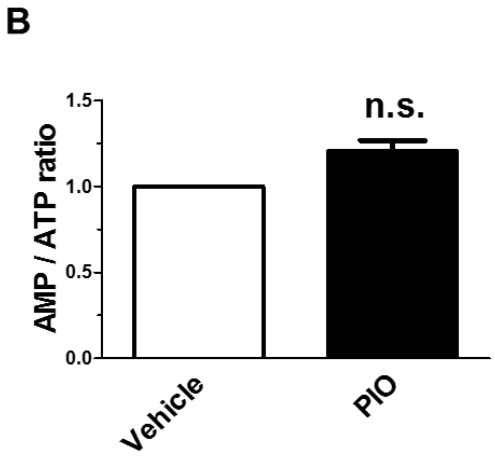
B
n.s.
AMP / ATP ratio
1.5
1.0
0.5
0.0
Vehicle
PIO

Fig. 3.5. Effects of PIO on PDGF-induced signaling events and protein synthesis in VSMCs. Serum-deprived VSMCs were pretreated with PIO (30 μM) or vehicle control for 30 min followed by exposure to: (**A-C**) PDGF (30 ng/ml, 48 hr) to determine the changes in protein phosphorylation; or (**D-E**) PDGF (30 ng/ml, 24 hr) to determine nascent protein synthesis. For protein phosphorylation, VSMC lysates were subjected to immunoblot analysis using primary antibodies specific for pERK1/2, pAkt, pGSK3β, pp70S6K, p4E-BP1, and pS6. *p <0.05 compared with vehicle control; $^{\$}$p < 0.05 compared with PIO alone; n.s. not significant compared with PDGF alone; n = 3.

FIG. 3.5A-E

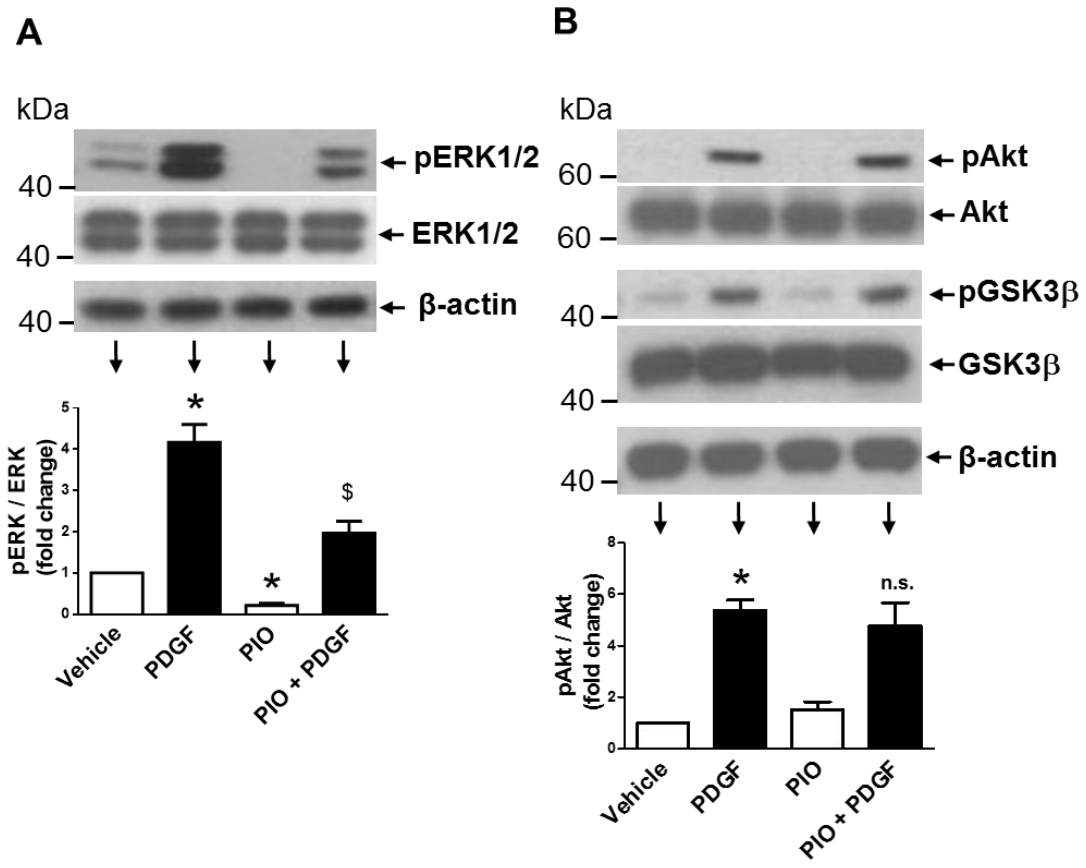
A
kDa
40
40
40
pERK1/2
ERK1/2
β-actin
pERK / ERK (fold change)
Vehicle
PDGF
PIO
PIO + PDGF
B
kDa
60
60
40
40
pAkt
Akt
pGSK3β
GSK3β
β-actin
pAkt / Akt (fold change)
n.s.
Vehicle
PDGF
PIO
PIO + PDGF

FIG. 3.5A-E
continued

C

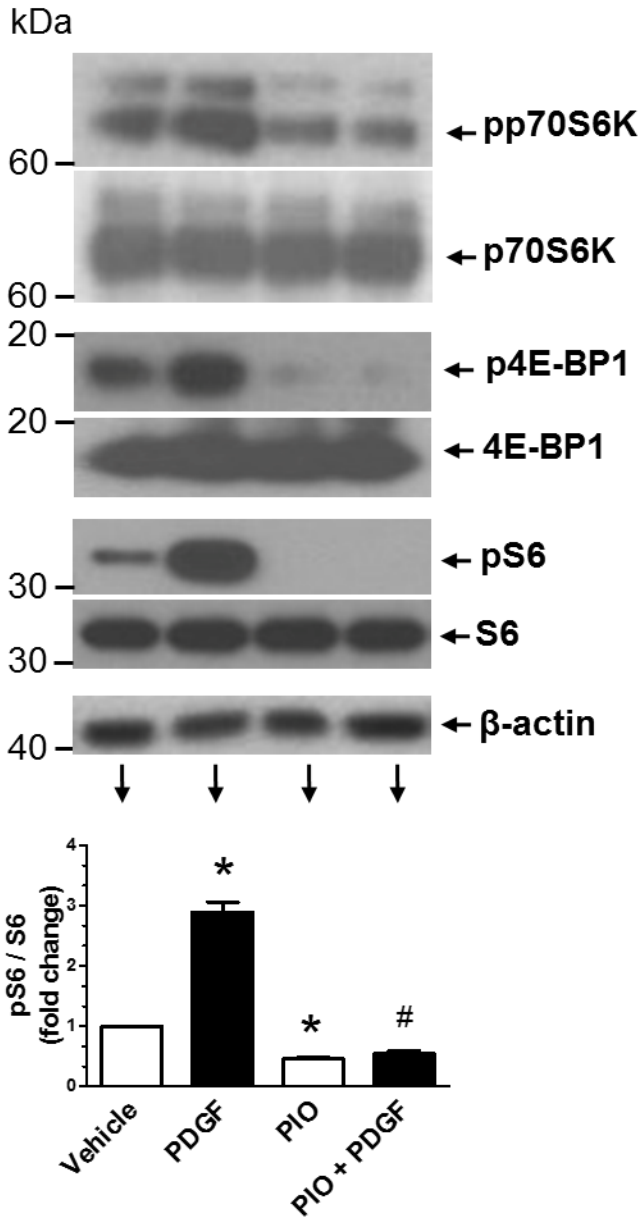

FIG. 3.5A-E
continued

D

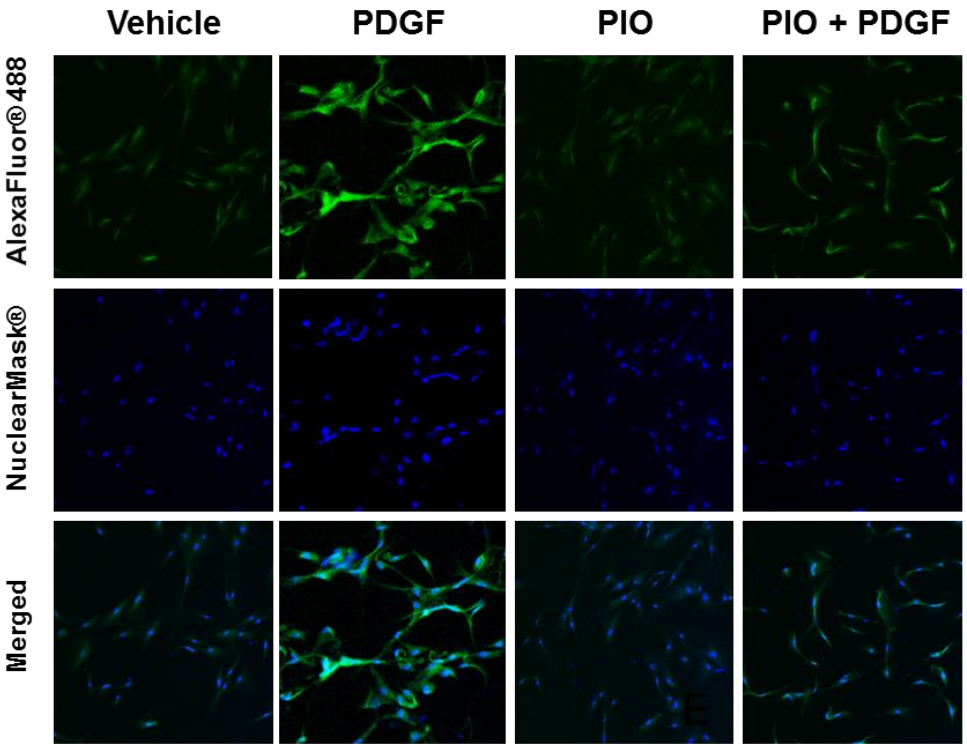

E

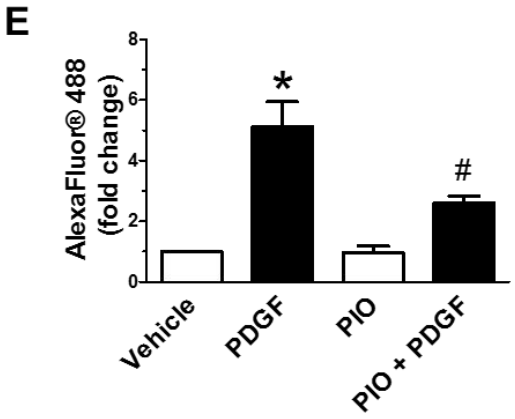

Fig. 3.6. Effects of AMPKα1 downregulation on PIO regulation of PDGF-induced signaling events. VSMCs were transfected with scrambled (Scr.), AMPKα1, or AMPKα2 siRNA followed by maintenance in culture for 48 hr. Subsequently, VSMCs were treated with: (**A-C**) PIO (30 μM, 48 hr) or vehicle control under serum-deprived conditions. VSMC lysates were then subjected to immunoblot analysis using primary antibodies specific for AMPKα1, AMPKα2, pAMPK and pACC. *$p < 0.05$ compared with scr. siRNA; or (**D-E**) PIO (30 μM, 30 min) or vehicle control followed by exposure to PDGF (30 ng/ml, 48 hr). VSMC lysates were then subjected to immunoblot analysis for pRaptor, pS6 and $p27^{kip1}$, pERK1/2, and cyclin D1. Immunoblots shown are representative of n = 3.

FIG. 3.6A-E

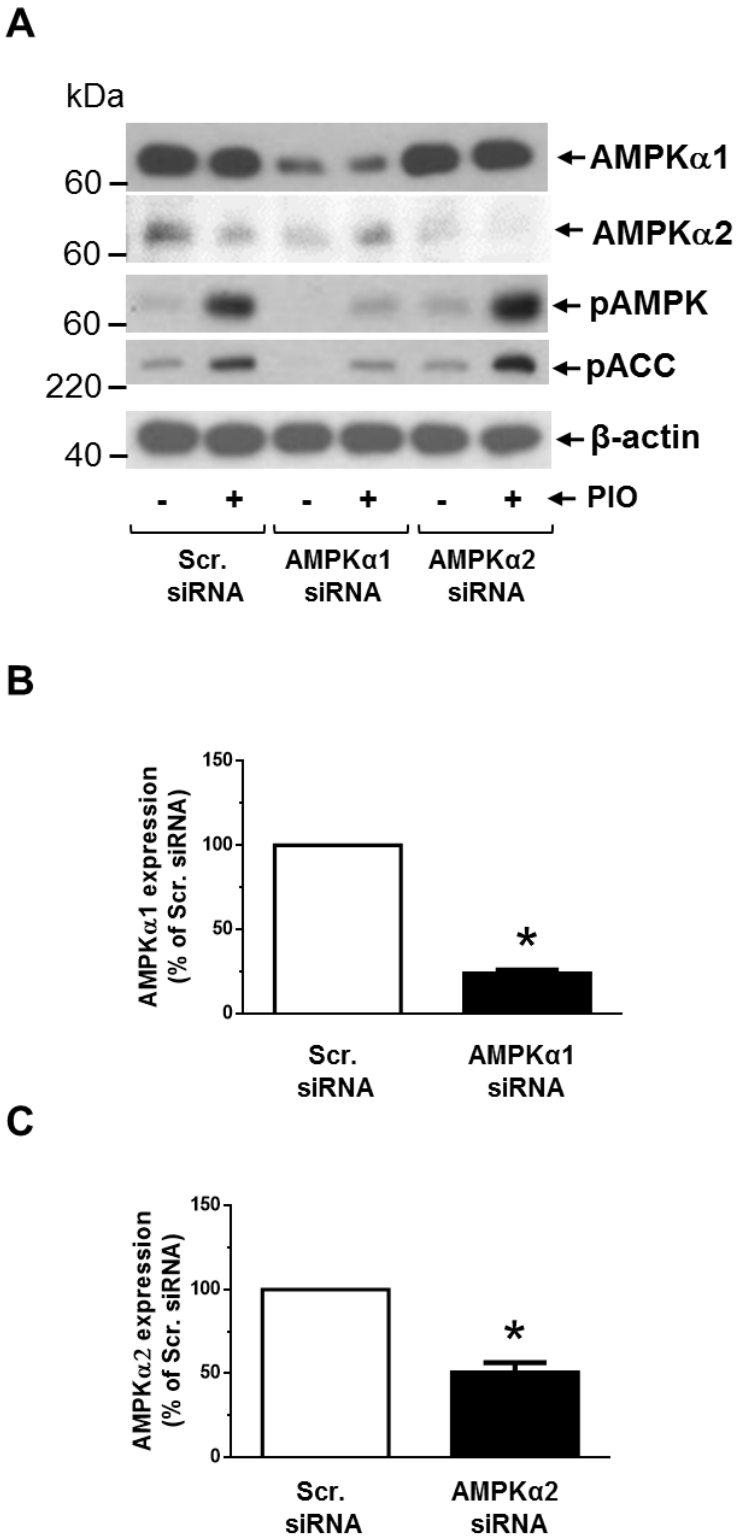
A
kDa
60
60
60
220
40
AMPKα1
AMPKα2
pAMPK
pACC
β-actin
- + - + - +
PIO
Scr. siRNA
AMPKα1 siRNA
AMPKα2 siRNA
B
AMPKα1 expression (% of Scr. siRNA)
150
100
50
0
*
Scr. siRNA
AMPKα1 siRNA
C
AMPKα2 expression (% of Scr. siRNA)
150
100
50
0
*
Scr. siRNA
AMPKα2 siRNA

FIG. 3.6A-E
continued

D

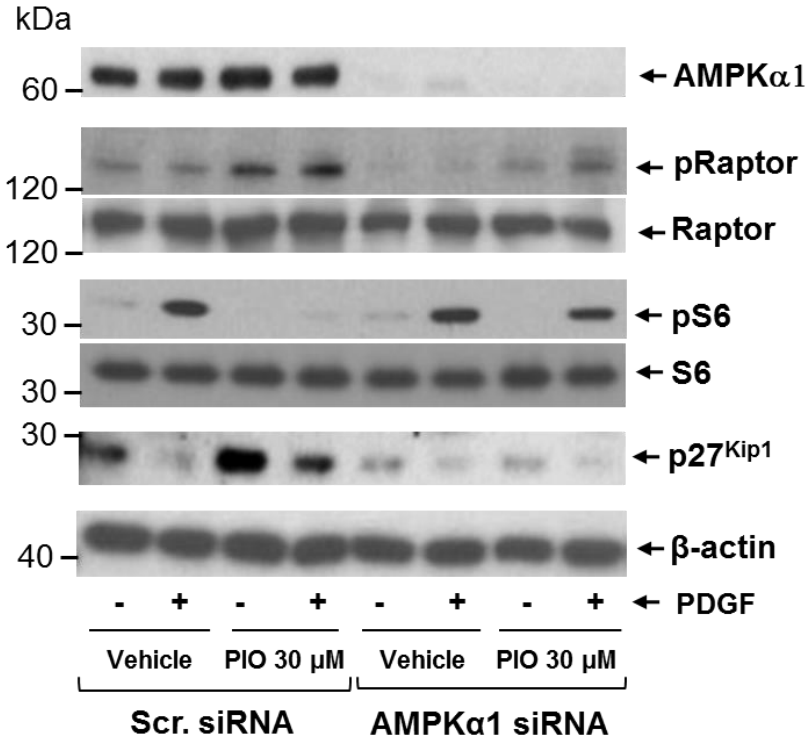

E

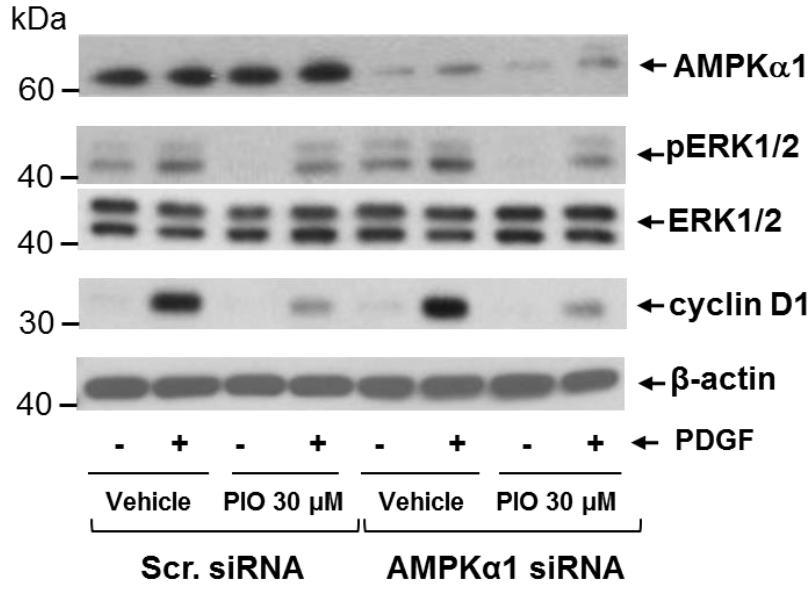

Fig. 3.7. Effects of PPARγ downregulation or PPARγ inhibition on PIO-induced changes in the phosphorylation of AMPK, S6, and ERK1/2, and cyclin D1 expression in VSMCs. **(A)** Serum-deprived VSMCs were treated with PIO (30 μM, 48 hr) or vehicle control. Subsequently, nuclear (Nuc.) and cytoplasmic (Cyt.) proteins (20 μg) were extracted for immunoblot analysis of PPARγ. Differentiated 3T3-L1 cell lysate (2 μg) was used as a positive control for the expression of PPARγ. Immunoblots shown are representative of n = 3. (**B-D**) VSMCs were transfected with scrambled (Scr.) or PPARγ siRNA followed by maintenance in culture for 48 hr. Subsequently, VSMCs were pretreated with PIO (30 μM, 30 min) or vehicle control followed by exposure to PDGF (30 ng/ml, 48 hr) under serum-deprived conditions. The respective VSMC lysates were then subjected to immunoblot analysis using primary antibodies specific for PPARγ, CD36, pAMPK, pS6, pERK1/2, and cyclin D1. *$p < 0.05$ compared with scr. siRNA. Immunoblots shown are representative of n = 3. (**E**) Serum-deprived VSMCs were pretreated with PPARγ inhibitor (GW-9662; 10 μM, 30 min) followed by exposure to PIO (30 μM, 30 min) or vehicle control and subsequent exposure to PDGF (30 ng/ml, 48 hr). VSMC lysates were then subjected to immunoblot analysis for pAMPK, pS6, pERK1/2 and cyclin D1. Immunoblots shown are representative of n = 3.

FIG. 3.7A-E

A

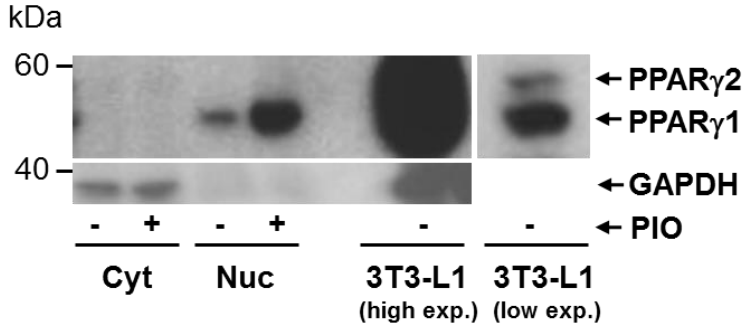
kDa
60
40
PPARγ2
PPARγ1
GAPDH
PIO
- + - + - -
Cyt
Nuc
3T3-L1 (high exp.)
3T3-L1 (low exp.)

B

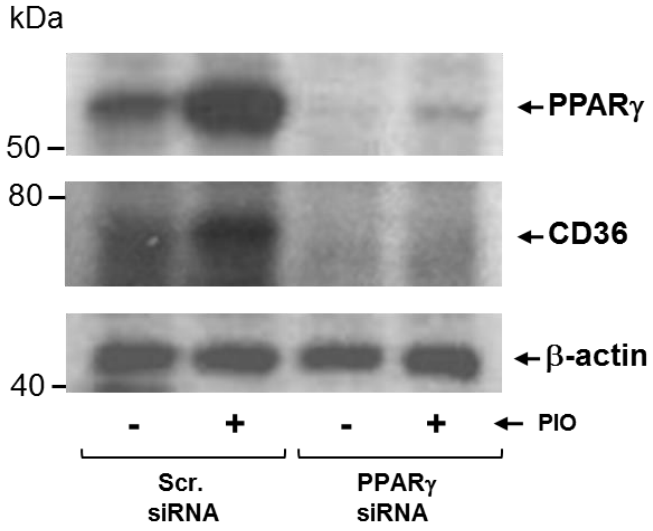
kDa
50
80
40
PPARγ
CD36
β-actin
- + - + PIO
Scr. siRNA
PPARγ siRNA

C

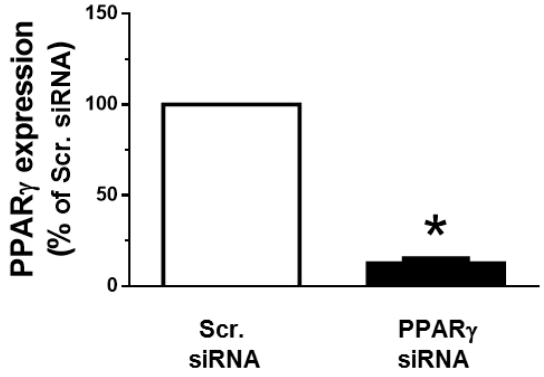
PPARγ expression (% of Scr. siRNA)
150
100
50
0
*
Scr. siRNA
PPARγ siRNA

FIG. 3.7A-E continued

D

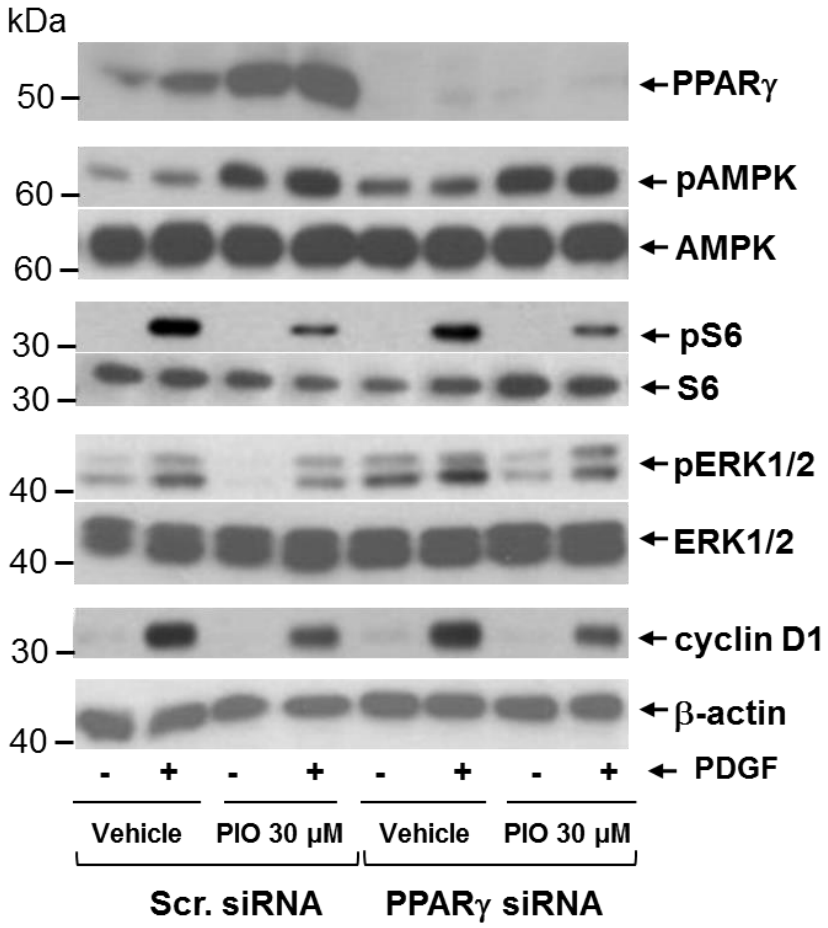

FIG. 3.7A-E
continued

E

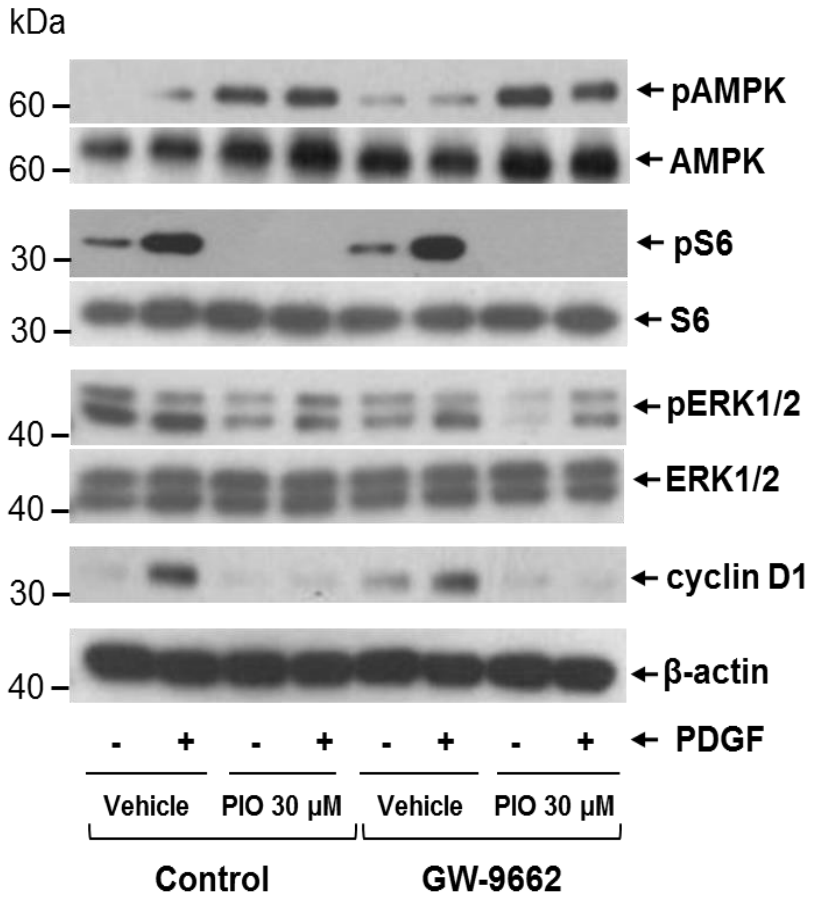

Fig. 3.8. PIO inhibits PDGF-induced VSMC proliferation *via* AMPK-dependent and AMPK-independent mechanisms. PIO activates AMPK to promote raptor phosphorylation, thereby inhibiting PDGF-induced mTOR/p70S6 kinase signaling to facilitate $p27^{kip1}$ accumulation. In addition, PIO inhibition of ERK1/2 phosphorylation (that occurs independently of AMPK or PPARγ) results in the suppression of cyclin D1 expression and Rb phosphorylation.

FIG. 3.8

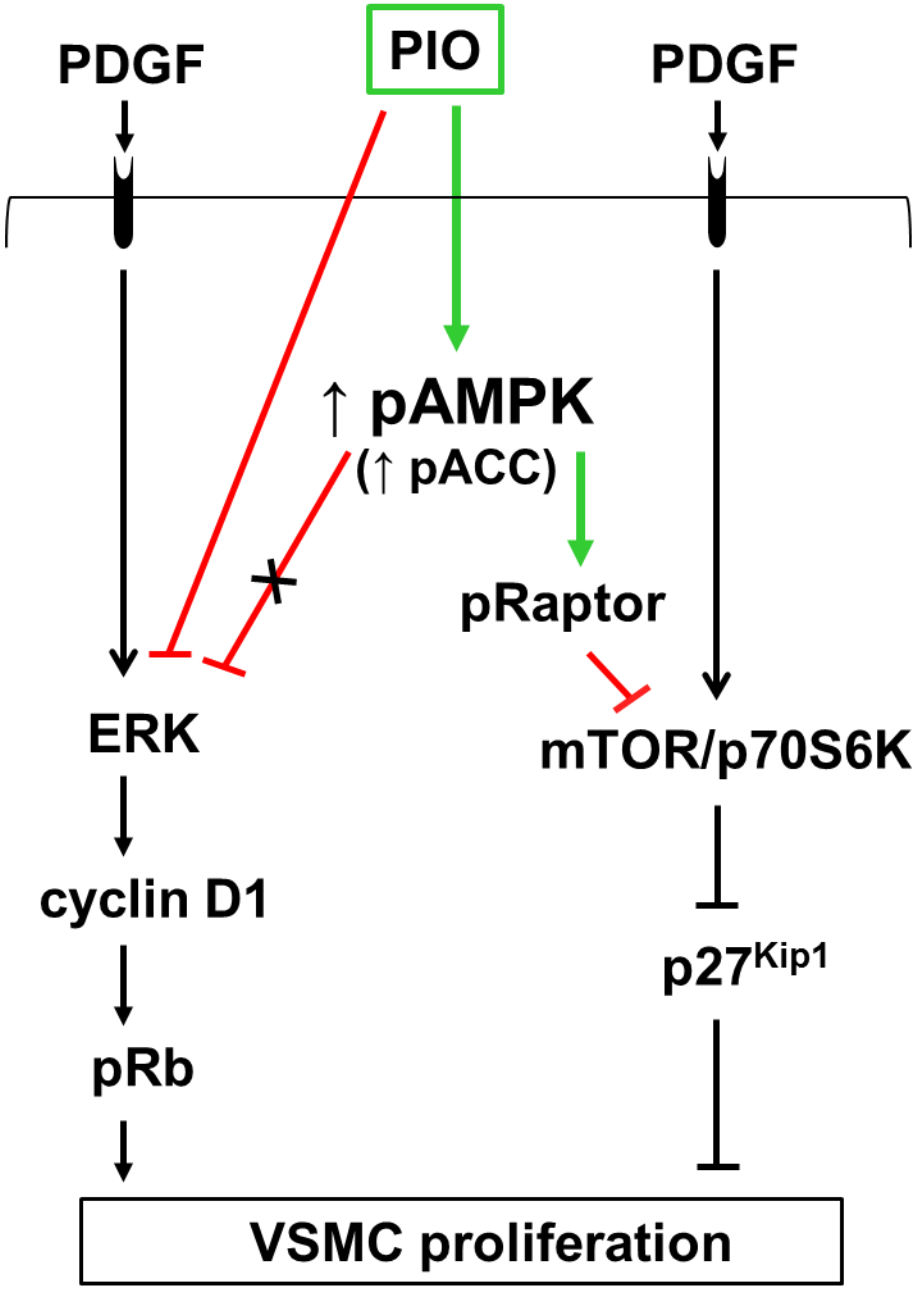
PDGF
PIO
PDGF
↑ pAMPK
(↑ pACC)
pRaptor
ERK
mTOR/p70S6K
cyclin D1
p27Kip1
pRb
VSMC proliferation

Bibliography

Arita, Y., S. Kihara, N. Ouchi, K. Maeda, H. Kuriyama, Y. Okamoto, M. Kumada, K. Hotta, M. Nishida, M. Takahashi, T. Nakamura, I. Shimomura, M. Muraguchi, Y. Ohmoto, T. Funahashi, and Y. Matsuzawa. 2002. Adipocyte-derived plasma protein adiponectin acts as a platelet-derived growth factor-BB-binding protein and regulates growth factor-induced common postreceptor signal in vascular smooth muscle cell. *Circulation* 105 (24):2893-8.

Benkirane, K., F. Amiri, Q. N. Diep, M. El Mabrouk, and E. L. Schiffrin. 2006. PPAR-gamma inhibits ANG II-induced cell growth via SHIP2 and 4E-BP1. *Am J Physiol Heart Circ Physiol* 290 (1):H390-7.

Benson, S., J. Wu, S. Padmanabhan, T. W. Kurtz, and H. A. Pershadsingh. 2000. Peroxisome proliferator-activated receptor (PPAR)-gamma expression in human vascular smooth muscle cells: inhibition of growth, migration, and c-fos expression by the peroxisome proliferator-activated receptor (PPAR)-gamma activator troglitazone. *Am J Hypertens* 13 (1 Pt 1):74-82.

Bishop-Bailey, D., T. Hla, and T. D. Warner. 2002. Intimal smooth muscle cells as a target for peroxisome proliferator-activated receptor-gamma ligand therapy. *Circ Res* 91 (3):210-7.

Boyle, J. G., P. J. Logan, M. A. Ewart, J. A. Reihill, S. A. Ritchie, J. M. Connell, S. J. Cleland, and I. P. Salt. 2008. Rosiglitazone stimulates nitric oxide synthesis in human aortic endothelial cells via AMP-activated protein kinase. *J Biol Chem* 283 (17):11210-7.

Braun-Dullaeus, R. C., M. J. Mann, U. Seay, L. Zhang, H. E. von Der Leyen, R. E. Morris, and V. J. Dzau. 2001. Cell cycle protein expression in vascular smooth muscle cells in vitro and in vivo is regulated through phosphatidylinositol 3-kinase and mammalian target of rapamycin. *Arterioscler Thromb Vasc Biol* 21 (7):1152-8.

Brunmair, B., K. Staniek, F. Gras, N. Scharf, A. Althaym, R. Clara, M. Roden, E. Gnaiger, H. Nohl, W. Waldhausl, and C. Furnsinn. 2004. Thiazolidinediones, like metformin, inhibit respiratory complex I: a common mechanism contributing to their antidiabetic actions? *Diabetes* 53 (4):1052-9.

Coletta, D. K., A. Sriwijitkamol, E. Wajcberg, P. Tantiwong, M. Li, M. Prentki, M. Madiraju, C. P. Jenkinson, E. Cersosimo, N. Musi, and R. A. Defronzo. 2009. Pioglitazone stimulates AMP-activated protein kinase signalling and increases the expression of genes involved in adiponectin signalling, mitochondrial function and fat oxidation in human skeletal muscle in vivo: a randomised trial. *Diabetologia* 52 (4):723-32.

de Dios, S. T., D. Bruemmer, R. J. Dilley, M. E. Ivey, G. L. Jennings, R. E. Law, and P. J. Little. 2003. Inhibitory activity of clinical thiazolidinedione peroxisome proliferator activating receptor-gamma ligands toward internal mammary artery, radial artery, and saphenous vein smooth muscle cell proliferation. *Circulation* 107 (20):2548-50.

Ding, M., A. C. Carrao, R. J. Wagner, Y. Xie, Y. Jin, E. M. Rzucidlo, J. Yu, W. Li, G. Tellides, J. Hwa, T. R. Aprahamian, and K. A. Martin. 2012. Vascular smooth

muscle cell-derived adiponectin: a paracrine regulator of contractile phenotype. *J Mol Cell Cardiol* 52 (2):474-84.

Ding, M., Y. Xie, R. J. Wagner, Y. Jin, A. C. Carrao, L. S. Liu, A. K. Guzman, R. J. Powell, J. Hwa, E. M. Rzucidlo, and K. A. Martin. 2011. Adiponectin induces vascular smooth muscle cell differentiation via repression of mammalian target of rapamycin complex 1 and FoxO4. *Arterioscler Thromb Vasc Biol* 31 (6):1403-10.

Divakaruni, A. S., S. E. Wiley, G. W. Rogers, A. Y. Andreyev, S. Petrosyan, M. Loviscach, E. A. Wall, N. Yadava, A. P. Heuck, D. A. Ferrick, R. R. Henry, W. G. McDonald, J. R. Colca, M. I. Simon, T. P. Ciaraldi, and A. N. Murphy. 2013. Thiazolidinediones are acute, specific inhibitors of the mitochondrial pyruvate carrier. *Proc Natl Acad Sci U S A* 110 (14):5422-7.

Dormandy, J. A., B. Charbonnel, D. J. Eckland, E. Erdmann, M. Massi-Benedetti, I. K. Moules, A. M. Skene, M. H. Tan, P. J. Lefebvre, G. D. Murray, E. Standl, R. G. Wilcox, L. Wilhelmsen, J. Betteridge, K. Birkeland, A. Golay, R. J. Heine, L. Koranyi, M. Laakso, M. Mokan, A. Norkus, V. Pirags, T. Podar, A. Scheen, W. Scherbaum, G. Schernthaner, O. Schmitz, J. Skrha, U. Smith, J. Taton, and P. ROactive investigators. 2005. Secondary prevention of macrovascular events in patients with type 2 diabetes in the PROactive Study (PROspective pioglitAzone Clinical Trial In macroVascular Events): a randomised controlled trial. *Lancet* 366 (9493):1279-89.

Fryer, L. G., A. Parbu-Patel, and D. Carling. 2002. The Anti-diabetic drugs rosiglitazone and metformin stimulate AMP-activated protein kinase through distinct signaling pathways. *J Biol Chem* 277 (28):25226-32.

Game, B. A., A. Maldonado, L. He, and Y. Huang. 2005. Pioglitazone inhibits MMP-1 expression in vascular smooth muscle cells through a mitogen-activated protein kinase-independent mechanism. *Atherosclerosis* 178 (2):249-56.

Goetze, S., X. P. Xi, K. Graf, E. Fleck, W. A. Hsueh, and R. E. Law. 1999. Troglitazone inhibits angiotensin II-induced extracellular signal-regulated kinase 1/2 nuclear translocation and activation in vascular smooth muscle cells. *FEBS Lett* 452 (3):277-82.

Gowans, G. J., S. A. Hawley, F. A. Ross, and D. G. Hardie. 2013. AMP is a true physiological regulator of AMP-activated protein kinase by both allosteric activation and enhancing net phosphorylation. *Cell Metab* 18 (4):556-66.

Guan, Y., C. Hao, D. R. Cha, R. Rao, W. Lu, D. E. Kohan, M. A. Magnuson, R. Redha, Y. Zhang, and M. D. Breyer. 2005. Thiazolidinediones expand body fluid volume through PPARgamma stimulation of ENaC-mediated renal salt absorption. *Nat Med* 11 (8):861-6.

Gwinn, D. M., D. B. Shackelford, D. F. Egan, M. M. Mihaylova, A. Mery, D. S. Vasquez, B. E. Turk, and R. J. Shaw. 2008. AMPK phosphorylation of raptor mediates a metabolic checkpoint. *Mol Cell* 30 (2):214-26.

Hanefeld, M. 2001. Pharmacokinetics and clinical efficacy of pioglitazone. *Int J Clin Pract Suppl* (121):19-25.

Hardie, D. G. 2008. AMPK and Raptor: matching cell growth to energy supply. *Mol Cell* 30 (3):263-5.

Hong, S. J., S. T. Kim, T. J. Kim, E. O. Kim, C. M. Ahn, J. H. Park, J. S. Kim, K. M. Lee, and D. S. Lim. 2010. Cellular and molecular changes associated with

inhibitory effect of pioglitazone on neointimal growth in patients with type 2 diabetes after zotarolimus-eluting stent implantation. *Arterioscler Thromb Vasc Biol* 30 (12):2655-65.

Hsueh, W. A., and R. E. Law. 2001. PPARgamma and atherosclerosis: effects on cell growth and movement. *Arterioscler Thromb Vasc Biol* 21 (12):1891-5.

Igarashi, M., A. Hirata, H. Yamaguchi, H. Tsuchiya, H. Ohnuma, M. Tominaga, M. Daimon, and T. Kato. 2001. Characterization of an inhibitory effect of pioglitazone on balloon-injured vascular smooth muscle cell growth. *Metabolism* 50 (8):955-62.

Igata, M., H. Motoshima, K. Tsuruzoe, K. Kojima, T. Matsumura, T. Kondo, T. Taguchi, K. Nakamaru, M. Yano, D. Kukidome, K. Matsumoto, T. Toyonaga, T. Asano, T. Nishikawa, and E. Araki. 2005. Adenosine monophosphate-activated protein kinase suppresses vascular smooth muscle cell proliferation through the inhibition of cell cycle progression. *Circ Res* 97 (8):837-44.

Inoki, K., J. Kim, and K. L. Guan. 2012. AMPK and mTOR in cellular energy homeostasis and drug targets. *Annu Rev Pharmacol Toxicol* 52:381-400.

Inzucchi, S. E., R. M. Bergenstal, J. B. Buse, M. Diamant, E. Ferrannini, M. Nauck, A. L. Peters, A. Tsapas, R. Wender, and D. R. Matthews. 2012. Management of hyperglycaemia in type 2 diabetes: a patient-centered approach. Position statement of the American Diabetes Association (ADA) and the European Association for the Study of Diabetes (EASD). *Diabetologia* 55 (6):1577-96.

Ishibashi, M., K. Egashira, K. Hiasa, S. Inoue, W. Ni, Q. Zhao, M. Usui, S. Kitamoto, T. Ichiki, and A. Takeshita. 2002. Antiinflammatory and antiarteriosclerotic effects of pioglitazone. *Hypertension* 40 (5):687-93.

Joner, M., K. Morimoto, H. Kasukawa, K. Steigerwald, S. Merl, G. Nakazawa, M. C. John, A. V. Finn, E. Acampado, F. D. Kolodgie, H. K. Gold, and R. Virmani. 2008. Site-specific targeting of nanoparticle prednisolone reduces in-stent restenosis in a rabbit model of established atheroma. *Arterioscler Thromb Vasc Biol* 28 (11):1960-6.

Kadowaki, T., T. Yamauchi, N. Kubota, K. Hara, K. Ueki, and K. Tobe. 2006. Adiponectin and adiponectin receptors in insulin resistance, diabetes, and the metabolic syndrome. *J Clin Invest* 116 (7):1784-92.

Kahn, B. B., T. Alquier, D. Carling, and D. G. Hardie. 2005. AMP-activated protein kinase: ancient energy gauge provides clues to modern understanding of metabolism. *Cell Metab* 1 (1):15-25.

Kahn, S. E., S. M. Haffner, M. A. Heise, W. H. Herman, R. R. Holman, N. P. Jones, B. G. Kravitz, J. M. Lachin, M. C. O'Neill, B. Zinman, G. Viberti, and Adopt Study Group. 2006. Glycemic durability of rosiglitazone, metformin, or glyburide monotherapy. *N Engl J Med* 355 (23):2427-43.

Kaul, S., A. F. Bolger, D. Herrington, R. P. Giugliano, and R. H. Eckel. 2010. Thiazolidinedione drugs and cardiovascular risks: a science advisory from the American Heart Association and American College of Cardiology Foundation. *Circulation* 121 (16):1868-77.

Kim, E. J., Y. K. Choi, Y. H. Han, H. J. Kim, I. K. Lee, and M. O. Lee. 2014. RORalpha suppresses proliferation of vascular smooth muscle cells through activation of AMP-activated protein kinase. *Int J Cardiol* 175 (3):515-21.

Konrad, D., A. Rudich, P. J. Bilan, N. Patel, C. Richardson, L. A. Witters, and A. Klip. 2005. Troglitazone causes acute mitochondrial membrane depolarisation and an AMPK-mediated increase in glucose phosphorylation in muscle cells. *Diabetologia* 48 (5):954-66.

Law, R. E., S. Goetze, X. P. Xi, S. Jackson, Y. Kawano, L. Demer, M. C. Fishbein, W. P. Meehan, and W. A. Hsueh. 2000. Expression and function of PPARgamma in rat and human vascular smooth muscle cells. *Circulation* 101 (11):1311-8.

Law, R. E., W. P. Meehan, X. P. Xi, K. Graf, D. A. Wuthrich, W. Coats, D. Faxon, and W. A. Hsueh. 1996. Troglitazone inhibits vascular smooth muscle cell growth and intimal hyperplasia. *J Clin Invest* 98 (8):1897-905.

Lee, C. S., Y. W. Kwon, H. M. Yang, S. H. Kim, T. Y. Kim, J. Hur, K. W. Park, H. J. Cho, H. J. Kang, Y. B. Park, and H. S. Kim. 2009. New mechanism of rosiglitazone to reduce neointimal hyperplasia: activation of glycogen synthase kinase-3beta followed by inhibition of MMP-9. *Arterioscler Thromb Vasc Biol* 29 (4):472-9.

Lee, K. P., G. W. Sudjarwo, S. H. Jung, D. Lee, D. Y. Lee, G. B. Lee, S. Baek, D. Y. Kim, H. M. Lee, B. Kim, S. C. Kwon, and K. J. Won. 2015. Carvacrol inhibits atherosclerotic neointima formation by downregulating reactive oxygen species production in vascular smooth muscle cells. *Atherosclerosis* 240 (2):367-73.

Li, J. M., S. Wheatcroft, L. M. Fan, M. T. Kearney, and A. M. Shah. 2004. Opposing roles of p47phox in basal versus angiotensin II-stimulated alterations in vascular O2- production, vascular tone, and mitogen-activated protein kinase activation. *Circulation* 109 (10):1307-13.

Lincoff, A. M., K. Wolski, S. J. Nicholls, and S. E. Nissen. 2007. Pioglitazone and risk of cardiovascular events in patients with type 2 diabetes mellitus: a meta-analysis of randomized trials. *Jama* 298 (10):1180-8.

Ma, X. M., and J. Blenis. 2009. Molecular mechanisms of mTOR-mediated translational control. *Nat Rev Mol Cell Biol* 10 (5):307-18.

Martin, A., J. V. Perez-Giron, R. Hernanz, R. Palacios, A. M. Briones, A. Fortuno, G. Zalba, M. Salaices, and M. J. Alonso. 2012. Peroxisome proliferator-activated receptor-gamma activation reduces cyclooxygenase-2 expression in vascular smooth muscle cells from hypertensive rats by interfering with oxidative stress. *J Hypertens* 30 (2):315-26.

Martinet, W., H. De Loof, and G. R. De Meyer. 2014. mTOR inhibition: a promising strategy for stabilization of atherosclerotic plaques. *Atherosclerosis* 233 (2):601-7.

Meredith, D., M. Panchatcharam, S. Miriyala, Y. S. Tsai, A. J. Morris, N. Maeda, G. A. Stouffer, and S. S. Smyth. 2009. Dominant-negative loss of PPARgamma function enhances smooth muscle cell proliferation, migration, and vascular remodeling. *Arterioscler Thromb Vasc Biol* 29 (4):465-71.

Motobayashi, Y., Y. Izawa-Ishizawa, K. Ishizawa, S. Orino, K. Yamaguchi, K. Kawazoe, S. Hamano, K. Tsuchiya, S. Tomita, and T. Tamaki. 2009. Adiponectin inhibits insulin-like growth factor-1-induced cell migration by the suppression of

extracellular signal-regulated kinase 1/2 activation, but not Akt in vascular smooth muscle cells. *Hypertens Res* 32 (3):188-93.

Nagahama, R., T. Matoba, K. Nakano, S. Kim-Mitsuyama, K. Sunagawa, and K. Egashira. 2012. Nanoparticle-mediated delivery of pioglitazone enhances therapeutic neovascularization in a murine model of hindlimb ischemia. *Arterioscler Thromb Vasc Biol* 32 (10):2427-34.

Nagata, D., R. Takeda, M. Sata, H. Satonaka, E. Suzuki, T. Nagano, and Y. Hirata. 2004. AMP-activated protein kinase inhibits angiotensin II-stimulated vascular smooth muscle cell proliferation. *Circulation* 110 (4):444-51.

Nesto, R. W., D. Bell, R. O. Bonow, V. Fonseca, S. M. Grundy, E. S. Horton, M. Le Winter, D. Porte, C. F. Semenkovich, S. Smith, L. H. Young, R. Kahn, Association American Heart, and Association American Diabetes. 2003. Thiazolidinedione use, fluid retention, and congestive heart failure: a consensus statement from the American Heart Association and American Diabetes Association. October 7, 2003. *Circulation* 108 (23):2941-8.

Ning, J., and D. R. Clemmons. 2010. AMP-activated protein kinase inhibits IGF-I signaling and protein synthesis in vascular smooth muscle cells via stimulation of insulin receptor substrate 1 S794 and tuberous sclerosis 2 S1345 phosphorylation. *Mol Endocrinol* 24 (6):1218-29.

Owens, G. K., M. S. Kumar, and B. R. Wamhoff. 2004. Molecular regulation of vascular smooth muscle cell differentiation in development and disease. *Physiol Rev* 84 (3):767-801.

Perez-Giron, J. V., R. Palacios, A. Martin, R. Hernanz, A. Aguado, S. Martinez-Revelles, M. T. Barrus, M. Salaices, and M. J. Alonso. 2014. Pioglitazone reduces angiotensin II-induced COX-2 expression through inhibition of ROS production and ET-1 transcription in vascular cells from spontaneously hypertensive rats. *Am J Physiol Heart Circ Physiol* 306 (11):H1582-93.

Peuler, J. D., S. M. Phare, A. R. Iannucci, and M. J. Hodorek. 1996. Differential inhibitory effects of antidiabetic drugs on arterial smooth muscle cell proliferation. *Am J Hypertens* 9 (2):188-92.

Phillips, J. W., K. G. Barringhaus, J. M. Sanders, Z. Yang, M. Chen, S. Hesselbacher, A. C. Czarnik, K. Ley, J. Nadler, and I. J. Sarembock. 2003. Rosiglitazone reduces the accelerated neointima formation after arterial injury in a mouse injury model of type 2 diabetes. *Circulation* 108 (16):1994-9.

Pyla, R., I. Osman, P. Pichavaram, P. Hansen, and L. Segar. 2014. Metformin exaggerates phenylephrine-induced AMPK phosphorylation independent of CaMKKbeta and attenuates contractile response in endothelium-denuded rat aorta. *Biochem Pharmacol*.

Pyla, R., N. Poulose, J. Y. Jun, and L. Segar. 2013. Expression of conventional and novel glucose transporters, GLUT1, -9, -10, and -12, in vascular smooth muscle cells. *Am J Physiol Cell Physiol* 304 (6):C574-89.

Ross, R. 1999. Atherosclerosis--an inflammatory disease. *N Engl J Med* 340 (2):115-26.

Saha, A. K., P. R. Avilucea, J. M. Ye, M. M. Assifi, E. W. Kraegen, and N. B. Ruderman. 2004. Pioglitazone treatment activates AMP-activated protein kinase

in rat liver and adipose tissue in vivo. *Biochem Biophys Res Commun* 314 (2):580-5.

Saha, A. K., X. J. Xu, E. Lawson, R. Deoliveira, A. E. Brandon, E. W. Kraegen, and N. B. Ruderman. 2010. Downregulation of AMPK accompanies leucine- and glucose-induced increases in protein synthesis and insulin resistance in rat skeletal muscle. *Diabetes* 59 (10):2426-34.

Satoh, N., Y. Ogawa, T. Usui, T. Tagami, S. Kono, H. Uesugi, H. Sugiyama, A. Sugawara, K. Yamada, A. Shimatsu, H. Kuzuya, and K. Nakao. 2003. Antiatherogenic effect of pioglitazone in type 2 diabetic patients irrespective of the responsiveness to its antidiabetic effect. *Diabetes Care* 26 (9):2493-9.

Sengupta, S., T. R. Peterson, and D. M. Sabatini. 2010. Regulation of the mTOR complex 1 pathway by nutrients, growth factors, and stress. *Mol Cell* 40 (2):310-22.

Staels, B., W. Koenig, A. Habib, R. Merval, M. Lebret, I. P. Torra, P. Delerive, A. Fadel, G. Chinetti, J. C. Fruchart, J. Najib, J. Maclouf, and A. Tedgui. 1998. Activation of human aortic smooth-muscle cells is inhibited by PPARalpha but not by PPARgamma activators. *Nature* 393 (6687):790-3.

Stone, J. D., A. Narine, P. R. Shaver, J. C. Fox, J. R. Vuncannon, and D. A. Tulis. 2013. AMP-activated protein kinase inhibits vascular smooth muscle cell proliferation and migration and vascular remodeling following injury. *Am J Physiol Heart Circ Physiol* 304 (3):H369-81.

Subramanian, V., J. Golledge, T. Ijaz, D. Bruemmer, and A. Daugherty. 2010. Pioglitazone-induced reductions in atherosclerosis occur via smooth muscle cell-specific interaction with PPAR{gamma}. *Circ Res* 107 (8):953-8.

Tanner, F. C., M. Boehm, L. M. Akyurek, H. San, Z. Y. Yang, J. Tashiro, G. J. Nabel, and E. G. Nabel. 2000. Differential effects of the cyclin-dependent kinase inhibitors p27(Kip1), p21(Cip1), and p16(Ink4) on vascular smooth muscle cell proliferation. *Circulation* 101 (17):2022-5.

Uemura, Y., R. Shibata, N. Kanemura, K. Ohashi, T. Kambara, M. Hiramatsu-Ito, T. Enomoto, D. Yuasa, Y. Joki, K. Matsuo, M. Ito, S. Hayakawa, H. Ogawa, T. Murohara, and N. Ouchi. 2015. Adipose-derived protein omentin prevents neointimal formation after arterial injury. *Faseb j* 29 (1):141-51.

Vasamsetti, S. B., S. Karnewar, A. K. Kanugula, A. R. Thatipalli, J. M. Kumar, and S. Kotamraju. 2015. Metformin inhibits monocyte-to-macrophage differentiation via AMPK-mediated inhibition of STAT3 activation: potential role in atherosclerosis. *Diabetes* 64 (6):2028-41.

Wakino, S., U. Kintscher, S. Kim, F. Yin, W. A. Hsueh, and R. E. Law. 2000. Peroxisome proliferator-activated receptor gamma ligands inhibit retinoblastoma phosphorylation and G1--> S transition in vascular smooth muscle cells. *J Biol Chem* 275 (29):22435-41.

Yoshimoto, T., M. Naruse, H. Shizume, K. Naruse, A. Tanabe, M. Tanaka, K. Tago, K. Irie, T. Muraki, H. Demura, and L. Zardi. 1999. Vasculo-protective effects of insulin sensitizing agent pioglitazone in neointimal thickening and hypertensive vascular hypertrophy. *Atherosclerosis* 145 (2):333-40.

Young, P. W., D. R. Buckle, B. C. Cantello, H. Chapman, J. C. Clapham, P. J. Coyle, D. Haigh, R. M. Hindley, J. C. Holder, H. Kallender, A. J. Latter, K. W. Lawrie, D. Mossakowska, G. J. Murphy, L. Roxbee Cox, and S. A. Smith. 1998.

Identification of high-affinity binding sites for the insulin sensitizer rosiglitazone (BRL-49653) in rodent and human adipocytes using a radioiodinated ligand for peroxisomal proliferator-activated receptor gamma. *J Pharmacol Exp Ther* 284 (2):751-9.

Yu, W., R. Liu-Bryan, S. Stevens, J. K. Damanahalli, and R. Terkeltaub. 2012. RAGE signaling mediates post-injury arterial neointima formation by suppression of liver kinase B1 and AMPK activity. *Atherosclerosis* 222 (2):417-25.

Zhang, H., A. Zhang, D. E. Kohan, R. D. Nelson, F. J. Gonzalez, and T. Yang. 2005. Collecting duct-specific deletion of peroxisome proliferator-activated receptor gamma blocks thiazolidinedione-induced fluid retention. *Proc Natl Acad Sci U S A* 102 (26):9406-11.

Zhang, L. L., C. Y. Gao, C. Q. Fang, Y. J. Wang, D. Gao, G. E. Yao, J. Xiang, J. Z. Wang, and J. C. Li. 2011. PPARgamma attenuates intimal hyperplasia by inhibiting TLR4-mediated inflammation in vascular smooth muscle cells. *Cardiovasc Res* 92 (3):484-93.

Zhao, Y., S. K. Biswas, P. H. McNulty, M. Kozak, J. Y. Jun, and L. Segar. 2011. PDGF-induced vascular smooth muscle cell proliferation is associated with dysregulation of insulin receptor substrates. *Am J Physiol Cell Physiol* 300 (6):C1375-85.

CHAPTER 4

PIOGLITAZONE ACTIVATES AMP-ACTIVATED PROTEIN KINASE *VIA* CAMKKβ IN VASCULAR SMOOTH MUSCLE CELLS AND INHIBITS NEOINTIMA FORMATION *IN VIVO* (**Osman** et al 2016)

Islam Osman, Arwa Fairaq, Lakshman Segar

To be submitted to Journal of Pharmacology

Abstract:

Despite the recent advances in drug-eluting stents, restenosis remains the major complication of coronary angioplasty. Pioglitazone (PIO), a classical insulin sensitizer that belongs to the family of peroxisome proliferator-activated receptor-γ (PPARγ) agonists, reduces intimal hyperplasia after coronary angioplasty in diabetic and nondiabetic subjects. However, the molecular mechanisms by which PIO inhibits neointima formation are not fully understood. We recently reported that PIO activates AMP-activated protein kinase (AMPK) in vascular smooth muscle cells (VSMCs) leading to inhibition of key proliferative signaling. However, the likely intermediary role of AMPK toward PIO inhibition of neointima formation remains unclear. Using genetic and pharmacological approaches, we demonstrate that $Ca2^{+}$/calmodulin-dependent protein kinase kinase-beta (CaMKKβ) is the major upstream kinase responsible for PIO activation of AMPK in human aortic VSMCs. In addition, we demonstrate that PIO-mediated inhibition of neointima formation is associated with AMPK activation in the vessel wall. Importantly, inhibition of AMPK by compound C reveals that PIO inhibits neointima formation *via* AMPK-dependent and -independent mechanisms. Altogether, our findings suggest that local delivery of PIO at the lesion site may limit restenosis after angioplasty without inducing PPARγ-mediated systemic adverse effects.

Introduction

Annually, ~500,000 patients undergo coronary angioplasty procedures in the U.S. alone (Go et al. 2014). Despite the recent advances in percutaneous coronary intervention, restenosis still occurs in ~10% of patients (Cassese et al. 2014; Mauri et al.

2008) and remains a major complication of coronary angioplasty, especially in diabetic patients (Scheen, Warzee, and Legrand 2004). Neointima formation characterized by enhanced proliferation of vascular smooth muscle cells (VSMCs) plays a major role in the development of restenosis after angioplasty (Ross 1999; Owens, Kumar, and Wamhoff 2004). Drug-eluting stent (e.g., rapamycin) has been shown to reduce the recurrence of restenosis (van der Hoeven et al. 2005) but is also associated with impaired re-endothelialization (Hofma et al. 2006).

Thiazolidinediones (TZDs) have been demonstrated to exhibit salutary effects in the vasculature (Yoshimoto et al. 1999; Phillips et al. 2003; Satoh et al. 2003) beyond their insulin-sensitizing action in patients with type 2 diabetes (Kahn et al. 2006). TZDs have strong inhibitory effects on mitogen-induced VSMC proliferation *in vitro* (Law et al. 2000; de Dios et al. 2003; Osman and Segar 2016) and injury-induced neointima formation *in vivo* (Law et al. 1996; Aizawa et al. 2001; Igarashi et al. 2001). However, the signaling mechanisms mediating TZD inhibition of neointima formation are not fully understood. We have recently reported that pioglitazone (PIO), a clinically available TZD, activates AMPK in a sustained manner in human aortic VSMCs, thereby leading to inhibition of VSMC proliferation *via* inhibition of mTOR/p70S6K signaling (Osman and Segar 2016). In addition, we reported that PIO activation of AMPK is neither associated with an increase in AMP/ATP ratio nor mitochondrial-membrane depolarization and is likely independent of the upstream kinase, liver kinase B1 (LKB1) (Osman and Segar 2016). In addition to LKB1, AMPK can be phosphorylated at Thr^{172}, and thus activated, by $Ca2^{+}$/calmodulin-dependent protein kinase kinase-beta (CaMKKβ) in response to high cytosolic free calcium levels (Hawley et al. 2005; Woods et al. 2005). However, the

intermediary role of CaMKKβ in mediating TZD activation of AMPK in VSMC is yet to be examined.

TZDs can activate AMPK in different tissues in experimental animals (Saha et al. 2004; LeBrasseur et al. 2006; Lessard et al. 2006; Morisaki et al. 2011). Hence, it is critically important to examine the likely intermediary role of AMPK toward TZD suppression of neointima formation *in vivo*. The objectives of the present study using human aortic VSMCs and CJ57BL/6 mice are to determine: i) the intermediary role of CaMKKβ in mediating PIO activation of AMPK in VSMC; ii) the extent to which PIO regulates the phosphorylation of AMPK in mouse aortic tissue *in vivo*; and iii) the likely intermediary role of AMPK toward PIO inhibition of neointima formation *in vivo*.

Materials and methods

Materials

Pioglitazone and compound C were purchased from Cayman Chemical Company (Ann Arbor, MI). All surgical tools were purchased from Roboz Surgical Instrument (Gaithersburg, MD). The primary antibodies for phospho-AMPKα^{Thr172} (2535), pan-AMPKα (2532), phospho-ACC^{Ser79} (11818), ACC (3676), LKB1 (3047), and β-actin (8457) were purchased from Cell Signaling Technology (Danvers, MA). The primary antibody for SM α-actin (ab5694) was purchased from Abcam (Cambridge, MA). The primary antibody for CaMKKβ was purchased from Bethyl Laboratories (Montgomery, TX). LKB1 and CaMKKβ Silencer® Select siRNAs, scrambled siRNA, goat anti-Rabbit IgG secondary antibody Alexa Fluor® 594 conjugate (A-11037) and prolong gold anti-

fade mountant with DAPI (P36931) were purchased from Life Technologies (Carlsbad, CA). STO-609 was purchased from Tocris Bioscience (Minneapolis, MN). All other chemicals were from Fisher Scientific (Fair Lawn, NJ) or Sigma Chemical (St. Louis, MO).

Animals

All animal experiments were performed in accordance with the Charlie Norwood Veterans Affairs Medical Center Institutional Animal Care and Use Committee guidelines and were approved by the committee. Male C57BL/6J mice (12 weeks of age, Jackson Laboratories, Bar Harbor, ME) were maintained in a room at a controlled temperature of 23°C with a 12:12-hr dark-light cycle and fed regular chow. For all surgical procedures, mice were anesthetized with isoflurane via inhalation (1-4% in oxygen).

Femoral artery guidewire injury and treatments

Guidewire injury was performed on CJ57BL/6 mice as previously described by Sata *et al* (Sata et al. 2000). Briefly, the injury was induced by inserting a straight spring wire (0.38 mm in diameter; Cook, Bloomington, IN) from the exposed muscular branch artery into the left femoral artery for >5 mm toward the iliac artery. The wire was left in place for 1 minute to denude and dilate the femoral artery. Then, the wire was removed and the proximal portion of the muscular branch artery was secured with silk sutures and blood flow was restored in the left femoral artery. The right femoral artery was not subjected to guidewire injury and therefore served as sham-operated controls. PIO (20 mg/kg/d) as a

suspension in 0.5% carboxymethylcellulose (CMC) or vehicle (0.5% CMC) treatments were initiated one day before surgery and were administered daily for three weeks until sacrifice. In select experiments, AMPK inhibitor compound C (20 mg/kg, every other day) dissolved in DMSO or vehicle (DMSO) were injected intraperitoneally every other day from one day before surgery until sacrifice (Uemura et al. 2014). Three weeks after arterial injury, mice were euthanized with isoflurane *via* inhalation and perfused at a constant pressure via the left ventricle with 0.9% NaCl solution, followed by perfusion fixation in 4% paraformaldehyde (PFA) in PBS, pH 7.4. The femoral artery was carefully excised, further fixed in 4% PFA overnight at 4°C, then washed in deionized water and kept in sucrose 30% for 24 hr at 4°C before cryosection.

Morphometric analysis of femoral artery

Cross-sections (5 µm) of femoral artery were stained with haematoxylin and eosin (H&E) for examination of overall morphology or elastica van Gieson's (EVG) to depict the internal elastic lamina (IEL) and the external elastic lamina (EEL), and the images were taken by AxioCam high-resolution camera (HRc) attached to an Observer Z1 microscope (Carl Zeiss Microimaging, Inc., Thornwood, NY). Sections were analyzed for intima-to-media ratios using image analysis software (Axiovision, release 4.8.2 SP3). The intimal area was determined by subtraction of the luminal area from the IEL area (i.e., intimal area = IEL area - luminal area). The medial area was determined by subtraction of the IEL area from the EEL area (i.e., medial area = EEL area - IEL area) (Basi et al. 2007).

Immunofluorescence analysis of femoral artery

Cross-sections (5 μm) of femoral artery were fixed in 4% PFA, and then blocked by incubation with 5% normal goat serum/0.3% Triton-x 100 in PBS for 1 hr. Subsequently, sections were exposed to the primary antibody specific for SM α-actin (1:200) for 1 hr at room temperature, washed 3 times with PBS, and then incubated with the secondary antibody (goat anti-rabbit IgG conjugated to Alexa fluor 594) for 1 hr at room temperature. Sections were mounted using prolong antifade with DAPI and the images were captured using a confocal microscope (Zeiss, Thornwood, NY).

Extraction and quantification of proteins in aortic tissues

Mice were euthanized with isoflurane via inhalation and perfused at a constant pressure via the left ventricle with 0.9% NaCl solution, then aortic tissues were carefully excised and cleared from fat and connective tissue, rinsed in ice-cold fresh phosphate-buffered saline, blotted to dryness, snap-frozen in liquid nitrogen, and stored at -80 °C until analysis. Aortic tissues were thawed and homogenized in 100 ml RIPA lysis buffer containing protease and phosphatase inhibitors (Thermo Scientific, Rockford, IL) using TissueLyser LT (Qiagen,Valencia, CA) at a setting of 50 Hz for 5 min with samples being placed on ice intermittently. The homogenates were incubated at 4 °C for 1 h on a rotator and centrifuged at 1000 x g for 10 min at 4 °C to remove tissue debris. The supernatants were mixed with 2x Laemmli sample buffer at a ratio of 1:1 followed by heating at 67.5 °C for 10 min. Proteins were quantified using Bio-Rad DC assay kit (Bio-Rad, Hercules, CA).

Cell culture and treatments

Human aortic VSMCs, vascular cell basal medium and smooth muscle growth supplement (SMGS) were purchased from ATCC (Manassas, VA). SMGS constituents and their final concentrations after addition to vascular cell basal medium were as follows: 5% FBS (vol/vol), 5 ng/ml human basic fibroblast growth factor, 5 ng/ml human epidermal growth factor, 5 μg/ml insulin, 50 μg/mL ascorbic acid, 10 mM L-Glutamine. VSMCs (passages 3–5) were incubated in vascular cell basal medium containing SMGS (complete medium) and 5.5 mM D-glucose along with antibiotic/antimycotic solution in a humidified atmosphere of 95% air and 5% CO_2 at 37°C. After the attainment of confluence (~6–7 days), VSMCs were trypsinized, centrifuged, and seeded onto Petri dishes or multiwell plates. Subconfluent VSMCs were maintained under SMGS (serum)-deprived conditions for 48 hours to achieve quiescence and then subjected to treatments as described in the legends to the respective figures. DMSO (0.1%) was used as the vehicle control for PIO treatment.

Immunoblot analysis

Immunoblot analysis was performed as described (Osman and Segar 2016). Mouse aortic tissue or VSMC lysates (20 μg protein per lane) were subjected to electrophoresis using precast 4–12% NuPage mini-gels (Life Technologies). The resolved proteins were then transferred to PVDF membranes (EMD Millipore, Billerica, MA). Subsequently, the membranes were blocked in 5% nonfat milk and probed with the respective primary antibodies. The immunoreactivity was detected using HRP-conjugated horse anti-mouse secondary antibody (7076; Cell Signaling) or goat anti-rabbit secondary antibody (7074;

Cell Signaling) followed by enhanced chemiluminescence (ECL; Thermo Scientific, Wilmington, DE). The protein bands were quantified by densitometric analysis using Image J.

Nucleofection of VSMCs with target-specific siRNAs

Subconfluent VSMCs were transfected with 500 pmoles of target-specific Silencer® Select Pre-Designed siRNAusing Amaxa nucleofector-II device U-025 program (Lonza, Germany), as previously described (Osman and Segar 2016). The scrambled siRNA- and target-specific siRNA-transfected VSMCs were incubated in complete medium for 48 hr. Subsequently, VSMCs were serum-deprived for 24 hr and then subjected to treatments as described in the legends to the respective figures.

Statistical analysis

Results are expressed as the means ± SEM of at least three separate experiments. Statistical analyses of the data were performed using one-way analysis of variance (ANOVA) followed by Bonferroni t-test for data involving more than two groups, or unpaired two-tailed t-test for data involving two groups only. Values of $p < 0.05$ were considered statistically significant.

Results

PIO activates AMPK in a CaMKKβ-dependent manner

We have recently reported that PIO activates AMPK in human aortic VSMCs (Osman and Segar 2016). In addition, we reported that PIO-induced AMPK activation is not

accompanied by changes in mitochondrial-membrane potential or adenine nucleotide levels, and remains essentially the same even after LKB1 downregulation (Osman and Segar 2016). In the current study, we investigated if PIO activation of AMPK in VSMCs is dependent on CaMKKβ, another key upstream kinase of AMPK (Hawley et al. 2005; Hurley et al. 2005; Woods et al. 2005). As shown in **Fig. 4.1A-C**, transfection of VSMCs with target-specific siRNA led to downregulation of LKB1 and CaMKKβ protein expression by ~73 ± 4% and ~76 ± 5%, respectively. Notably, downregulation of CaMKKβ, but not LKB1, resulted in a significant reduction of basal phosphorylation of AMPK by ~93 ± 2%, and PIO-induced phosphorylation of AMPK by ~74 ± 11% (**Fig. 4.1A**). In addition, pretreatment of VSMCs with STO-609 (10 μM, 30 min), a pharmacological inhibitor of CaMKKβ (Tokumitsu et al. 2002), reduced PIO-induced phosphorylation of AMPK at 24 and 48 hr time points by 66 ± 10% and 80 ± 3%, respectively (**Fig. 4.2**). Similarly, pretreatment with STO-609 reduced PIO-induced phosphorylation of acetyl-CoA carboxylase (ACC), a key downstream target of AMPK (Kahn et al. 2005) at 24 and 48 hr time points. Together, these data indicate the PIO activates AMPK in a CaMKKβ-dependent manner in VSMCs.

PIO inhibits neointima formation in CJ57BL/6 mice.

Previous reports indicate that TZDs, including PIO, reduce neointima formation experimentally (Igarashi et al. 1997; Yoshimoto et al. 1999; Aizawa et al. 2001) and clinically in both diabetic (Takagi et al. 2003; Nishio et al. 2006; Riche, Valderrama, and Henyan 2007; Patel et al. 2011) and non-diabetic subjects (Marx et al. 2005; Geng et al. 2009). In the current study, we examined the effects of PIO on neointima formation in

CJ57BL/6 mice. As shown in **Fig. 4.3** (**A-C**), femoral artery injury in CJ57BL/6 mice resulted in extensive neointima formation. In addition, most cells in the intimal area were positive for SM α-actin, a marker for SMCs (**Fig. 4.3D**). PIO treatment (20 mg/kg/d, P.O.) led to a significant decrease in injury-induced neointima/media ratio by ~50 ± 6% (**Fig. 4.3A-D**). The medial area was not significantly different between all groups (data not shown).

PIO enhances the phosphorylation of AMPK in the mouse aorta

Next, we examined if PIO inhibition of neointima formation is associated with activation of AMPK in the vasculature. As shown in **Fig. 4.4**, PIO administration in CJ57BL/6 mice led to enhanced phosphorylation of AMPK in isolated aortic tissue by ~55 ± 12%. These results suggest that activation of AMPK in the vascular wall contributes, at least in part, to PIO inhibition of neointima formation.

Inhibition of AMPK partially reverses PIO inhibition of neointima formation

To examine the intermediary role of AMPK in mediating PIO inhibitory effects against neointima formation, CJ57BL/6 mice were treated with AMPK inhibitor, compound C (20 mg/kg 3 times per week, I.P.), either alone or in combination with PIO (20 mg/kg/d, P.O.). As shown in **Fig. 4.5A-C**, compound C by itself led an increase in neointima formation by ~33 ± 8%. However, this increase did not reach statistical significance ($p = 0.058$). Notably, in the presence of compound C, PIO inhibited neointima formation by ~29 ± 15%, while in the absence of compound C, PIO inhibited neointima formation by ~55 ± 12%. Together, these data suggest that inhibition of

endogenous AMPK activity enhances neointima formation and that AMPK contributes, in part, to PIO inhibition of neointima formation.

Discussion

We have recently reported that PIO activates AMPK in a sustained manner in human aortic VSMCs and thus leading to inhibition of PDGF-induced VSMC proliferation *via* inhibition of mTOR/p70S6K signaling (Osman and Segar 2016). In addition, we reported that PIO activation of AMPK is neither associated with an increase in AMP/ATP ratio nor mitochondrial-membrane depolarization and is likely independent of the upstream kinase, LKB1 (Osman and Segar 2016). In the current study, we extend our findings by identifying CaMKKβ as the upstream kinase mediating PIO activation of AMPK in VSMCs. In addition, we report that PIO administration in CJ57BL/6 mice leads to sustained activation of AMPK in the vasculature, and thus contributing, in part, to PIO inhibition of neointima formation.

While TZDs are traditionally viewed as PPARγ agonists, recent reports have ascribed some of their pharmacological effects to PPARγ-independent activation of AMPK. For instance, gene silencing of AMPK reduces the troglitazone-mediated increase in 2-deoxyglucose uptake in muscle cells (Konrad et al. 2005). In addition, infection of human aortic endothelial cells with adenoviruses expressing dominant negative AMPK attenuates rosiglitazone-induced phosphorylation of eNOS-Ser-1177 and the subsequent increase in NO production (Boyle et al. 2008). From a mechanistic perspective, TZD activation of AMPK is commonly ascribed to inhibition of mitochondrial activity and alteration of AMP/ATP ratio (Fryer, Parbu-Patel, and Carling 2002; Brunmair et al. 2004;

LeBrasseur et al. 2006; Boyle et al. 2008; Hawley et al. 2010). However, some previous findings by our group and others suggest that PIO may activate AMPK via a different mechanism (Brunmair et al. 2004; Osman and Segar 2016). For instance, the inhibitory effects of PIO on mitochondrial function in homogenates of skeletal muscle are only evident at very high concentrations (100 μM), while the inhibitory effects of rosiglitazone are evident at concentrations as low as 10 μM (Brunmair et al. 2004). In addition, we have recently reported that PIO activates AMPK in VSMCs at concentrations as low as 3 μM (Osman and Segar 2016). In addition, PIO activation of AMPK in VSMCs is neither associated with an increase in AMP/ATP ratio nor mitochondrial-membrane depolarization and is likely independent of LKB1 (Osman and Segar 2016). These findings raise the possibility that PIO may activate AMPK via a different mechanism in VSMCs.

In addition to LKB1, AMPK can be phosphorylated at Thr^{172}, and thus activated, by CaMKKβ in response to high cytosolic free calcium levels (Hawley et al. 2005; Woods et al. 2005). Previously, we and several other investigators have shown that vasoactive peptides that evoke a rise in cytosolic free calcium levels in vascular smooth muscle promote an increase in AMPK phosphorylation through an intermediary activation of CaMKKβ (Horman et al. 2008; Pyla et al. 2014). Recently, rosiglitazone was reported to inhibit the endoplasmic reticulum calcium ATPase in monocytic cells (Caddy et al. 2008) and VSMCs (Caddy et al. 2010) and thus leading to an increase intracellular calcium levels. These earlier observations suggest that PIO may activate AMPK through CaMKKβ in VSMCs. In accordance with these reports, downregulation of endogenous CaMKKβ by target-specific siRNA reveals that CaMKKβ is the key upstream kinase

responsible for basal and PIO activation of AMPK in VSMCs. To confirm the intermediary role of CaMKKβ in mediating PIO activation of AMPK, we employed an additional approach involving VSMC treatment with STO-609. Pharmacological inhibition of CaMKKβ by STO-609 yielded results similar to that observed in CaMKKβ siRNA-treated VSMCs. Together, these studies suggest that PIO activates AMPK in a CaMKKβ-dependent manner in VSMCs. Future studies are clearly warranted that should investigate the likely effects of PIO on calcium signaling in VSMCs.

In addition to the previously described TZD activation of AMPK in cells in culture (Fryer, Parbu-Patel, and Carling 2002; Brunmair et al. 2004; LeBrasseur et al. 2006; Boyle et al. 2008; Hawley et al. 2010; Konrad et al. 2005; Osman and Segar 2016), TZDs activate AMPK in different tissues in experimental animals (Saha et al. 2004; LeBrasseur et al. 2006; Lessard et al. 2006; Morisaki et al. 2011). Moreover, PIO activates AMPK in human skeletal muscle *in vivo* and increases the expression of genes involved in adiponectin signaling, mitochondrial function and fat oxidation (Coletta et al. 2009). Recently, PIO was reported to enhance the phosphorylation of AMPK in rabbit vein grafts (Morisaki et al. 2011). In this study, we extend previous findings by demonstrating that PIO activates AMPK in mouse aortic tissues in a sustained manner. From a mechanistic perspective, PIO activation of PPARγ in adipose tissue enhances circulatory levels of adiponectin (Kadowaki et al. 2006), which in turn is expected to activate AMPK in VSMCs (Ding et al. 2012; Ding et al. 2011). In addition, we recently reported that PIO activates AMPK in VSMCs directly and independent of PPARγ activation (Osman and Segar 2016). Thus, it is likely that PIO activates AMPK in the vasculature (this

study) *via* direct and indirect effects and that this activation mediates at least some of its pharmacological effects in the vessel wall.

Previous studies have shown that TZDs have strong inhibitory effects on neointima formation in different experimental models including normal rats (Law et al. 1996; Aizawa et al. 2001; Igarashi et al. 2001), insulin-resistant Zucker fatty rats (Shinohara et al. 1998), stroke-prone spontaneously hypertensive rats (Yoshimoto et al. 1999), and hypercholesterolemic rabbits (Pakala et al. 2006). In addition, TZDs inhibit neointima formation after coronary stenting in nondiabetic patients with metabolic syndrome (Katayama et al. 2007), and in patients with type 2 diabetes mellitus (Takagi et al. 2000; Nishio et al. 2006; Choi et al. 2004; Patel et al. 2011). However, the signaling mechanisms mediating TZD inhibition of neointima formation are not fully understood. For instance, *in vivo* transfer of the PPARγ-WT gene was found to inhibit smooth muscle proliferation, sustain apoptosis, and reduce neointima formation after balloon injury in rats (Lim et al. 2006). On the other hand, rosiglitazone has been shown to inhibit neointimal formation *via* PPARγ-independent activation of glycogen synthase kinase-3β (Lee et al. 2009). We have recently reported that PIO inhibits PDGF-induced VSMC proliferation *via* activation of AMPK/mTOR signaling axis (Osman and Segar 2016). In this study, we extend our findings by showing that AMPK mediates, in part, to PIO inhibition of neointima formation *in vivo*.

Several cytokines and pharmacological agents are reported to inhibit neointima formation *via* activation of AMPK. For instance, 5-aminoimidazole-4-carboxamide-1-beta-d-ribofuranoside (AICAR) (Stone et al. 2013), adiponectin (Takaoka et al. 2009), metformin (Lu et al. 2013), retinoic acid-related orphan receptor alpha (Kim et al. 2014),

muscle-derived follistatin-like 1 protein (Miyabe et al. 2014) , diclofenac (MacAskill et al. 2015), and omentin (Uemura et al. 2015) inhibit neointima formation that appears to be dependent on AMPK activation. In addition, genetic ablation of AMPK enhances neointima formation *in vivo* (Song et al. 2011; Song et al. 2013). Moreover, receptor for advanced glycation endproducts (RAGE) signaling enhances neointima formation *via* the suppression of AMPK (Yu et al. 2012). Accordingly, AMPK may represent a viable pharmacological target to treat restenosis after balloon injury.

TZDs have been demonstrated to exhibit salutary effects in the vasculature (Yoshimoto et al. 1999; Phillips et al. 2003; Satoh et al. 2003) beyond their insulin-sensitizing action in patients with type 2 diabetes (Kahn et al. 2006). However, TZD treatment is associated with several adverse effects, including weight gain, fluid retention, and congestive heart failure, thus raising concerns about their cardiovascular safety (Nesto et al. 2003). These unfavorable effects are attributed in part to activation of PPARγ (Guan et al. 2005; Zhang et al. 2005). Since, PIO inhibits neointima formation, in part, *via* activation of AMPK, strategies that utilize nanoparticle-mediated PIO delivery at the lesion site may limit restenosis after angioplasty without inducing PPARγ-mediated systemic adverse effects (Nagahama et al. 2012; Joner et al. 2008).

Figure legends

Fig. 4.1. Effects of LKB1 or CaMKKβ downregulation on PIO activation of AMPK in VSMCs. (**A-C**) VSMCs were transfected with scrambled (Scr.), LKB1, or CaMKKβ siRNA followed by maintenance in culture for 48 hr. Subsequently, VSMCs were treated with PIO (30 μM, 3 hr) or vehicle control under serum-deprived conditions. VSMC lysates were then subjected to immunoblot analysis using primary antibodies specific for LKB1, CaMKKβ, pAMPK, and pACC. *$p < 0.05$ compared with scr. siRNA vehicle control; # $p < 0.05$ compared with LKB1 siRNA vehicle control; n.s. not significant compared with CaMKKβ siRNA vehicle control; n = 3.

FIG. 4A-C

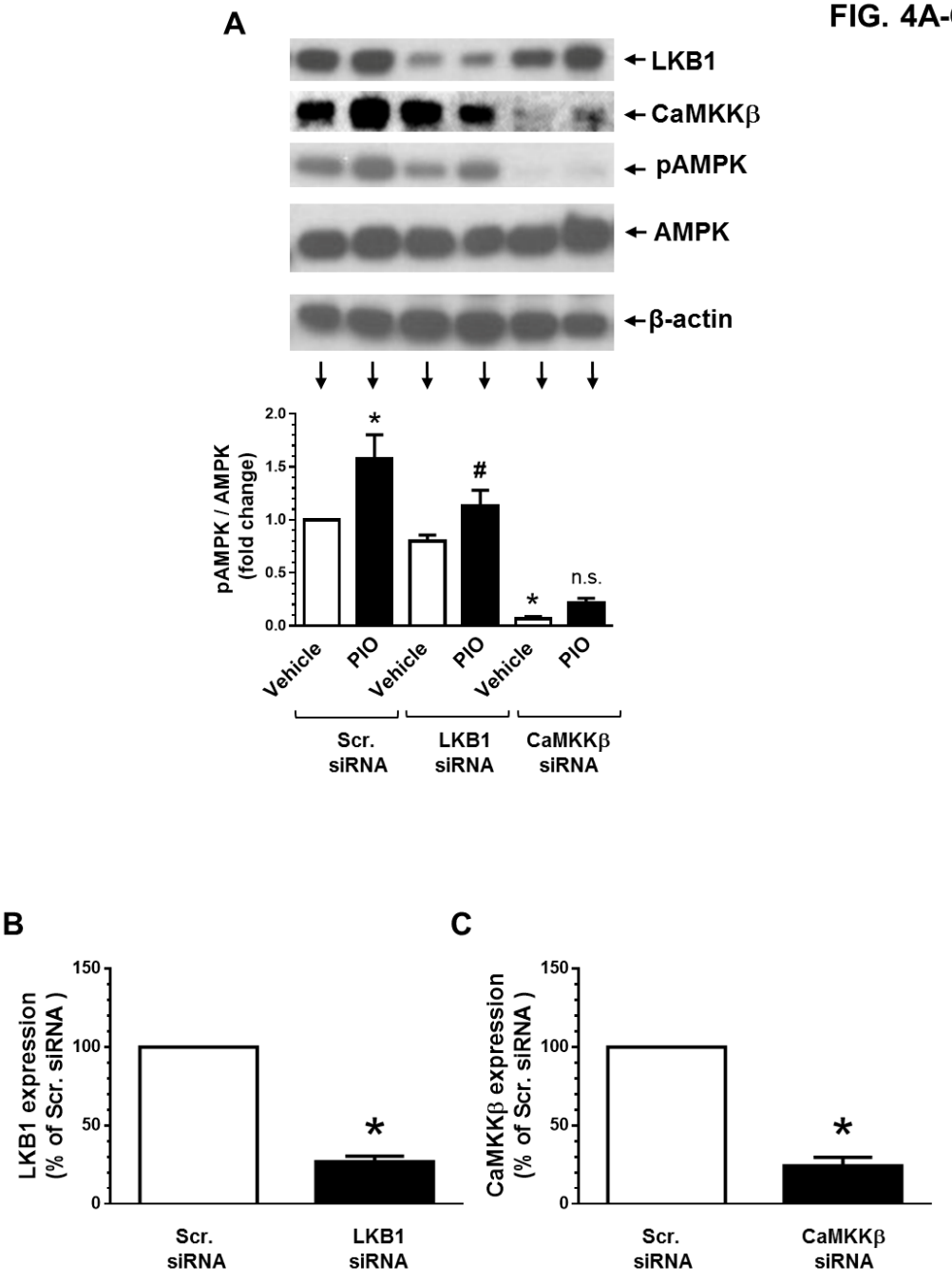
A
LKB1
CaMKKβ
pAMPK
AMPK
β-actin
pAMPK / AMPK
(fold change)
2.0
1.5
1.0
0.5
0.0
*
#
*
n.s.
Vehicle
PIO
Vehicle
PIO
Vehicle
PIO
Scr.
siRNA
LKB1
siRNA
CaMKKβ
siRNA
B
LKB1 expression
(% of Scr. siRNA)
150
100
50
0
*
Scr.
siRNA
LKB1
siRNA
C
CaMKKβ expression
(% of Scr. siRNA)
150
100
50
0
*
Scr.
siRNA
CaMKKβ
siRNA

Fig. 4.2. Effects of STO-609 on PIO activation of AMPK in VSMCs. Serum-deprived VSMCs were pretreated with AMPK inhibitor (STO-609; 10 μM) for 30 min, followed by exposure to PIO (30 μM) or vehicle control for 24 or 48 hr. VSMC lysates were then subjected to immunoblot analysis using primary antibodies specific for pAMPK and pACC. *$p < 0.05$ compared with vehicle control; n.s. not significant compared with STO-609 alone; n = 3.

FIG. 4.2

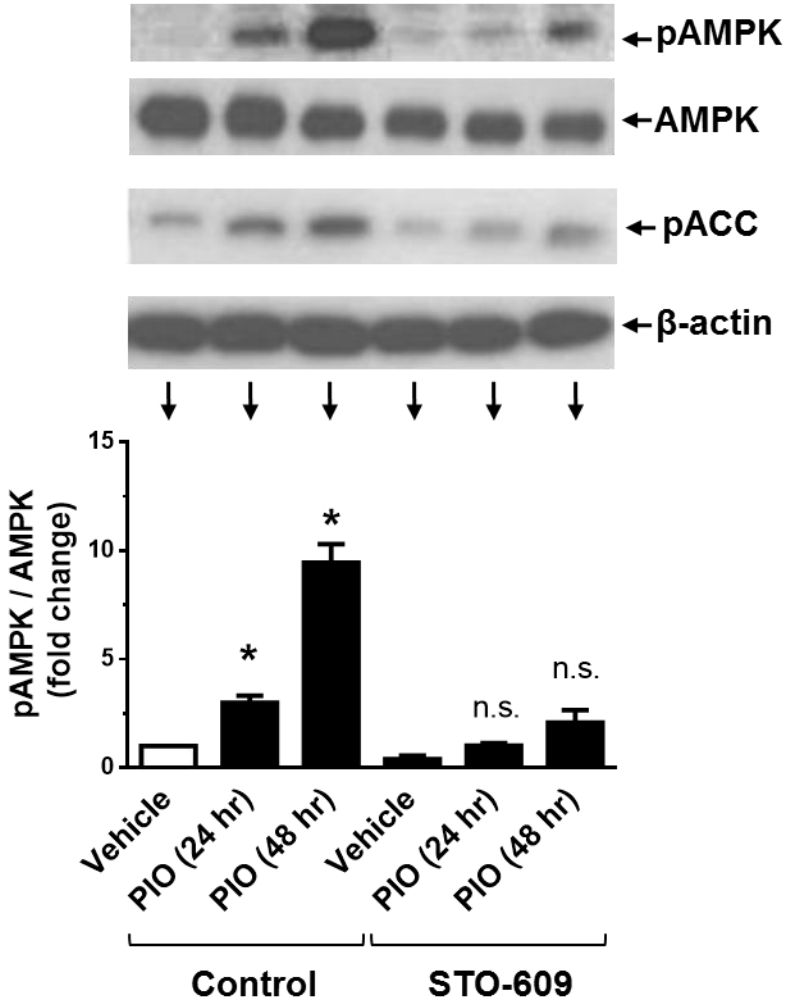
pAMPK
AMPK
pACC
β-actin
pAMPK / AMPK
(fold change)
15
10
5
0
*
*
n.s.
n.s.
Vehicle
PIO (24 hr)
PIO (48 hr)
Vehicle
PIO (24 hr)
PIO (48 hr)
Control
STO-609

Fig. 4.3. Effects of PIO on neointima formation after femoral artery injury in CJ57BL/6 mice. PIO was administered orally by gavage (20 mg/kg/d) in CJ57BL/6 mice starting from 1 day before surgery and for three weeks until sacrifice. **A**) EVG and H&E staining of injured femoral arteries from CJ57BL/6 mice (-/+ PIO); arrows indicate internal and external elastic laminae; **B)** Morphometric analyses of the intimal area in injured femoral arteries; **C**) Morphometric analyses of neointima/media ratio in injured femoral arteries. *$p < 0.05$ compared with vehicle control; $n = 6$. **D**) Confocal immunofluorescence analysis of smooth muscle (SM) α-actin (red), elastin autofluorescence (laminae, green), nuclei (DAPI, blue), and merged images in the injured femoral arteries. Images shown in all panels are representative of $n = 6$.

FIG. 4.3A-D

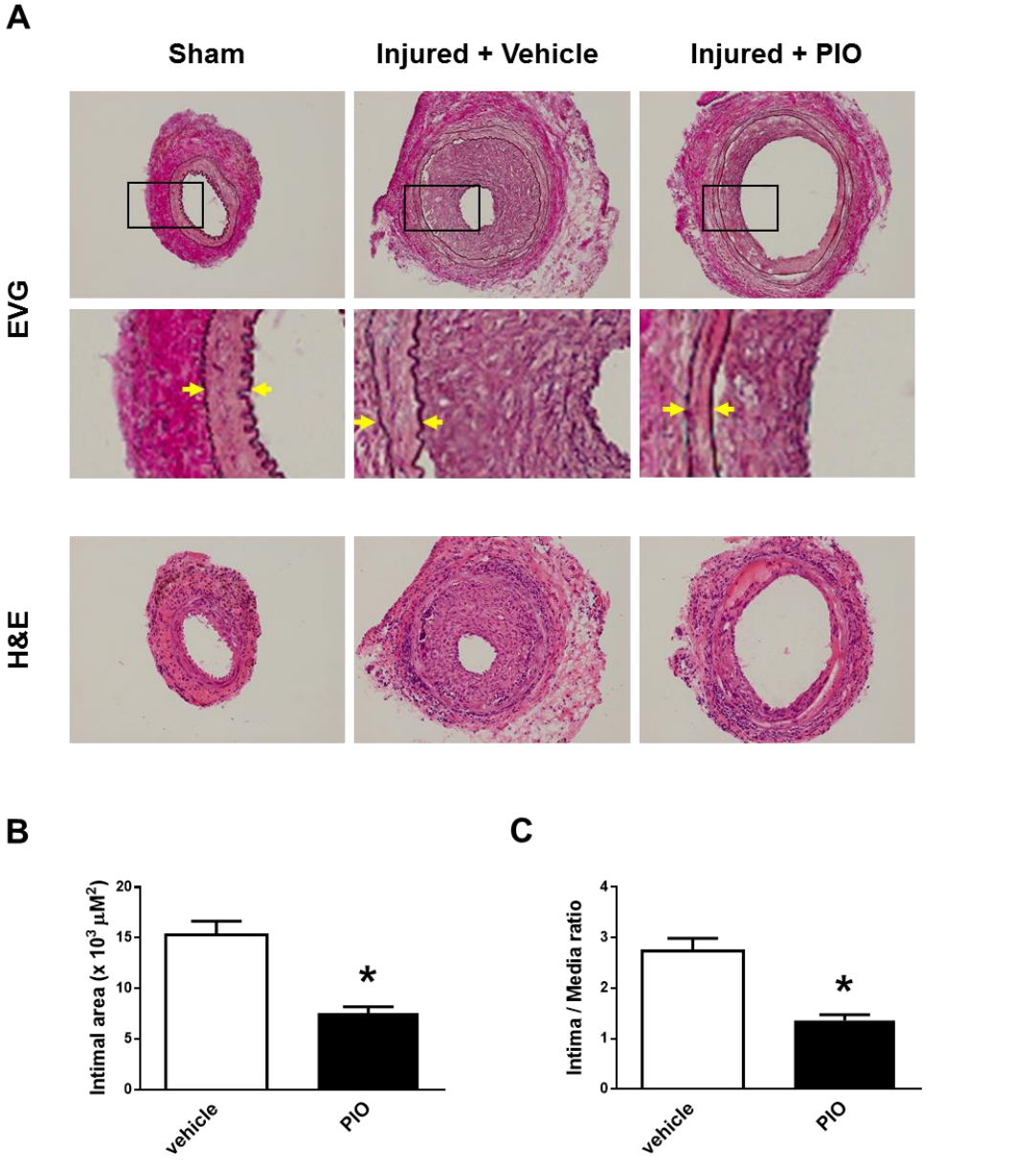
A
Sham
Injured + Vehicle
Injured + PIO
EVG
H&E
B
Intimal area (x 10^3 µM^2)
20
15
10
5
0
*
vehicle
PIO
C
Intima / Media ratio
4
3
2
1
0
*
vehicle
PIO

FIG. 4.3A-D
continued

D

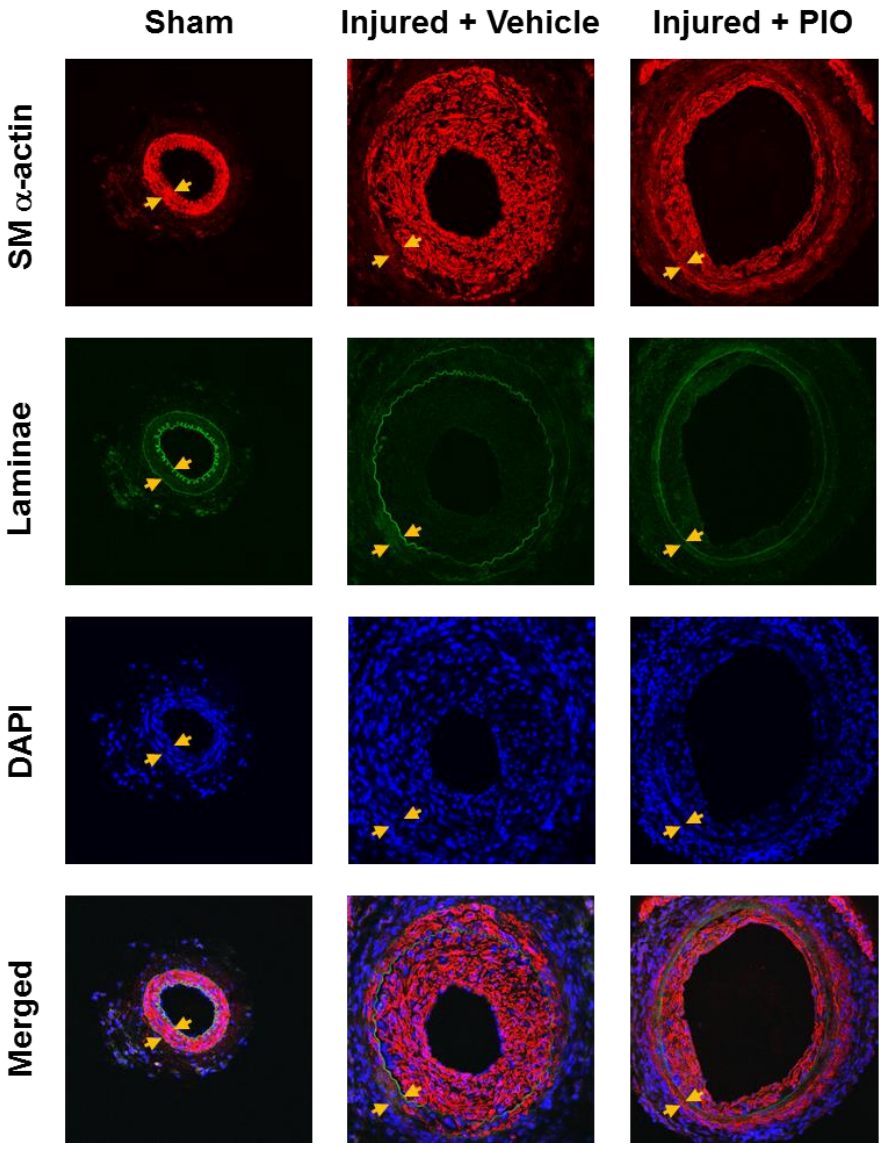

Fig. 4.4. Effects of PIO on AMPK phosphorylation in the aorta of CJ5/BL/6 mice. PIO was administered orally by gavage (20 mg/kg/d) in CJ57BL/6 mice starting from 1 day before surgery and for three weeks until sacrifice. Aortic tissue lysates were then subjected to immunoblot analysis using primary antibodies specific for pAMPK. *$p < 0.05$ compared with vehicle control; $n = 6$.

FIG. 4.4

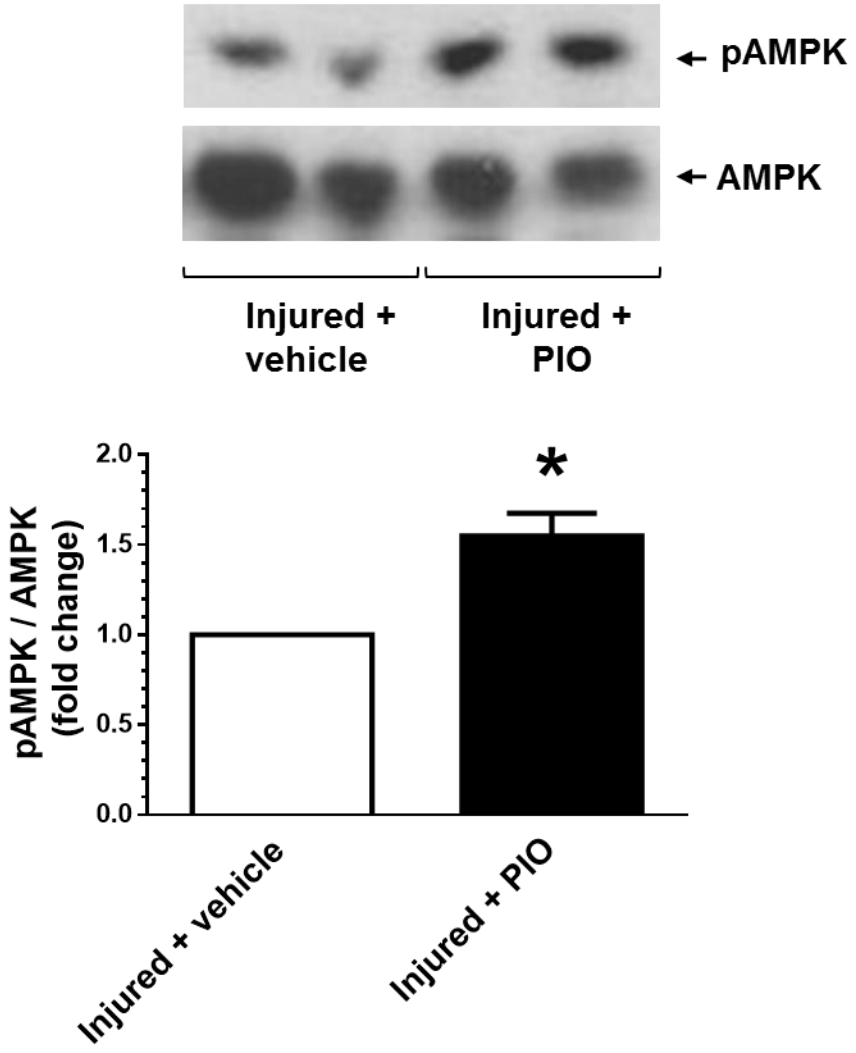
pAMPK
AMPK
Injured + vehicle
Injured + PIO
pAMPK / AMPK (fold change)
2.0
1.5
1.0
0.5
0.0
*
Injured + vehicle
Injured + PIO

Fig. 4.5. Effects of compound C on PIO-mediated inhibitory effects on neointima formation in CJ57BL/6 mice. AMPK inhibitor compound C (Comp C; 20 mg/kg, every other day) or vehicle control were injected intraperitoneally every other day from one day before surgery until sacrifice. Simultaneously, PIO was administered orally by gavage (20 mg/kg/d) starting from 1 day before surgery and for three weeks until sacrifice. **A**) EVG and H&E staining of injured femoral arteries from CJ57BL/6 mice (-/+ Comp C and -/+ PIO); arrows indicate internal and external elastic laminae; **B)** Morphometric analyses of the intimal area in injured femoral arteries; **C**) Morphometric analyses of neointima/media ratio in injured femoral arteries. *$p < 0.05$ compared with vehicle control; $n = 6$.

FIG.
4.5A-C

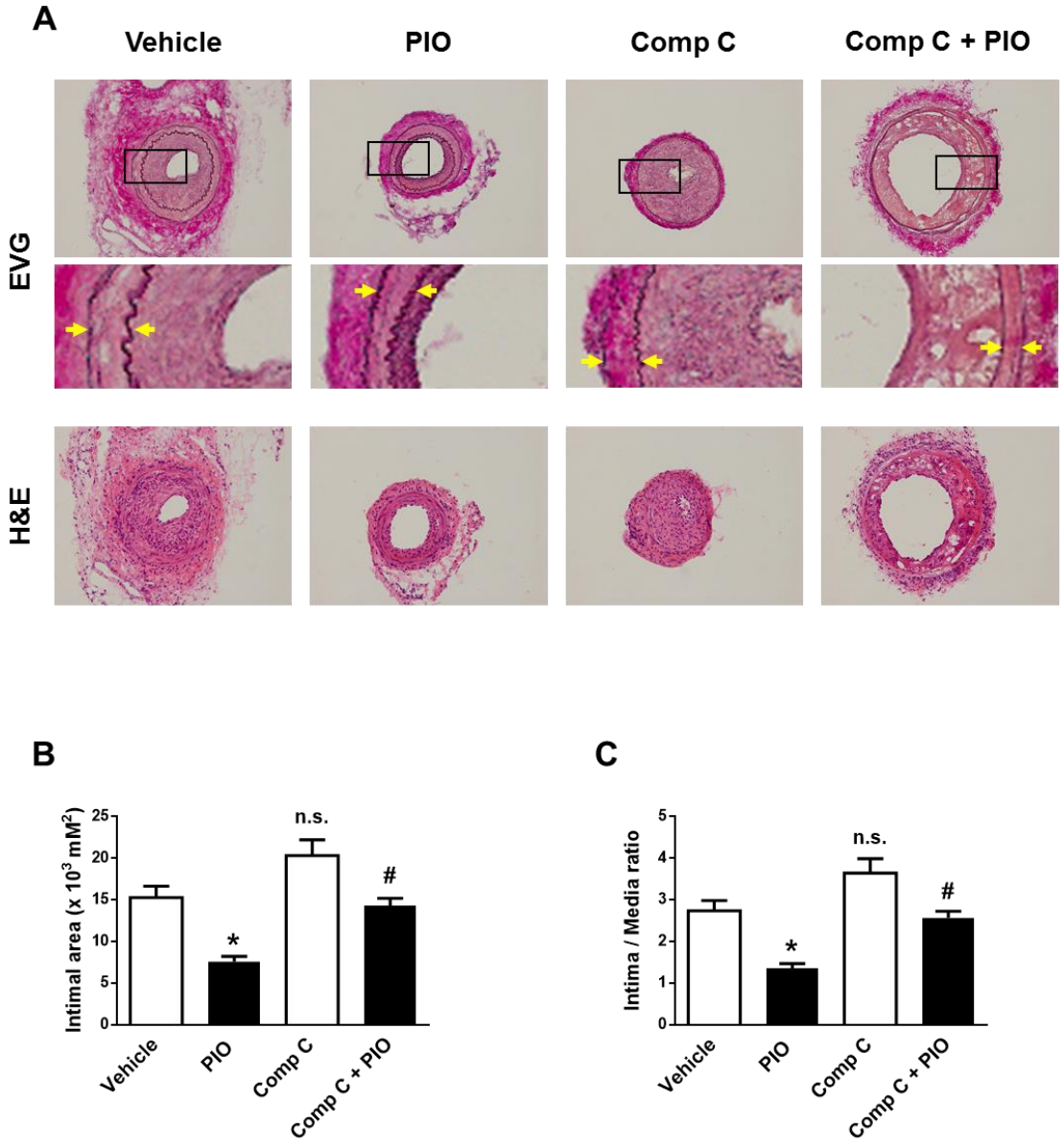
A
Vehicle
PIO
Comp C
Comp C + PIO
EVG
H&E
B
Intimal area (x 10³ mM²)
25
20
15
10
5
0
n.s.
*
#
Vehicle
PIO
Comp C
Comp C + PIO
C
Intima / Media ratio
5
4
3
2
1
0
n.s.
*
#
Vehicle
PIO
Comp C
Comp C + PIO

Bibliography

Aizawa, Y., J. Kawabe, N. Hasebe, N. Takehara, and K. Kikuchi. 2001. Pioglitazone enhances cytokine-induced apoptosis in vascular smooth muscle cells and reduces intimal hyperplasia. *Circulation* 104 (4):455-60.

Aizawa, Y., J. i Kawabe, N. Hasebe, N. Takehara, and K. Kikuchi. 2001. Pioglitazone Enhances Cytokine-Induced Apoptosis in Vascular Smooth Muscle Cells and Reduces Intimal Hyperplasia. *Circulation* 104 (4):455-460.

Basi, D.L., N. Adhikari, A. Mariash, Q. Li, E. Kao, S.V. Mullegama, and J.L. Hall. 2007. Femoral artery neointimal hyperplasia is reduced after wire injury in Ref-1+/- mice. *Am.J.Physiol Heart Circ.Physiol* 292 (1):H516-H521.

Boyle, J. G., P. J. Logan, M. A. Ewart, J. A. Reihill, S. A. Ritchie, J. M. Connell, S. J. Cleland, and I. P. Salt. 2008. Rosiglitazone stimulates nitric oxide synthesis in human aortic endothelial cells via AMP-activated protein kinase. *J Biol Chem* 283 (17):11210-7.

Brunmair, B., K. Staniek, F. Gras, N. Scharf, A. Althaym, R. Clara, M. Roden, E. Gnaiger, H. Nohl, W. Waldhausl, and C. Furnsinn. 2004. Thiazolidinediones, like metformin, inhibit respiratory complex I: a common mechanism contributing to their antidiabetic actions? *Diabetes* 53 (4):1052-9.

Caddy, J., S. Isa, L. S. Mainwaring, E. Adam, A. Roberts, D. Lang, R. H. Morris, A. W. Thomas, and R. Webb. 2010. Rosiglitazone induces the unfolded protein response, but has no significant effect on cell viability, in monocytic and vascular smooth muscle cells. *Biochem Biophys Res Commun* 400 (4):689-95.

Caddy, J., N. Singh, L. Atkin, M. Ahluwalia, A. Roberts, D. Lang, A. W. Thomas, and R. Webb. 2008. Rosiglitazone transiently disturbs calcium homeostasis in monocytic cells. *Biochemical and Biophysical Research Communications* 366 (1):149-155.

Cassese, S., R. A. Byrne, T. Tada, S. Pinieck, M. Joner, T. Ibrahim, L. A. King, M. Fusaro, K. L. Laugwitz, and A. Kastrati. 2014. Incidence and predictors of restenosis after coronary stenting in 10 004 patients with surveillance angiography. *Heart* 100 (2):153-9.

Choi, D., S. K. Kim, S. H. Choi, Y. G. Ko, C. W. Ahn, Y. Jang, S. K. Lim, H. C. Lee, and B. S. Cha. 2004. Preventative effects of rosiglitazone on restenosis after coronary stent implantation in patients with type 2 diabetes. *Diabetes Care* 27 (11):2654-60.

Coletta, D. K., A. Sriwijitkamol, E. Wajcberg, P. Tantiwong, M. Li, M. Prentki, M. Madiraju, C. P. Jenkinson, E. Cersosimo, N. Musi, and R. A. Defronzo. 2009. Pioglitazone stimulates AMP-activated protein kinase signalling and increases the expression of genes involved in adiponectin signalling, mitochondrial function and fat oxidation in human skeletal muscle in vivo: a randomised trial. *Diabetologia* 52 (4):723-32.

de Dios, S. T., D. Bruemmer, R. J. Dilley, M. E. Ivey, G. L. Jennings, R. E. Law, and P. J. Little. 2003. Inhibitory activity of clinical thiazolidinedione peroxisome proliferator activating receptor-gamma ligands toward internal mammary artery, radial artery, and saphenous vein smooth muscle cell proliferation. *Circulation* 107 (20):2548-50.

Ding, M., A. C. Carrao, R. J. Wagner, Y. Xie, Y. Jin, E. M. Rzucidlo, J. Yu, W. Li, G. Tellides, J. Hwa, T. R. Aprahamian, and K. A. Martin. 2012. Vascular smooth muscle cell-derived adiponectin: a paracrine regulator of contractile phenotype. *J Mol Cell Cardiol* 52 (2):474-84.

Ding, M., Y. Xie, R. J. Wagner, Y. Jin, A. C. Carrao, L. S. Liu, A. K. Guzman, R. J. Powell, J. Hwa, E. M. Rzucidlo, and K. A. Martin. 2011. Adiponectin induces vascular smooth muscle cell differentiation via repression of mammalian target of rapamycin complex 1 and FoxO4. *Arterioscler Thromb Vasc Biol* 31 (6):1403-10.

Fryer, L. G., A. Parbu-Patel, and D. Carling. 2002. The Anti-diabetic drugs rosiglitazone and metformin stimulate AMP-activated protein kinase through distinct signaling pathways. *J Biol Chem* 277 (28):25226-32.

Geng, D. F., D. M. Jin, W. Wu, Z. Wang, and J. F. Wang. 2009. Effect of thiazolidinediones on in-stent restenosis in patients after coronary stenting: a meta-analysis of randomized controlled trials. *Atherosclerosis* 202 (2):521-8.

Go, A. S., D. Mozaffarian, V. L. Roger, E. J. Benjamin, J. D. Berry, M. J. Blaha, S. Dai, E. S. Ford, C. S. Fox, S. Franco, H. J. Fullerton, C. Gillespie, S. M. Hailpern, J. A. Heit, V. J. Howard, M. D. Huffman, S. E. Judd, B. M. Kissela, S. J. Kittner, D. T. Lackland, J. H. Lichtman, L. D. Lisabeth, R. H. Mackey, D. J. Magid, G. M. Marcus, A. Marelli, D. B. Matchar, D. K. McGuire, E. R. Mohler, 3rd, C. S. Moy, M. E. Mussolino, R. W. Neumar, G. Nichol, D. K. Pandey, N. P. Paynter, M. J. Reeves, P. D. Sorlie, J. Stein, A. Towfighi, T. N. Turan, S. S. Virani, N. D. Wong, D. Woo, M. B. Turner, Committee American Heart Association Statistics, and Subcommittee Stroke Statistics. 2014. Heart disease and stroke statistics--2014

update: a report from the American Heart Association. *Circulation* 129 (3):e28-e292.

Guan, Y., C. Hao, D. R. Cha, R. Rao, W. Lu, D. E. Kohan, M. A. Magnuson, R. Redha, Y. Zhang, and M. D. Breyer. 2005. Thiazolidinediones expand body fluid volume through PPARgamma stimulation of ENaC-mediated renal salt absorption. *Nat Med* 11 (8):861-6.

Hawley, S. A., D. A. Pan, K. J. Mustard, L. Ross, J. Bain, A. M. Edelman, B. G. Frenguelli, and D. G. Hardie. 2005. Calmodulin-dependent protein kinase kinase-beta is an alternative upstream kinase for AMP-activated protein kinase. *Cell Metab* 2 (1):9-19.

Hawley, S. A., F. A. Ross, C. Chevtzoff, K. A. Green, A. Evans, S. Fogarty, M. C. Towler, L. J. Brown, O. A. Ogunbayo, A. M. Evans, and D. G. Hardie. 2010. Use of cells expressing gamma subunit variants to identify diverse mechanisms of AMPK activation. *Cell Metab* 11 (6):554-65.

Hofma, S. H., W. J. van der Giessen, B. M. van Dalen, P. A. Lemos, E. P. McFadden, G. Sianos, J. M. Ligthart, D. van Essen, P. J. de Feyter, and P. W. Serruys. 2006. Indication of long-term endothelial dysfunction after sirolimus-eluting stent implantation. *Eur Heart J* 27 (2):166-70.

Horman, S., N. Morel, D. Vertommen, N. Hussain, D. Neumann, C. Beauloye, N. El Najjar, C. Forcet, B. Viollet, M. P. Walsh, L. Hue, and M. H. Rider. 2008. AMP-activated protein kinase phosphorylates and desensitizes smooth muscle myosin light chain kinase. *J Biol Chem* 283 (27):18505-12.

Hurley, R. L., K. A. Anderson, J. M. Franzone, B. E. Kemp, A. R. Means, and L. A. Witters. 2005. The Ca2+/calmodulin-dependent protein kinase kinases are AMP-activated protein kinase kinases. *J Biol Chem* 280 (32):29060-6.

Igarashi, M., A. Hirata, H. Yamaguchi, H. Tsuchiya, H. Ohnuma, M. Tominaga, M. Daimon, and T. Kato. 2001. Characterization of an inhibitory effect of pioglitazone on balloon-injured vascular smooth muscle cell growth. *Metabolism* 50 (8):955-62.

Igarashi, M., Y. Takeda, N. Ishibashi, K. Takahashi, S. Mori, M. Tominaga, and Y. Saito. 1997. Pioglitazone reduces smooth muscle cell density of rat carotid arterial intima induced by balloon catheterization. *Horm Metab Res* 29 (9):444-9.

Joner, M., K. Morimoto, H. Kasukawa, K. Steigerwald, S. Merl, G. Nakazawa, M. C. John, A. V. Finn, E. Acampado, F. D. Kolodgie, H. K. Gold, and R. Virmani. 2008. Site-specific targeting of nanoparticle prednisolone reduces in-stent restenosis in a rabbit model of established atheroma. *Arterioscler Thromb Vasc Biol* 28 (11):1960-6.

Kadowaki, T., T. Yamauchi, N. Kubota, K. Hara, K. Ueki, and K. Tobe. 2006. Adiponectin and adiponectin receptors in insulin resistance, diabetes, and the metabolic syndrome. *J Clin Invest* 116 (7):1784-92.

Kahn, B. B., T. Alquier, D. Carling, and D. G. Hardie. 2005. AMP-activated protein kinase: ancient energy gauge provides clues to modern understanding of metabolism. *Cell Metab* 1 (1):15-25.

Kahn, S. E., S. M. Haffner, M. A. Heise, W. H. Herman, R. R. Holman, N. P. Jones, B. G. Kravitz, J. M. Lachin, M. C. O'Neill, B. Zinman, G. Viberti, and Adopt Study

Group. 2006. Glycemic durability of rosiglitazone, metformin, or glyburide monotherapy. *N Engl J Med* 355 (23):2427-43.

Katayama, T., H. Ueba, K. Tsuboi, N. Kubo, T. Yasu, M. Kuroki, M. Saito, S. Momomura, and M. Kawakami. 2007. Reduction of neointimal hyperplasia after coronary stenting by pioglitazone in nondiabetic patients with metabolic syndrome. *Am Heart J* 153 (5):762 e1-7.

Kim, E. J., Y. K. Choi, Y. H. Han, H. J. Kim, I. K. Lee, and M. O. Lee. 2014. RORalpha suppresses proliferation of vascular smooth muscle cells through activation of AMP-activated protein kinase. *Int J Cardiol* 175 (3):515-21.

Konrad, D., A. Rudich, P. J. Bilan, N. Patel, C. Richardson, L. A. Witters, and A. Klip. 2005. Troglitazone causes acute mitochondrial membrane depolarisation and an AMPK-mediated increase in glucose phosphorylation in muscle cells. *Diabetologia* 48 (5):954-66.

Law, R. E., S. Goetze, X. P. Xi, S. Jackson, Y. Kawano, L. Demer, M. C. Fishbein, W. P. Meehan, and W. A. Hsueh. 2000. Expression and function of PPARgamma in rat and human vascular smooth muscle cells. *Circulation* 101 (11):1311-8.

Law, R. E., W. P. Meehan, X. P. Xi, K. Graf, D. A. Wuthrich, W. Coats, D. Faxon, and W. A. Hsueh. 1996. Troglitazone inhibits vascular smooth muscle cell growth and intimal hyperplasia. *J Clin Invest* 98 (8):1897-905.

LeBrasseur, N. K., M. Kelly, T. S. Tsao, S. R. Farmer, A. K. Saha, N. B. Ruderman, and E. Tomas. 2006. Thiazolidinediones can rapidly activate AMP-activated protein kinase in mammalian tissues. *Am J Physiol Endocrinol Metab* 291 (1):E175-81.

Lee, C. S., Y. W. Kwon, H. M. Yang, S. H. Kim, T. Y. Kim, J. Hur, K. W. Park, H. J. Cho, H. J. Kang, Y. B. Park, and H. S. Kim. 2009. New mechanism of rosiglitazone to reduce neointimal hyperplasia: activation of glycogen synthase kinase-3beta followed by inhibition of MMP-9. *Arterioscler Thromb Vasc Biol* 29 (4):472-9.

Lessard, S. J., Z. P. Chen, M. J. Watt, M. Hashem, J. J. Reid, M. A. Febbraio, B. E. Kemp, and J. A. Hawley. 2006. Chronic rosiglitazone treatment restores AMPKalpha2 activity in insulin-resistant rat skeletal muscle. *Am J Physiol Endocrinol Metab* 290 (2):E251-7.

Lim, S., C. J. Jin, M. Kim, S. S. Chung, H. S. Park, I. K. Lee, C. T. Lee, Y. M. Cho, H. K. Lee, and K. S. Park. 2006. PPARgamma gene transfer sustains apoptosis, inhibits vascular smooth muscle cell proliferation, and reduces neointima formation after balloon injury in rats. *Arterioscler Thromb Vasc Biol* 26 (4):808-13.

Lu, J., J. Ji, H. Meng, D. Wang, B. Jiang, L. Liu, E. Randell, K. Adeli, and Q. H. Meng. 2013. The protective effect and underlying mechanism of metformin on neointima formation in fructose-induced insulin resistant rats. *Cardiovasc Diabetol* 12:58.

MacAskill, M. G., D. G. Watson, M. A. Ewart, R. Wadsworth, A. Jackson, E. Aitken, G. MacKenzie, D. Kingsmore, S. Currie, and P. Coats. 2015. Improving arteriovenous fistula patency: Transdermal delivery of diclofenac reduces cannulation-dependent neointimal hyperplasia via AMPK activation. *Vascul Pharmacol* 71:108-15.

Marx, N., J. Wohrle, T. Nusser, D. Walcher, A. Rinker, V. Hombach, W. Koenig, and M. Hoher. 2005. Pioglitazone reduces neointima volume after coronary stent implantation: a randomized, placebo-controlled, double-blind trial in nondiabetic patients. *Circulation* 112 (18):2792-8.

Mauri, L., T. S. Silbaugh, R. E. Wolf, K. Zelevinsky, A. Lovett, Z. Zhou, F. S. Resnic, and S. L. Normand. 2008. Long-term clinical outcomes after drug-eluting and bare-metal stenting in Massachusetts. *Circulation* 118 (18):1817-27.

Miyabe, M., K. Ohashi, R. Shibata, Y. Uemura, Y. Ogura, D. Yuasa, T. Kambara, Y. Kataoka, T. Yamamoto, K. Matsuo, Y. Joki, T. Enomoto, S. Hayakawa, M. Hiramatsu-Ito, M. Ito, M. J. Van Den Hoff, K. Walsh, T. Murohara, and N. Ouchi. 2014. Muscle-derived follistatin-like 1 functions to reduce neointimal formation after vascular injury. *Cardiovasc Res* 103 (1):111-20.

Morisaki, K., R. Shibata, N. Takahashi, N. Ouchi, Y. Maehara, T. Murohara, and K. Komori. 2011. Pioglitazone prevents intimal hyperplasia in experimental rabbit vein grafts. *J Vasc Surg* 54 (6):1753-9.

Nagahama, R., T. Matoba, K. Nakano, S. Kim-Mitsuyama, K. Sunagawa, and K. Egashira. 2012. Nanoparticle-mediated delivery of pioglitazone enhances therapeutic neovascularization in a murine model of hindlimb ischemia. *Arterioscler Thromb Vasc Biol* 32 (10):2427-34.

Nesto, R. W., D. Bell, R. O. Bonow, V. Fonseca, S. M. Grundy, E. S. Horton, M. Le Winter, D. Porte, C. F. Semenkovich, S. Smith, L. H. Young, R. Kahn, Association American Heart, and Association American Diabetes. 2003. Thiazolidinedione use, fluid retention, and congestive heart failure: a consensus

statement from the American Heart Association and American Diabetes Association. October 7, 2003. *Circulation* 108 (23):2941-8.

Nishio, K., M. Sakurai, T. Kusuyama, M. Shigemitsu, T. Fukui, K. Kawamura, S. Itoh, N. Konno, and T. Katagiri. 2006. A randomized comparison of pioglitazone to inhibit restenosis after coronary stenting in patients with type 2 diabetes. *Diabetes Care* 29 (1):101-6.

Osman, I., and L. Segar. 2016. Pioglitazone, a PPARgamma agonist, attenuates PDGF-induced vascular smooth muscle cell proliferation through AMPK-dependent and AMPK-independent inhibition of mTOR/p70S6K and ERK signaling. *Biochem Pharmacol* 101:54-70.

Owens, G. K., M. S. Kumar, and B. R. Wamhoff. 2004. Molecular regulation of vascular smooth muscle cell differentiation in development and disease. *Physiol Rev* 84 (3):767-801.

Pakala, R., C. Dilcher, R. Baffour, D. Hellinga, R. Seabron, M. Joner, F. Kolodgie, R. Virmani, and R. Waksman. 2006. Peroxisome proliferator-activated receptor gamma ligand pioglitazone alters neointimal composition in a balloon-denuded and radiated hypercholesterolemic rabbit. *J Cardiovasc Pharmacol* 48 (6):299-305.

Patel, D., B. Walitt, J. Lindsay, and R. L. Wilensky. 2011. Role of pioglitazone in the prevention of restenosis and need for revascularization after bare-metal stent implantation: a meta-analysis. *JACC Cardiovasc Interv* 4 (3):353-60.

Phillips, J. W., K. G. Barringhaus, J. M. Sanders, Z. Yang, M. Chen, S. Hesselbacher, A. C. Czarnik, K. Ley, J. Nadler, and I. J. Sarembock. 2003. Rosiglitazone reduces

the accelerated neointima formation after arterial injury in a mouse injury model of type 2 diabetes. *Circulation* 108 (16):1994-9.

Pyla, R., I. Osman, P. Pichavaram, P. Hansen, and L. Segar. 2014. Metformin exaggerates phenylephrine-induced AMPK phosphorylation independent of CaMKKbeta and attenuates contractile response in endothelium-denuded rat aorta. *Biochem Pharmacol* 92 (2):266-79.

Riche, D. M., R. Valderrama, and N. N. Henyan. 2007. Thiazolidinediones and risk of repeat target vessel revascularization following percutaneous coronary intervention: a meta-analysis. *Diabetes Care* 30 (2):384-8.

Ross, R. 1999. Atherosclerosis--an inflammatory disease. *N Engl J Med* 340 (2):115-26.

Saha, A. K., P. R. Avilucea, J. M. Ye, M. M. Assifi, E. W. Kraegen, and N. B. Ruderman. 2004. Pioglitazone treatment activates AMP-activated protein kinase in rat liver and adipose tissue in vivo. *Biochem Biophys Res Commun* 314 (2):580-5.

Sata, M., Y. Maejima, F. Adachi, K. Fukino, A. Saiura, S. Sugiura, T. Aoyagi, Y. Imai, H. Kurihara, K. Kimura, M. Omata, M. Makuuchi, Y. Hirata, and R. Nagai. 2000. A mouse model of vascular injury that induces rapid onset of medial cell apoptosis followed by reproducible neointimal hyperplasia. *J.Mol.Cell Cardiol.* 32 (11):2097-2104.

Satoh, N., Y. Ogawa, T. Usui, T. Tagami, S. Kono, H. Uesugi, H. Sugiyama, A. Sugawara, K. Yamada, A. Shimatsu, H. Kuzuya, and K. Nakao. 2003. Antiatherogenic effect of pioglitazone in type 2 diabetic patients irrespective of the responsiveness to its antidiabetic effect. *Diabetes Care* 26 (9):2493-9.

Scheen, A. J., F. Warzee, and V. M. Legrand. 2004. Drug-eluting stents: meta-analysis in diabetic patients. *Eur Heart J* 25 (23):2167-8; author reply 2168-9.

Shinohara, E., S. Kihara, N. Ouchi, T. Funahashi, T. Nakamura, S. Yamashita, K. Kameda-Takemura, and Y. Matsuzawa. 1998. Troglitazone suppresses intimal formation following balloon injury in insulin-resistant Zucker fatty rats. *Atherosclerosis* 136 (2):275-9.

Song, P., S. Wang, C. He, S. Wang, B. Liang, B. Viollet, and M. H. Zou. 2011. AMPKalpha2 deletion exacerbates neointima formation by upregulating Skp2 in vascular smooth muscle cells. *Circ Res* 109 (11):1230-9.

Song, P., Y. Zhou, K. A. Coughlan, X. Dai, H. Xu, B. Viollet, and M. H. Zou. 2013. Adenosine monophosphate-activated protein kinase-alpha2 deficiency promotes vascular smooth muscle cell migration via S-phase kinase-associated protein 2 upregulation and E-cadherin downregulation. *Arterioscler Thromb Vasc Biol* 33 (12):2800-9.

Stone, J. D., A. Narine, P. R. Shaver, J. C. Fox, J. R. Vuncannon, and D. A. Tulis. 2013. AMP-activated protein kinase inhibits vascular smooth muscle cell proliferation and migration and vascular remodeling following injury. *Am J Physiol Heart Circ Physiol* 304 (3):H369-81.

Takagi, T., T. Akasaka, A. Yamamuro, Y. Honda, T. Hozumi, S. Morioka, and K. Yoshida. 2000. Troglitazone reduces neointimal tissue proliferation after coronary stent implantation in patients with non-insulin dependent diabetes mellitus: a serial intravascular ultrasound study. *J Am Coll Cardiol* 36 (5):1529-35.

Takagi, T., A. Yamamuro, K. Tamita, K. Yamabe, M. Katayama, S. Mizoguchi, M. Ibuki, T. Tani, K. Tanabe, K. Nagai, K. Shiratori, S. Morioka, and J. Yoshikawa. 2003. Pioglitazone reduces neointimal tissue proliferation after coronary stent implantation in patients with type 2 diabetes mellitus: an intravascular ultrasound scanning study. *Am Heart J* 146 (2):E5.

Takaoka, M., D. Nagata, S. Kihara, I. Shimomura, Y. Kimura, Y. Tabata, Y. Saito, R. Nagai, and M. Sata. 2009. Periadventitial adipose tissue plays a critical role in vascular remodeling. *Circ Res* 105 (9):906-11.

Tokumitsu, H., H. Inuzuka, Y. Ishikawa, M. Ikeda, I. Saji, and R. Kobayashi. 2002. STO-609, a specific inhibitor of the Ca(2+)/calmodulin-dependent protein kinase kinase. *J Biol Chem* 277 (18):15813-8.

Uemura, Y., R. Shibata, N. Kanemura, K. Ohashi, T. Kambara, M. Hiramatsu-Ito, T. Enomoto, D. Yuasa, Y. Joki, K. Matsuo, M. Ito, S. Hayakawa, H. Ogawa, T. Murohara, and N. Ouchi. 2014. Adipose-derived protein omentin prevents neointimal formation after arterial injury. *FASEB J*.

———. 2015. Adipose-derived protein omentin prevents neointimal formation after arterial injury. *Faseb j* 29 (1):141-51.

van der Hoeven, B. L., N. M. Pires, H. M. Warda, P. V. Oemrawsingh, B. J. van Vlijmen, P. H. Quax, M. J. Schalij, E. E. van der Wall, and J. W. Jukema. 2005. Drug-eluting stents: results, promises and problems. *Int J Cardiol* 99 (1):9-17.

Woods, A., K. Dickerson, R. Heath, S. P. Hong, M. Momcilovic, S. R. Johnstone, M. Carlson, and D. Carling. 2005. Ca2+/calmodulin-dependent protein kinase kinase-

beta acts upstream of AMP-activated protein kinase in mammalian cells. *Cell Metab* 2 (1):21-33.

Yoshimoto, T., M. Naruse, H. Shizume, K. Naruse, A. Tanabe, M. Tanaka, K. Tago, K. Irie, T. Muraki, H. Demura, and L. Zardi. 1999. Vasculo-protective effects of insulin sensitizing agent pioglitazone in neointimal thickening and hypertensive vascular hypertrophy. *Atherosclerosis* 145 (2):333-40.

Yu, W., R. Liu-Bryan, S. Stevens, J. K. Damanahalli, and R. Terkeltaub. 2012. RAGE signaling mediates post-injury arterial neointima formation by suppression of liver kinase B1 and AMPK activity. *Atherosclerosis* 222 (2):417-25.

Zhang, H., A. Zhang, D. E. Kohan, R. D. Nelson, F. J. Gonzalez, and T. Yang. 2005. Collecting duct-specific deletion of peroxisome proliferator-activated receptor gamma blocks thiazolidinedione-induced fluid retention. *Proc Natl Acad Sci U S A* 102 (26):9406-11.

CHAPTER 5

INTEGRATED DISCUSSION

The aim of this dissertation was to investigate the effects of VSMC-specific dysregulated insulin receptor signaling on VSMC proliferation, and to investigate the molecular mechanisms by which PIO, an insulin sensitizer, inhibits VSMC proliferation and intimal hyperplasia. In the second chapter, we demonstrated that, in comparison with PDGF, neither fructose nor insulin enhanced VSMC proliferation and cyclin D1 expression. D-[^{14}C(U)] fructose uptake studies revealed a progressive increase in fructose uptake in a time-dependent manner. Concentration-dependent studies with high fructose (5 to 25 mM) showed marked increases in IRS-1 serine phosphorylation, a key adapter protein in insulin receptor signaling. Accordingly, high fructose treatment led to significant diminutions in insulin-induced phosphorylation of downstream signaling components including Akt and S6. In addition, high fructose significantly diminished insulin-induced ERK phosphorylation. Nevertheless, high fructose did not affect PDGF-induced key proliferative signaling events including phosphorylation of Akt, S6, and ERK and expression of cyclin D1 protein. Together, high fructose dysregulates IRS-1 phosphorylation state and proximal insulin receptor signaling in VSMCs but does not affect PDGF-induced proliferative signaling. In conclusion, although high fructose disrupts VSMC-specific insulin receptor signaling, the metabolic abnormalities (e.g.,

dyslipidemia) associated with high fructose consumption may play a major role in enhanced atherosclerosis and intimal hyperplasia.

In the third chapter, we demonstrated that PIO activates AMPK in VSMCs in a sustained manner thereby contributing in part to inhibition of key proliferative signaling events. In particular, PIO at 30 μM concentration activated AMPK to induce raptor phosphorylation, which diminished PDGF-induced mTOR activity as evidenced by decreased phosphorylation of p70S6K, 4E-BP1, and S6 and increased accumulation of $p27^{kip1}$, a cell cycle inhibitor. In addition, PIO inhibited the basal phosphorylation of ERK in VSMCs. Downregulation of endogenous AMPK by target-specific siRNA revealed an AMPK-independent effect for PIO inhibition of ERK, which contributed in part to diminutions in cyclin D1 expression and Rb phosphorylation and the suppression of VSMC proliferation. Furthermore, AMPK-dependent inhibition of mTOR/p70S6K and AMPK-independent inhibition of ERK signaling occurred regardless of PPARγ expression/activation in VSMCs as evidenced by gene silencing and pharmacological inhibition of PPARγ. In the fourth chapter, we demonstrated that PIO activates AMPK *via* CaMKKβ in VSMCs. In addition, we demonstrated that PIO activates AMPK in aortic tissues *in vivo*. Pharmacological inhibition of AMPK by compound C revealed that PIO inhibits neointima formation *via* AMPK-dependent and –independent mechanisms.

Previous studies have shown that in rodents fed a 20-40% fructose diet, circulating concentration of fructose increases at a range of 0.2 to 1 mM (Patel et al. 2015). Fructose is known to be transported passively into several tissues including skeletal muscle and adipocytes through plasma membrane-localized fructose transporter (glucose transporter-5, GLUT5) (Douard and Ferraris 2008). Our study provides evidence for fructose uptake

in VSMCs for the first time using radiolabeled ^{14}C-fructose. Furthermore, we and several other investigators have demonstrated the expression of GLUT5 mRNA in VSMCs and aortic tissues (Liu et al. 2011; Pyla et al. 2013). In addition to the contribution from GLUT5-mediated fructose uptake, elevation of intracellular fructose concentration can occur through *de novo* synthesis from high glucose. This is achieved through the polyol pathway that involves the activation of aldose reductase (a rate-limiting enzyme) and the intermediary formation of sorbitol (Yasunari et al. 1995; Lanaspa et al. 2013). In this regard, exposure of VSMCs to 25 mM glucose results in the elevation of polyol pathway metabolites including sorbitol and fructose (Liu et al. 2011). Importantly, 25 mM fructose treatment has been shown to enhance intracellular fructose to a similar level with an accompanying induction of GLUT5 mRNA in VSMCs (Liu et al. 2011). Our findings reveal that at 11 to 25 mM concentrations, fructose has the potential to enhance IRS-1serine phosphorylation in VSMCs, thereby attenuating insulin-induced phosphorylation of downstream signaling components such as Akt and ribosomal protein S6. In addition, high fructose treatment inhibits insulin-induced phosphorylation of ERK. Contrary to our hypothesis, high fructose-mediated disruption of insulin receptor signaling does not affect PDGF-induced key proliferative signaling events as evidenced by sustenance in the phosphorylation state of Akt, S6, and ERK and the expression level of cyclin D1.

Our findings on fructose dysregulation of insulin receptor signaling in VSMCs are in conformity with previous studies, which demonstrate high fructose-induced insulin resistance in hepatic tissue and skeletal muscle (Bezerra et al. 2000; Wei, Wang, and Pagliassotti 2005). For instance, high-fructose diet in rats leads to significant decreases in insulin-induced IRS-1 tyrosine phosphorylation and IRS-1 association with PI 3-kinase

in the liver and skeletal muscle (Bezerra et al. 2000). In rat primary hepatocytes treated with high fructose, IRS-1 serine phosphorylation is increased with an accompanying decrease in insulin-induced IRS-1 tyrosine phosphorylation (Wei, Wang, and Pagliassotti 2005). From a mechanistic standpoint, fructose-mediated dysregulation of IRS-1 and the resultant suppression of downstream signaling events may be attributable to several factors including methylglyoxal accumulation and c-jun N-terminal kinase (JNK) activation (Riboulet-Chavey et al. 2006; Liu et al. 2011; Wei, Wang, and Pagliassotti 2005; Dhar et al. 2008). It is noteworthy that, in high-fructose diet-fed rats, a significant accumulation of methylglyoxal has been observed in aortic tissues (Liu et al. 2011). In addition, high fructose treatment (15 to 25 mM) under *in vitro* conditions has been shown to enhance methylglyoxal accumulation in aortic VSMCs (Wang et al. 2006; Liu et al. 2011). Together, these findings suggest that high fructose-mediated accumulation of methylglyoxal may promote IRS-1 serine phosphorylation, thereby disrupting insulin receptor signaling in VSMCs.

Previous studies have shown that in a rat model of obesity, there is a selective resistance to PI 3-kinase/Akt signaling but not ERK pathway in aortic tissues (Jiang et al. 1999). Furthermore, in VSMCs isolated from insulin receptor-deficient mice, a decrease in insulin-induced Akt phosphorylation is associated with an increase in ERK phosphorylation, which may decrease $p27^{Kip1}$ expression to enhance proliferation (Lightell, Moss, and Woods 2011). Such selective insulin resistance in vascular cells would augment the atherogenic potential in insulin-resistant states (Jiang et al. 1999; Gogg, Smith, and Jansson 2009). However, high fructose treatment diminishes insulin-induced activation of Akt, S6 (a downstream target of mTOR), and ERK in VSMCs

(present study). Notably, methylglyoxal, an intermediary metabolite of fructose, has been previously shown to inhibit not only IRS-1 tyrosine phosphorylation and Akt signaling but also insulin-induced activation of ERK (Riboulet-Chavey et al. 2006). Thus, high fructose-mediated disruption of insulin receptor signaling including ERK does not result in enhanced VSMC proliferation, as evidenced in the present study.

To further understand the relationship between high fructose exposure and VSMC proliferative phenotype, our study has also examined whether dysregulated insulin receptor signaling is associated with altered PDGF receptor signaling. Previously, high glucose has been shown to increase aldose reductase activity and fructose formation thereby upregulating PDGF receptor-β expression (Campbell et al. 2003; Kasuya et al. 1999), which in turn results in enhanced PDGF-induced VSMC proliferation. Our findings reveal that in high fructose-treated VSMCs, PDGF receptor-β expression remains unchanged. In addition, PDGF-induced phosphorylation of key proliferative signaling events (e.g., Akt, S6, and ERK) and the expression of cell cycle protein (e.g., cyclin D1) remain essentially the same with our without high fructose treatment. These findings suggest that, under the conditions of VSMC-specific insulin resistance resulting from high fructose-induced IRS-1 serine phosphorylation, the growth-promoting effects of PDGF will be preserved in the vessel wall.

It is noteworthy that previous observations on insulin resistance and exaggerated neointima formation in IRS-1-deficient mice have been attributed to altered metabolic milieu (Kubota et al. 2003). High fructose consumption is known to induce metabolic changes in the liver including enhanced *de novo* lipogenesis (Samuel 2011). In addition, high fructose may impair the hepatic clearance of triglyceride-rich lipoproteins (Dekker

et al. 2010). Recently, high fructose has been shown to elevate the circulating concentration of proprotein convertase subtilisin/kexin type 9 (PCSK9), which accelerates hepatic LDL receptor degradation to promote hypercholesterolemia (Dong et al. 2015). In conclusion, although high fructose disrupts VSMC-specific insulin receptor signaling, the metabolic abnormalities including dyslipidemia associated with high fructose consumption may play a major role in enhanced atherosclerosis and intimal hyperplasia.

Next, the present study demonstrates that the antidiabetic drug, PIO, activates AMPK in a sustained manner thereby contributing in part to inhibition of key proliferative signaling events in VSMCs. In particular, PIO at 30 μM concentration activates AMPK to induce raptor phosphorylation, which diminishes PDGF-induced mTOR activity as evidenced by decreased phosphorylation of p70S6K, 4E-BP1, and S6 and increased accumulation of $p27^{kip1}$, a cell cycle inhibitor. In addition, PIO inhibits the basal phosphorylation of ERK in VSMCs. Downregulation of endogenous AMPK by target-specific siRNA reveals an AMPK-independent effect for PIO inhibition of ERK, which contributes in part to diminutions in cyclin D1 expression and Rb phosphorylation and the suppression of VSMC proliferation. Furthermore, AMPK-dependent inhibition of mTOR/p70S6K and AMPK-independent inhibition of ERK signaling occur regardless of PPARγ expression/activation in VSMCs as evidenced by gene silencing and pharmacological inhibition of PPARγ. Strategies that utilize nanoparticle-mediated PIO delivery at the lesion site may limit restenosis after angioplasty without inducing PPARγ-mediated systemic adverse effects (Nagahama et al. 2012; Joner et al. 2008).

Previous studies demonstrate that AMPK activation suppresses VSMC proliferation (Nagata et al. 2004; Igata et al. 2005; Stone et al. 2013; Uemura et al. 2015), whereas genetic and pharmacological strategies to inactivate AMPK restore VSMC proliferative response (Nagata et al. 2004; Igata et al. 2005; Uemura et al. 2015). Unlike these earlier observations with an AMPK activator (e.g., AICAR) (Nagata et al. 2004; Igata et al. 2005; Stone et al. 2013), our findings with a TZD derivative (e.g., PIO) highlight its role in AMPK activation that mediates the suppression of VSMC proliferative signaling in a partial manner. Notably, ectopic expression of dominant-negative AMPK to inhibit AMPK activity (Nagata et al. 2004; Igata et al. 2005) prevents AICAR inhibition of serum-induced VSMC proliferation and the associated phosphorylation of Rb (Igata et al. 2005). In the present study, downregulation of endogenous AMPK by target-specific siRNA abolishes PIO-mediated accumulation of $p27^{Kip1}$ (a cell cycle inhibitor) (Tanner et al. 2000) but does not prevent PIO inhibition of PDGF-induced cyclin D1 expression. Together, our findings reveal that PIO has the potential to inhibit VSMC proliferation through AMPK-dependent and AMPK-independent mechanisms beyond its role as a PPARγ agonist. Furthermore, AMPK activation by AICAR results in increased p53 phosphorylation/expression and $p21^{Cip1}$ expression, which in turn inhibits Rb phosphorylation to suppress VSMC proliferation (Igata et al. 2005). Our findings reveal that PIO does not affect p53 phosphorylation/expression but it decreases $p21^{Cip1}$ expression, suggesting that p53-p21 axis may not play an intermediary role in PIO inhibition of VSMC proliferation.

Studies with AICAR and adipokines have shown that AMPK activation is associated with diminished ERK activation (Nagata et al. 2004; Motobayashi et al. 2009; Uemura et

al. 2015), which in turn is attributable to the suppression of VSMC proliferation (Nagata et al. 2004; Uemura et al. 2015). However, there is no apparent causal link between the observed AMPK activation and diminished ERK phosphorylation toward PIO inhibition of VSMC proliferation (present study). For instance, while AICAR activates AMPK and inhibits agonist-induced ERK phosphorylation (Nagata et al. 2004; Motobayashi et al. 2009), overexpression of dominant-negative AMPK abrogates the downstream signal (e.g., ACC phosphorylation) and augments agonist-induced ERK phosphorylation to promote VSMC proliferation (Nagata et al. 2004). In addition, adipokines such as omentin and adiponectin activate AMPK to inhibit ERK phosphorylation in VSMCs (Uemura et al. 2015; Motobayashi et al. 2009). In particular, genetic blockade of AMPK activation prevents omentin inhibition of PDGF-induced ERK phosphorylation to restore VSMC proliferation (Uemura et al. 2015). In contrast to AICAR and the aforementioned adipokines, our findings show that PIO inhibition of basal ERK phosphorylation remains essentially the same after AMPK downregulation and the associated abrogation of ACC phosphorylation. This is further supported by the persistent decrease in PDGF-induced cyclin D1 expression by PIO after AMPK downregulation, thereby suggesting that PIO inhibition of VSMC proliferation occurs in part through mechanisms independent of AMPK activation.

Several lines of evidence suggest that AMPK activation results in the inhibition of mTOR/p70S6K signaling (and *vice versa*) in different tissues/cell types (Inoki, Kim, and Guan 2012; Saha et al. 2010), including VSMCs (Kim et al. 2014). In particular, AMPK activation in nonvascular cells promotes raptor phosphorylation to inhibit the activity of mTOR (Gwinn et al. 2008), a key signaling component that regulates protein synthesis

(Sengupta, Peterson, and Sabatini 2010; Ning and Clemmons 2010), cell cycle progression and cell proliferation (Martinet, De Loof, and De Meyer 2014). Recent studies with VSMCs demonstrate that ectopic expression of retinoic acid receptor-related orphan receptor-α (RORα) enhances AMPK phosphorylation to inhibit mTOR/p70S6K phosphorylation, thereby suppressing VSMC proliferation (Kim et al. 2014). Our findings reveal that PIO not only activates AMPK but also promotes raptor phosphorylation to inhibit mTOR signaling (e.g., ↓ phosphorylation of p70S6K, 4E-BP1, and S6) and protein synthesis in VSMCs. This novel observation is supported by AMPK downregulation studies using target-specific siRNA. Importantly, downregulation of AMPK diminishes PIO-mediated phosphorylation of ACC and raptor, thereby restoring S6 phosphorylation with an accompanying blockade in the accumulation of $p27^{Kip1}$ (a cell cycle inhibitor) (Tanner et al. 2000). Together, these findings suggest that in addition to strategies that overexpress RORα in VSMCs (Kim et al. 2014), treatment with PIO may provide another promising approach to attenuate exaggerated VSMC growth through ↑AMPK → ↓mTOR axis.

While our findings with PIO point toward AMPK-independent (*via* ↓ ERK) and AMPK-dependent (*via* ↓ mTOR/p70S6K) mechanisms to suppress VSMC proliferation, it is critically important to know whether PPARγ regulates these signaling events. Previously, loss-of-function studies (e.g., dominant-negative PPARγ mutation that suppresses endogenous PPARγ function) have revealed exaggerated neointima formation in mice but without any changes in growth factor-induced ERK phosphorylation, suggesting that endogenous PPARγ does not regulate ERK activation during VSMC proliferation (Meredith et al. 2009). In a different study, rosiglitazone inhibits PDGF- or

arterial injury-induced ERK activation in a PPARγ-independent manner, as evidenced by the use of dominant-negative PPARγ mutant (Lee et al. 2009). In conformity with these earlier findings, our study demonstrates that PIO, while upregulating PPARγ expression in the nucleus, exerts an inhibitory effect on ERK phosphorylation and cyclin D1 expression. Importantly, PIO inhibition of ERK phosphorylation and cyclin D1 expression is unaffected after PPARγ downregulation (~87%) by target-specific siRNA. Since the contribution of ~13% residual PPARγ expression (in PPARγ siRNA-treated VSMCs) cannot be fully excluded, we employed an additional approach involving VSMC treatment with GW-9662. Pharmacological inhibition of PPARγ by GW-9662 yielded results similar to that observed in PPARγ siRNA-treated VSMCs. Together, these studies suggest that PIO inhibition of key proliferative signaling events (e.g., pERK and cyclin D1) occurs by mechanisms independent of PPARγ in VSMCs. It is noteworthy that the basal ERK phosphorylation in vascular cells is mediated in part by reactive oxygen species (ROS), including superoxide (O_2^-) (Li et al. 2004; Lee et al. 2015). In addition, PIO has been shown to inhibit NADPH oxidase-mediated generation of ROS in aortic tissues and VSMCs (Martin et al. 2012; Perez-Giron et al. 2014). Thus, it is likely that PIO inhibits the basal ERK activation by suppressing ROS production in VSMCs.

It is widely accepted that TZD activation of PPARγ in adipocytes results in the synthesis and release of adiponectin (Kadowaki et al. 2006). Recent studies demonstrate that exposure of VSMCs to rosiglitazone for 24 hours enhances the expression of adiponectin (Ding et al. 2012), which in turn can act in an autocrine/paracrine manner to activate AMPK in VSMCs (Ding et al. 2012; Ding et al. 2011). From our findings that

reveal PIO activation of AMPK, it may, therefore, be argued that PPARγ-mediated adiponectin synthesis/release is a critical transcriptional event for such an effect. However, our experimental approaches involving siRNA-mediated PPARγ downregulation, chemical inhibition of PPARγ by GW-9662, and time course studies do not support the likely intermediary role of adiponectin toward PIO activation of AMPK in VSMCs. First, neither PPARγ downregulation nor GW-9662 affects PIO activation of AMPK or PIO inhibition of PDGF-induced S6 phosphorylation. Second, PIO activation of AMPK occurs as early as 1 to 3 hours (present study) in contrast to a much longer time frame (≥ 24 hr) that is required for adiponectin upregulation and subsequent AMPK activation (Ding et al. 2012; Ding et al. 2011) in VSMCs. Third, PIO is several folds less potent than rosiglitazone as a PPARγ activator (Young et al. 1998). Together, these studies suggest that PIO activation of AMPK occurs by PPARγ- and adiponectin-independent mechanisms in VSMCs.

TZD derivative(s) have been shown to activate AMPK through ↓ mitochondrial respiratory chain complex I (Brunmair et al. 2004), ↓ mitochondrial membrane potential (Konrad et al. 2005), ↑AMP/ATP ratio (Fryer, Parbu-Patel, and Carling 2002; Saha et al. 2004), and/or LKB1 (Boyle et al. 2008) in insulin-responsive tissues and HeLa cells. In particular, ROSI but not PIO at 10 μM and 30 μM concentrations significantly inhibits respiratory complex I enzyme activity in rat skeletal muscle and liver (Brunmair et al. 2004), suggesting that PIO activation of AMPK in VSMCs may not involve inhibition of respiratory complex I. Although TRO has been shown to activate AMPK by acutely reducing mitochondrial membrane potential in skeletal muscle cells (Konrad et al. 2005), our findings from TMRM fluorescence studies do not support the possibility for

mitochondrial membrane depolarization by PIO as a likely intermediary event in VSMCs *at least* under the chosen time intervals. In view of the critical link between ↑AMP/ATP ratio and AMPK activation (Fryer, Parbu-Patel, and Carling 2002; Saha et al. 2004), we have also analyzed adenine nucleotide levels in PIO-treated VSMCs. While ROSI at 200 μM concentration increases AMP/ATP ratio in skeletal muscle cells (Fryer, Parbu-Patel, and Carling 2002), PIO treatment in VSMCs shows a trend toward ↑AMP/ATP ratio but without statistical significance. Given that LKB1 is a catalytic enzyme, the contribution of ~14% residual LKB1 protein (in LKB1 siRNA-treated VSMCs) cannot be fully excluded with regard to AMPK activation. Furthermore, PIO treatment enhances the phosphorylation of ACC, a key downstream target of AMPK (Kahn et al. 2005) prior to AMPKα^{Thr172} phosphorylation in VSMCs as revealed in our time course study. This may be attributed to an apparent allosteric activation of AMPK without AMPKα^{Thr172} phosphorylation as has been evidenced previously in human melanoma cells upon treatment with A769662, a direct AMPK activator that does not increase intracellular AMP or ADP levels (Gowans et al. 2013). Future studies are clearly warranted that should compare the role of PIO *versus* ROSI/TRO toward inducing temporal changes in mitochondrial function, including the potential inhibitory effects on mitochondrial pyruvate carrier (Divakaruni et al. 2013), to identify the upstream signaling events critical for PIO activation of AMPK in VSMCs.

From a clinical standpoint, the findings from the meta-analysis of randomized trials suggest that, in comparison with rosiglitazone that may increase the risk of ischemic events, PIO has a more favorable effect on ischemic vascular complications (Lincoff et al. 2007). PROactive study (PROspective pioglitAzone Clinical Trial In macroVascular

Events) reveals that PIO treatment is associated with improved cardiovascular outcomes in patients with type 2 diabetes and macrovascular disease (Dormandy et al. 2005). Nevertheless, the precise mechanisms for such vasoprotective effects remain largely unknown due to the pleiotropic actions of PIO. Notably, PIO has been shown to lower blood pressure (Hsueh and Law 2001) and improve endothelial function (Hsueh and Law 2001). It also exhibits anti-inflammatory (Ishibashi et al. 2002), anti-migratory (Game et al. 2005), and anti-proliferative (Yoshimoto et al. 1999) effects in VSMCs. The concentration of PIO used in the present *in vitro* study with VSMCs is nearly one order of magnitude higher than the peak plasma concentration (~3 μM) observed in human subjects on PIO treatment (Hanefeld 2001). At this juncture, it is important to note that in comparison with the inhibitory effects of 10-30 μM PIO added directly to VSMCs in culture (our findings and previous studies) (Hong et al. 2010), a pronounced inhibition of VSMC proliferation occurs upon *in vitro* addition of serum samples obtained from PIO-treated type 2 diabetic subjects (Hong et al. 2010). These data suggest that, under *in vivo* conditions, circulating PIO has the potential to exert direct and indirect inhibitory effects on VSMC proliferation. The indirect inhibitory effects of PIO may be attributable to its role in anti-inflammatory action and enhanced adiponectin release. It is well accepted that PIO activation of PPARγ in adipose tissue would enhance circulatory levels of adiponectin (Kadowaki et al. 2006), which in turn would suppress neointima formation (Arita et al. 2002) through AMPK activation in VSMCs (Ding et al. 2012; Ding et al. 2011). The present findings suggest a yet another mechanism for PIO inhibition of VSMC proliferation through AMPK-dependent and AMPK-independent signaling mechanisms regardless of PPARγ expression. Notably, AMPK activation by AICAR has

been shown to inhibit neointima formation in balloon-injured rat carotid artery (Stone et al. 2013). Recent studies demonstrate that AICAR and metformin inhibit the differentiation of monocytes to macrophages through AMPKα1 activation *in vitro* (Vasamsetti et al. 2015). In addition, oral administration of metformin attenuates atherosclerotic lesion by inhibiting macrophage accumulation in apoE-deficient mouse aorta (Vasamsetti et al. 2015). Future studies should compare the effects of the therapeutically relevant concentration of PIO *versus* metformin/AICAR on neointima formation after arterial injury in AMPKα1-deficient mice.

In conclusion, PIO has the potential to inhibit VSMC proliferation through indirect effects involving adiponectin/AMPK (Kadowaki et al. 2006; Ding et al. 2012; Ding et al. 2011; Arita et al. 2002), and in part through direct effects involving AMPK-dependent and AMPK-independent regulation of cell cycle regulatory proteins.

We extend our findings by identifying CaMKKβ as the upstream kinase mediating PIO activation of AMPK in VSMCs. In addition, we report that PIO administration in CJ57BL/6 mice leads to sustained activation of AMPK in the vasculature, and thus contributing, in part, to PIO inhibition of neointima formation.

While TZDs are traditionally viewed as PPARγ agonists, recent reports have ascribed some of their pharmacological effects to PPARγ-independent activation of AMPK. For instance, gene silencing of AMPK reduces the troglitazone-mediated increase in 2-deoxyglucose uptake in muscle cells (Konrad et al. 2005). In addition, infection of human aortic endothelial cells with adenoviruses expressing dominant-negative AMPK attenuates rosiglitazone-induced phosphorylation of eNOS-Ser-1177 and the subsequent increase in NO production (Boyle et al. 2008). From a mechanistic perspective, TZD

activation of AMPK is commonly ascribed to inhibition of mitochondrial activity and alteration of AMP/ATP ratio (Fryer, Parbu-Patel, and Carling 2002; Brunmair et al. 2004; LeBrasseur et al. 2006; Boyle et al. 2008; Hawley et al. 2010). However, some previous findings by our group and others suggest that PIO may activate AMPK via a different mechanism (Brunmair et al. 2004; Osman and Segar 2016). For instance, the inhibitory effects of PIO on mitochondrial function in homogenates of skeletal muscle are only evident at very high concentrations (100 μM), while the inhibitory effects of rosiglitazone are evident at concentrations as low as 10 μM (Brunmair et al. 2004). In addition, we have recently reported that PIO activates AMPK in VSMCs at concentrations as low as 3 μM (Osman and Segar 2016). In addition, PIO activation of AMPK in VSMCs is neither associated with an increase in AMP/ATP ratio nor mitochondrial-membrane depolarization and is likely independent of LKB1 (Osman and Segar 2016). These findings raise the possibility that PIO may activate AMPK *via* a different mechanism in VSMCs.

In addition to LKB1, AMPK can be phosphorylated at Thr^{172}, and thus activated, by CaMKKβ in response to high cytosolic free calcium levels (Hawley et al. 2005; Woods et al. 2005). Previously, we and several other investigators have shown that vasoactive peptides that evoke a rise in cytosolic free calcium levels in vascular smooth muscle promote an increase in AMPK phosphorylation through an intermediary activation of CaMKKβ (Horman et al. 2008; Pyla et al. 2014). Recently, rosiglitazone was reported to inhibit the endoplasmic reticulum calcium ATPase in monocytic cells (Caddy et al. 2008) and VSMCs (Caddy et al. 2010) and thus leading to an increase intracellular calcium levels. These earlier observations suggest that PIO may activate AMPK through

CaMKKβ in VSMCs. In accordance with these reports, downregulation of endogenous CaMKKβ by target-specific siRNA reveals that CaMKKβ is the key upstream kinase responsible for basal and PIO activation of AMPK in VSMCs. To confirm the intermediary role of CaMKKβ in mediating PIO activation of AMPK, we employed an additional approach involving VSMC treatment with STO-609. Pharmacological inhibition of CaMKKβ by STO-609 yielded results similar to that observed in CaMKKβ siRNA-treated VSMCs. Together, these studies suggest that PIO activates AMPK in a CaMKKβ-dependent manner in VSMCs. Future studies are clearly warranted that should investigate the likely effects of PIO on calcium signaling in VSMCs.

In addition to the previously described TZD activation of AMPK in cells in culture (Fryer, Parbu-Patel, and Carling 2002; Brunmair et al. 2004; LeBrasseur et al. 2006; Boyle et al. 2008; Hawley et al. 2010; Konrad et al. 2005; Osman and Segar 2016), TZDs activate AMPK in different tissues in experimental animals (Saha et al. 2004; LeBrasseur et al. 2006; Lessard et al. 2006; Morisaki et al. 2011). Moreover, PIO activates AMPK in human skeletal muscle *in vivo* and increases the expression of genes involved in adiponectin signaling, mitochondrial function and fat oxidation (Coletta et al. 2009). Recently, PIO was reported to enhance the phosphorylation of AMPK in rabbit vein grafts (Morisaki et al. 2011). In this study, we extend previous findings by demonstrating that PIO activates AMPK in mouse aortic tissues in a sustained manner. From a mechanistic perspective, PIO activation of PPARγ in adipose tissue enhances circulatory levels of adiponectin (Kadowaki et al. 2006), which in turn is expected to activate AMPK in VSMCs (Ding et al. 2012; Ding et al. 2011). In addition, we recently reported that PIO activates AMPK in VSMCs directly and independent of PPARγ activation (Osman

and Segar 2016). Thus, it is likely that PIO activates AMPK in the vasculature (this study) *via* direct and indirect effects and that this activation mediates at least some of its pharmacological effects in the vessel wall.

Previous studies have shown that TZDs have strong inhibitory effects on neointima formation in different experimental models including normal rats (Law et al. 1996; Aizawa et al. 2001; Igarashi et al. 2001), insulin-resistant Zucker fatty rats (Shinohara et al. 1998), stroke-prone spontaneously hypertensive rats (Yoshimoto et al. 1999), and hypercholesterolemic rabbits (Pakala et al. 2006). In addition, TZDs inhibit neointima formation after coronary stenting in nondiabetic patients with metabolic syndrome (Katayama et al. 2007), and in patients with type 2 diabetes mellitus (Takagi et al. 2000; Nishio et al. 2006; Choi et al. 2004; Patel et al. 2011). However, the signaling mechanisms mediating TZD inhibition of neointima formation are not fully understood. For instance, *in vivo* transfer of the PPARγ-WT gene was found to inhibit smooth muscle proliferation, sustain apoptosis, and reduce neointima formation after balloon injury in rats (Lim et al. 2006). On the other hand, rosiglitazone has been shown to inhibit neointimal formation *via* PPARγ-independent activation of glycogen synthase kinase-3β (Lee et al. 2009). We have recently reported that PIO inhibits PDGF-induced VSMC proliferation *via* activation of AMPK/mTOR signaling axis (Osman and Segar 2016). In this study, we extend our findings by showing that AMPK mediates, in part, to PIO inhibition of neointima formation *in vivo*.

Several cytokines and pharmacological agents are reported to inhibit neointima formation *via* activation of AMPK. For instance, 5-aminoimidazole-4-carboxamide-1-beta-d-ribofuranoside (AICAR) (Stone et al. 2013), adiponectin (Takaoka et al. 2009),

metformin (Lu et al. 2013), retinoic acid-related orphan receptor alpha (Kim et al. 2014), muscle-derived follistatin-like 1 protein (Miyabe et al. 2014) , diclofenac (MacAskill et al. 2015), and omentin (Uemura et al. 2015) inhibit neointima formation that appears to be dependent on AMPK activation. In addition, genetic ablation of AMPK enhances neointima formation *in vivo* (Song et al. 2011; Song et al. 2013). Moreover, receptor for advanced glycation endproducts (RAGE) signaling enhances neointima formation *via* the suppression of AMPK (Yu et al. 2012). Accordingly, AMPK may represent a viable pharmacological target to treat restenosis after balloon injury.

TZDs have been demonstrated to exhibit salutary effects in the vasculature (Yoshimoto et al. 1999; Phillips et al. 2003; Satoh et al. 2003) beyond their insulin-sensitizing action in patients with type 2 diabetes (Kahn et al. 2006). However, TZD treatment is associated with several adverse effects, including weight gain, fluid retention, and congestive heart failure, thus raising concerns about their cardiovascular safety (Nesto et al. 2003). These unfavorable effects are attributed in part to activation of PPARγ (Guan et al. 2005; Zhang et al. 2005). Since, PIO inhibits neointima formation, in part, *via* activation of AMPK, strategies that utilize nanoparticle-mediated PIO delivery at the lesion site may limit restenosis after angioplasty without inducing PPARγ-mediated systemic adverse effects (Nagahama et al. 2012; Joner et al. 2008).

Bibliography

Aizawa, Y., J. i Kawabe, N. Hasebe, N. Takehara, and K. Kikuchi. 2001. Pioglitazone Enhances Cytokine-Induced Apoptosis in Vascular Smooth Muscle Cells and Reduces Intimal Hyperplasia. *Circulation* 104 (4):455-460.

Arita, Y., S. Kihara, N. Ouchi, K. Maeda, H. Kuriyama, Y. Okamoto, M. Kumada, K. Hotta, M. Nishida, M. Takahashi, T. Nakamura, I. Shimomura, M. Muraguchi, Y. Ohmoto, T. Funahashi, and Y. Matsuzawa. 2002. Adipocyte-derived plasma protein adiponectin acts as a platelet-derived growth factor-BB-binding protein and regulates growth factor-induced common postreceptor signal in vascular smooth muscle cell. *Circulation* 105 (24):2893-8.

Bezerra, R. M., M. Ueno, M. S. Silva, D. Q. Tavares, C. R. Carvalho, and M. J. Saad. 2000. A high fructose diet affects the early steps of insulin action in muscle and liver of rats. *J Nutr* 130 (6):1531-5.

Boyle, J. G., P. J. Logan, M. A. Ewart, J. A. Reihill, S. A. Ritchie, J. M. Connell, S. J. Cleland, and I. P. Salt. 2008. Rosiglitazone stimulates nitric oxide synthesis in human aortic endothelial cells via AMP-activated protein kinase. *J Biol Chem* 283 (17):11210-7.

Brunmair, B., K. Staniek, F. Gras, N. Scharf, A. Althaym, R. Clara, M. Roden, E. Gnaiger, H. Nohl, W. Waldhausl, and C. Furnsinn. 2004. Thiazolidinediones, like metformin, inhibit respiratory complex I: a common mechanism contributing to their antidiabetic actions? *Diabetes* 53 (4):1052-9.

Caddy, J., S. Isa, L. S. Mainwaring, E. Adam, A. Roberts, D. Lang, R. H. Morris, A. W. Thomas, and R. Webb. 2010. Rosiglitazone induces the unfolded protein

response, but has no significant effect on cell viability, in monocytic and vascular smooth muscle cells. *Biochem Biophys Res Commun* 400 (4):689-95.

Caddy, J., N. Singh, L. Atkin, M. Ahluwalia, A. Roberts, D. Lang, A. W. Thomas, and R. Webb. 2008. Rosiglitazone transiently disturbs calcium homeostasis in monocytic cells. *Biochemical and Biophysical Research Communications* 366 (1):149-155.

Campbell, M., W. E. Allen, J. A. Silversides, and E. R. Trimble. 2003. Glucose-induced phosphatidylinositol 3-kinase and mitogen-activated protein kinase-dependent upregulation of the platelet-derived growth factor-beta receptor potentiates vascular smooth muscle cell chemotaxis. *Diabetes* 52 (2):519-26.

Choi, D., S. K. Kim, S. H. Choi, Y. G. Ko, C. W. Ahn, Y. Jang, S. K. Lim, H. C. Lee, and B. S. Cha. 2004. Preventative effects of rosiglitazone on restenosis after coronary stent implantation in patients with type 2 diabetes. *Diabetes Care* 27 (11):2654-60.

Coletta, D. K., A. Sriwijitkamol, E. Wajcberg, P. Tantiwong, M. Li, M. Prentki, M. Madiraju, C. P. Jenkinson, E. Cersosimo, N. Musi, and R. A. Defronzo. 2009. Pioglitazone stimulates AMP-activated protein kinase signalling and increases the expression of genes involved in adiponectin signalling, mitochondrial function and fat oxidation in human skeletal muscle in vivo: a randomised trial. *Diabetologia* 52 (4):723-32.

Dekker, M. J., Q. Su, C. Baker, A. C. Rutledge, and K. Adeli. 2010. Fructose: a highly lipogenic nutrient implicated in insulin resistance, hepatic steatosis, and the metabolic syndrome. *Am J Physiol Endocrinol Metab* 299 (5):E685-94.

Dhar, A., K. Desai, M. Kazachmov, P. Yu, and L. Wu. 2008. Methylglyoxal production in vascular smooth muscle cells from different metabolic precursors. *Metabolism* 57 (9):1211-20.

Ding, M., A. C. Carrao, R. J. Wagner, Y. Xie, Y. Jin, E. M. Rzucidlo, J. Yu, W. Li, G. Tellides, J. Hwa, T. R. Aprahamian, and K. A. Martin. 2012. Vascular smooth muscle cell-derived adiponectin: a paracrine regulator of contractile phenotype. *J Mol Cell Cardiol* 52 (2):474-84.

Ding, M., Y. Xie, R. J. Wagner, Y. Jin, A. C. Carrao, L. S. Liu, A. K. Guzman, R. J. Powell, J. Hwa, E. M. Rzucidlo, and K. A. Martin. 2011. Adiponectin induces vascular smooth muscle cell differentiation via repression of mammalian target of rapamycin complex 1 and FoxO4. *Arterioscler Thromb Vasc Biol* 31 (6):1403-10.

Divakaruni, A. S., S. E. Wiley, G. W. Rogers, A. Y. Andreyev, S. Petrosyan, M. Loviscach, E. A. Wall, N. Yadava, A. P. Heuck, D. A. Ferrick, R. R. Henry, W. G. McDonald, J. R. Colca, M. I. Simon, T. P. Ciaraldi, and A. N. Murphy. 2013. Thiazolidinediones are acute, specific inhibitors of the mitochondrial pyruvate carrier. *Proc Natl Acad Sci U S A* 110 (14):5422-7.

Dong, B., A. B. Singh, S. Azhar, N. G. Seidah, and J. Liu. 2015. High-fructose feeding promotes accelerated degradation of hepatic LDL receptor and hypercholesterolemia in hamsters via elevated circulating PCSK9 levels. *Atherosclerosis* 239 (2):364-74.

Dormandy, J. A., B. Charbonnel, D. J. Eckland, E. Erdmann, M. Massi-Benedetti, I. K. Moules, A. M. Skene, M. H. Tan, P. J. Lefebvre, G. D. Murray, E. Standl, R. G. Wilcox, L. Wilhelmsen, J. Betteridge, K. Birkeland, A. Golay, R. J. Heine, L.

Koranyi, M. Laakso, M. Mokan, A. Norkus, V. Pirags, T. Podar, A. Scheen, W. Scherbaum, G. Schernthaner, O. Schmitz, J. Skrha, U. Smith, J. Taton, and P. ROactive investigators. 2005. Secondary prevention of macrovascular events in patients with type 2 diabetes in the PROactive Study (PROspective pioglitAzone Clinical Trial In macroVascular Events): a randomised controlled trial. *Lancet* 366 (9493):1279-89.

Douard, V., and R. P. Ferraris. 2008. Regulation of the fructose transporter GLUT5 in health and disease. *Am J Physiol Endocrinol Metab* 295 (2):E227-37.

Fryer, L. G., A. Parbu-Patel, and D. Carling. 2002. The Anti-diabetic drugs rosiglitazone and metformin stimulate AMP-activated protein kinase through distinct signaling pathways. *J Biol Chem* 277 (28):25226-32.

Game, B. A., A. Maldonado, L. He, and Y. Huang. 2005. Pioglitazone inhibits MMP-1 expression in vascular smooth muscle cells through a mitogen-activated protein kinase-independent mechanism. *Atherosclerosis* 178 (2):249-56.

Gogg, S., U. Smith, and P. A. Jansson. 2009. Increased MAPK activation and impaired insulin signaling in subcutaneous microvascular endothelial cells in type 2 diabetes: the role of endothelin-1. *Diabetes* 58 (10):2238-45.

Gowans, G. J., S. A. Hawley, F. A. Ross, and D. G. Hardie. 2013. AMP is a true physiological regulator of AMP-activated protein kinase by both allosteric activation and enhancing net phosphorylation. *Cell Metab* 18 (4):556-66.

Guan, Y., C. Hao, D. R. Cha, R. Rao, W. Lu, D. E. Kohan, M. A. Magnuson, R. Redha, Y. Zhang, and M. D. Breyer. 2005. Thiazolidinediones expand body fluid volume

through PPARgamma stimulation of ENaC-mediated renal salt absorption. *Nat Med* 11 (8):861-6.

Gwinn, D. M., D. B. Shackelford, D. F. Egan, M. M. Mihaylova, A. Mery, D. S. Vasquez, B. E. Turk, and R. J. Shaw. 2008. AMPK phosphorylation of raptor mediates a metabolic checkpoint. *Mol Cell* 30 (2):214-26.

Hanefeld, M. 2001. Pharmacokinetics and clinical efficacy of pioglitazone. *Int J Clin Pract Suppl* (121):19-25.

Hawley, S. A., D. A. Pan, K. J. Mustard, L. Ross, J. Bain, A. M. Edelman, B. G. Frenguelli, and D. G. Hardie. 2005. Calmodulin-dependent protein kinase kinase-beta is an alternative upstream kinase for AMP-activated protein kinase. *Cell Metab* 2 (1):9-19.

Hawley, S. A., F. A. Ross, C. Chevtzoff, K. A. Green, A. Evans, S. Fogarty, M. C. Towler, L. J. Brown, O. A. Ogunbayo, A. M. Evans, and D. G. Hardie. 2010. Use of cells expressing gamma subunit variants to identify diverse mechanisms of AMPK activation. *Cell Metab* 11 (6):554-65.

Hong, S. J., S. T. Kim, T. J. Kim, E. O. Kim, C. M. Ahn, J. H. Park, J. S. Kim, K. M. Lee, and D. S. Lim. 2010. Cellular and molecular changes associated with inhibitory effect of pioglitazone on neointimal growth in patients with type 2 diabetes after zotarolimus-eluting stent implantation. *Arterioscler Thromb Vasc Biol* 30 (12):2655-65.

Horman, S., N. Morel, D. Vertommen, N. Hussain, D. Neumann, C. Beauloye, N. El Najjar, C. Forcet, B. Viollet, M. P. Walsh, L. Hue, and M. H. Rider. 2008. AMP-

activated protein kinase phosphorylates and desensitizes smooth muscle myosin light chain kinase. *J Biol Chem* 283 (27):18505-12.

Hsueh, W. A., and R. E. Law. 2001. PPARgamma and atherosclerosis: effects on cell growth and movement. *Arterioscler Thromb Vasc Biol* 21 (12):1891-5.

Igarashi, M., A. Hirata, H. Yamaguchi, H. Tsuchiya, H. Ohnuma, M. Tominaga, M. Daimon, and T. Kato. 2001. Characterization of an inhibitory effect of pioglitazone on balloon-injured vascular smooth muscle cell growth. *Metabolism* 50 (8):955-62.

Igata, M., H. Motoshima, K. Tsuruzoe, K. Kojima, T. Matsumura, T. Kondo, T. Taguchi, K. Nakamaru, M. Yano, D. Kukidome, K. Matsumoto, T. Toyonaga, T. Asano, T. Nishikawa, and E. Araki. 2005. Adenosine monophosphate-activated protein kinase suppresses vascular smooth muscle cell proliferation through the inhibition of cell cycle progression. *Circ Res* 97 (8):837-44.

Inoki, K., J. Kim, and K. L. Guan. 2012. AMPK and mTOR in cellular energy homeostasis and drug targets. *Annu Rev Pharmacol Toxicol* 52:381-400.

Ishibashi, M., K. Egashira, K. Hiasa, S. Inoue, W. Ni, Q. Zhao, M. Usui, S. Kitamoto, T. Ichiki, and A. Takeshita. 2002. Antiinflammatory and antiarteriosclerotic effects of pioglitazone. *Hypertension* 40 (5):687-93.

Jiang, Z. Y., Y. W. Lin, A. Clemont, E. P. Feener, K. D. Hein, M. Igarashi, T. Yamauchi, M. F. White, and G. L. King. 1999. Characterization of selective resistance to insulin signaling in the vasculature of obese Zucker (fa/fa) rats. *J Clin Invest* 104 (4):447-57.

Joner, M., K. Morimoto, H. Kasukawa, K. Steigerwald, S. Merl, G. Nakazawa, M. C. John, A. V. Finn, E. Acampado, F. D. Kolodgie, H. K. Gold, and R. Virmani. 2008. Site-specific targeting of nanoparticle prednisolone reduces in-stent restenosis in a rabbit model of established atheroma. *Arterioscler Thromb Vasc Biol* 28 (11):1960-6.

Kadowaki, T., T. Yamauchi, N. Kubota, K. Hara, K. Ueki, and K. Tobe. 2006. Adiponectin and adiponectin receptors in insulin resistance, diabetes, and the metabolic syndrome. *J Clin Invest* 116 (7):1784-92.

Kahn, B. B., T. Alquier, D. Carling, and D. G. Hardie. 2005. AMP-activated protein kinase: ancient energy gauge provides clues to modern understanding of metabolism. *Cell Metab* 1 (1):15-25.

Kahn, S. E., S. M. Haffner, M. A. Heise, W. H. Herman, R. R. Holman, N. P. Jones, B. G. Kravitz, J. M. Lachin, M. C. O'Neill, B. Zinman, G. Viberti, and Adopt Study Group. 2006. Glycemic durability of rosiglitazone, metformin, or glyburide monotherapy. *N Engl J Med* 355 (23):2427-43.

Kasuya, Y., J. Nakamura, Y. Hamada, M. Nakayama, H. Sasaki, T. Komori, S. Chaya, G. Watanabe, K. Naruse, E. Nakashima, K. Kato, and N. Hotta. 1999. An aldose reductase inhibitor prevents the glucose-induced increase in PDGF-beta receptor in cultured rat aortic smooth muscle cells. *Biochem Biophys Res Commun* 261 (3):853-8.

Katayama, T., H. Ueba, K. Tsuboi, N. Kubo, T. Yasu, M. Kuroki, M. Saito, S. Momomura, and M. Kawakami. 2007. Reduction of neointimal hyperplasia after

coronary stenting by pioglitazone in nondiabetic patients with metabolic syndrome. *Am Heart J* 153 (5):762 e1-7.

Kim, E. J., Y. K. Choi, Y. H. Han, H. J. Kim, I. K. Lee, and M. O. Lee. 2014. RORalpha suppresses proliferation of vascular smooth muscle cells through activation of AMP-activated protein kinase. *Int J Cardiol* 175 (3):515-21.

Konrad, D., A. Rudich, P. J. Bilan, N. Patel, C. Richardson, L. A. Witters, and A. Klip. 2005. Troglitazone causes acute mitochondrial membrane depolarisation and an AMPK-mediated increase in glucose phosphorylation in muscle cells. *Diabetologia* 48 (5):954-66.

Kubota, T., N. Kubota, M. Moroi, Y. Terauchi, T. Kobayashi, K. Kamata, R. Suzuki, K. Tobe, A. Namiki, S. Aizawa, R. Nagai, T. Kadowaki, and T. Yamaguchi. 2003. Lack of insulin receptor substrate-2 causes progressive neointima formation in response to vessel injury. *Circulation* 107 (24):3073-80.

Lanaspa, M. A., T. Ishimoto, N. Li, C. Cicerchi, D. J. Orlicky, P. Ruzycki, C. Rivard, S. Inaba, C. A. Roncal-Jimenez, E. S. Bales, C. P. Diggle, A. Asipu, J. M. Petrash, T. Kosugi, S. Maruyama, L. G. Sanchez-Lozada, J. L. McManaman, D. T. Bonthron, Y. Y. Sautin, and R. J. Johnson. 2013. Endogenous fructose production and metabolism in the liver contributes to the development of metabolic syndrome. *Nat Commun* 4:2434.

Law, R. E., W. P. Meehan, X. P. Xi, K. Graf, D. A. Wuthrich, W. Coats, D. Faxon, and W. A. Hsueh. 1996. Troglitazone inhibits vascular smooth muscle cell growth and intimal hyperplasia. *J Clin Invest* 98 (8):1897-905.

LeBrasseur, N. K., M. Kelly, T. S. Tsao, S. R. Farmer, A. K. Saha, N. B. Ruderman, and E. Tomas. 2006. Thiazolidinediones can rapidly activate AMP-activated protein kinase in mammalian tissues. *Am J Physiol Endocrinol Metab* 291 (1):E175-81.

Lee, C. S., Y. W. Kwon, H. M. Yang, S. H. Kim, T. Y. Kim, J. Hur, K. W. Park, H. J. Cho, H. J. Kang, Y. B. Park, and H. S. Kim. 2009. New mechanism of rosiglitazone to reduce neointimal hyperplasia: activation of glycogen synthase kinase-3beta followed by inhibition of MMP-9. *Arterioscler Thromb Vasc Biol* 29 (4):472-9.

Lee, K. P., G. W. Sudjarwo, S. H. Jung, D. Lee, D. Y. Lee, G. B. Lee, S. Baek, D. Y. Kim, H. M. Lee, B. Kim, S. C. Kwon, and K. J. Won. 2015. Carvacrol inhibits atherosclerotic neointima formation by downregulating reactive oxygen species production in vascular smooth muscle cells. *Atherosclerosis* 240 (2):367-73.

Lessard, S. J., Z. P. Chen, M. J. Watt, M. Hashem, J. J. Reid, M. A. Febbraio, B. E. Kemp, and J. A. Hawley. 2006. Chronic rosiglitazone treatment restores AMPKalpha2 activity in insulin-resistant rat skeletal muscle. *Am J Physiol Endocrinol Metab* 290 (2):E251-7.

Li, J. M., S. Wheatcroft, L. M. Fan, M. T. Kearney, and A. M. Shah. 2004. Opposing roles of p47phox in basal versus angiotensin II-stimulated alterations in vascular O2- production, vascular tone, and mitogen-activated protein kinase activation. *Circulation* 109 (10):1307-13.

Lightell, D. J., Jr., S. C. Moss, and T. C. Woods. 2011. Loss of canonical insulin signaling accelerates vascular smooth muscle cell proliferation and migration through changes in p27Kip1 regulation. *Endocrinology* 152 (2):651-8.

Lim, S., C. J. Jin, M. Kim, S. S. Chung, H. S. Park, I. K. Lee, C. T. Lee, Y. M. Cho, H. K. Lee, and K. S. Park. 2006. PPARgamma gene transfer sustains apoptosis, inhibits vascular smooth muscle cell proliferation, and reduces neointima formation after balloon injury in rats. *Arterioscler Thromb Vasc Biol* 26 (4):808-13.

Lincoff, A. M., K. Wolski, S. J. Nicholls, and S. E. Nissen. 2007. Pioglitazone and risk of cardiovascular events in patients with type 2 diabetes mellitus: a meta-analysis of randomized trials. *Jama* 298 (10):1180-8.

Liu, J., R. Wang, K. Desai, and L. Wu. 2011. Upregulation of aldolase B and overproduction of methylglyoxal in vascular tissues from rats with metabolic syndrome. *Cardiovasc Res* 92 (3):494-503.

Lu, J., J. Ji, H. Meng, D. Wang, B. Jiang, L. Liu, E. Randell, K. Adeli, and Q. H. Meng. 2013. The protective effect and underlying mechanism of metformin on neointima formation in fructose-induced insulin resistant rats. *Cardiovasc Diabetol* 12:58.

MacAskill, M. G., D. G. Watson, M. A. Ewart, R. Wadsworth, A. Jackson, E. Aitken, G. MacKenzie, D. Kingsmore, S. Currie, and P. Coats. 2015. Improving arteriovenous fistula patency: Transdermal delivery of diclofenac reduces cannulation-dependent neointimal hyperplasia via AMPK activation. *Vascul Pharmacol* 71:108-15.

Martin, A., J. V. Perez-Giron, R. Hernanz, R. Palacios, A. M. Briones, A. Fortuno, G. Zalba, M. Salaices, and M. J. Alonso. 2012. Peroxisome proliferator-activated receptor-gamma activation reduces cyclooxygenase-2 expression in vascular

smooth muscle cells from hypertensive rats by interfering with oxidative stress. *J Hypertens* 30 (2):315-26.

Martinet, W., H. De Loof, and G. R. De Meyer. 2014. mTOR inhibition: a promising strategy for stabilization of atherosclerotic plaques. *Atherosclerosis* 233 (2):601-7.

Meredith, D., M. Panchatcharam, S. Miriyala, Y. S. Tsai, A. J. Morris, N. Maeda, G. A. Stouffer, and S. S. Smyth. 2009. Dominant-negative loss of PPARgamma function enhances smooth muscle cell proliferation, migration, and vascular remodeling. *Arterioscler Thromb Vasc Biol* 29 (4):465-71.

Miyabe, M., K. Ohashi, R. Shibata, Y. Uemura, Y. Ogura, D. Yuasa, T. Kambara, Y. Kataoka, T. Yamamoto, K. Matsuo, Y. Joki, T. Enomoto, S. Hayakawa, M. Hiramatsu-Ito, M. Ito, M. J. Van Den Hoff, K. Walsh, T. Murohara, and N. Ouchi. 2014. Muscle-derived follistatin-like 1 functions to reduce neointimal formation after vascular injury. *Cardiovasc Res* 103 (1):111-20.

Morisaki, K., R. Shibata, N. Takahashi, N. Ouchi, Y. Maehara, T. Murohara, and K. Komori. 2011. Pioglitazone prevents intimal hyperplasia in experimental rabbit vein grafts. *J Vasc Surg* 54 (6):1753-9.

Motobayashi, Y., Y. Izawa-Ishizawa, K. Ishizawa, S. Orino, K. Yamaguchi, K. Kawazoe, S. Hamano, K. Tsuchiya, S. Tomita, and T. Tamaki. 2009. Adiponectin inhibits insulin-like growth factor-1-induced cell migration by the suppression of extracellular signal-regulated kinase 1/2 activation, but not Akt in vascular smooth muscle cells. *Hypertens Res* 32 (3):188-93.

Nagahama, R., T. Matoba, K. Nakano, S. Kim-Mitsuyama, K. Sunagawa, and K. Egashira. 2012. Nanoparticle-mediated delivery of pioglitazone enhances

therapeutic neovascularization in a murine model of hindlimb ischemia. *Arterioscler Thromb Vasc Biol* 32 (10):2427-34.

Nagata, D., R. Takeda, M. Sata, H. Satonaka, E. Suzuki, T. Nagano, and Y. Hirata. 2004. AMP-activated protein kinase inhibits angiotensin II-stimulated vascular smooth muscle cell proliferation. *Circulation* 110 (4):444-51.

Nesto, R. W., D. Bell, R. O. Bonow, V. Fonseca, S. M. Grundy, E. S. Horton, M. Le Winter, D. Porte, C. F. Semenkovich, S. Smith, L. H. Young, R. Kahn, Association American Heart, and Association American Diabetes. 2003. Thiazolidinedione use, fluid retention, and congestive heart failure: a consensus statement from the American Heart Association and American Diabetes Association. October 7, 2003. *Circulation* 108 (23):2941-8.

Ning, J., and D. R. Clemmons. 2010. AMP-activated protein kinase inhibits IGF-I signaling and protein synthesis in vascular smooth muscle cells via stimulation of insulin receptor substrate 1 S794 and tuberous sclerosis 2 S1345 phosphorylation. *Mol Endocrinol* 24 (6):1218-29.

Nishio, K., M. Sakurai, T. Kusuyama, M. Shigemitsu, T. Fukui, K. Kawamura, S. Itoh, N. Konno, and T. Katagiri. 2006. A randomized comparison of pioglitazone to inhibit restenosis after coronary stenting in patients with type 2 diabetes. *Diabetes Care* 29 (1):101-6.

Osman, I., and L. Segar. 2016. Pioglitazone, a PPARgamma agonist, attenuates PDGF-induced vascular smooth muscle cell proliferation through AMPK-dependent and AMPK-independent inhibition of mTOR/p70S6K and ERK signaling. *Biochem Pharmacol* 101:54-70.

Pakala, R., C. Dilcher, R. Baffour, D. Hellinga, R. Seabron, M. Joner, F. Kolodgie, R. Virmani, and R. Waksman. 2006. Peroxisome proliferator-activated receptor gamma ligand pioglitazone alters neointimal composition in a balloon-denuded and radiated hypercholesterolemic rabbit. *J Cardiovasc Pharmacol* 48 (6):299-305.

Patel, C., K. Sugimoto, V. Douard, A. Shah, H. Inui, T. Yamanouchi, and R. P. Ferraris. 2015. Effect of dietary fructose on portal and systemic serum fructose levels in rats and in KHK-/- and GLUT5-/- mice. *Am J Physiol Gastrointest Liver Physiol* 309 (9):G779-90.

Patel, D., B. Walitt, J. Lindsay, and R. L. Wilensky. 2011. Role of pioglitazone in the prevention of restenosis and need for revascularization after bare-metal stent implantation: a meta-analysis. *JACC Cardiovasc Interv* 4 (3):353-60.

Perez-Giron, J. V., R. Palacios, A. Martin, R. Hernanz, A. Aguado, S. Martinez-Revelles, M. T. Barrus, M. Salaices, and M. J. Alonso. 2014. Pioglitazone reduces angiotensin II-induced COX-2 expression through inhibition of ROS production and ET-1 transcription in vascular cells from spontaneously hypertensive rats. *Am J Physiol Heart Circ Physiol* 306 (11):H1582-93.

Phillips, J. W., K. G. Barringhaus, J. M. Sanders, Z. Yang, M. Chen, S. Hesselbacher, A. C. Czarnik, K. Ley, J. Nadler, and I. J. Sarembock. 2003. Rosiglitazone reduces the accelerated neointima formation after arterial injury in a mouse injury model of type 2 diabetes. *Circulation* 108 (16):1994-9.

Pyla, R., I. Osman, P. Pichavaram, P. Hansen, and L. Segar. 2014. Metformin exaggerates phenylephrine-induced AMPK phosphorylation independent of

CaMKKbeta and attenuates contractile response in endothelium-denuded rat aorta. *Biochem Pharmacol* 92 (2):266-79.

Pyla, R., N. Poulose, J. Y. Jun, and L. Segar. 2013. Expression of conventional and novel glucose transporters, GLUT1, -9, -10, and -12, in vascular smooth muscle cells. *Am J Physiol Cell Physiol* 304 (6):C574-89.

Riboulet-Chavey, A., A. Pierron, I. Durand, J. Murdaca, J. Giudicelli, and E. Van Obberghen. 2006. Methylglyoxal impairs the insulin signaling pathways independently of the formation of intracellular reactive oxygen species. *Diabetes* 55 (5):1289-99.

Saha, A. K., P. R. Avilucea, J. M. Ye, M. M. Assifi, E. W. Kraegen, and N. B. Ruderman. 2004. Pioglitazone treatment activates AMP-activated protein kinase in rat liver and adipose tissue in vivo. *Biochem Biophys Res Commun* 314 (2):580-5.

Saha, A. K., X. J. Xu, E. Lawson, R. Deoliveira, A. E. Brandon, E. W. Kraegen, and N. B. Ruderman. 2010. Downregulation of AMPK accompanies leucine- and glucose-induced increases in protein synthesis and insulin resistance in rat skeletal muscle. *Diabetes* 59 (10):2426-34.

Samuel, V. T. 2011. Fructose induced lipogenesis: from sugar to fat to insulin resistance. *Trends Endocrinol Metab* 22 (2):60-5.

Satoh, N., Y. Ogawa, T. Usui, T. Tagami, S. Kono, H. Uesugi, H. Sugiyama, A. Sugawara, K. Yamada, A. Shimatsu, H. Kuzuya, and K. Nakao. 2003. Antiatherogenic effect of pioglitazone in type 2 diabetic patients irrespective of the responsiveness to its antidiabetic effect. *Diabetes Care* 26 (9):2493-9.

Sengupta, S., T. R. Peterson, and D. M. Sabatini. 2010. Regulation of the mTOR complex 1 pathway by nutrients, growth factors, and stress. *Mol Cell* 40 (2):310-22.

Shinohara, E., S. Kihara, N. Ouchi, T. Funahashi, T. Nakamura, S. Yamashita, K. Kameda-Takemura, and Y. Matsuzawa. 1998. Troglitazone suppresses intimal formation following balloon injury in insulin-resistant Zucker fatty rats. *Atherosclerosis* 136 (2):275-9.

Song, P., S. Wang, C. He, S. Wang, B. Liang, B. Viollet, and M. H. Zou. 2011. AMPKalpha2 deletion exacerbates neointima formation by upregulating Skp2 in vascular smooth muscle cells. *Circ Res* 109 (11):1230-9.

Song, P., Y. Zhou, K. A. Coughlan, X. Dai, H. Xu, B. Viollet, and M. H. Zou. 2013. Adenosine monophosphate-activated protein kinase-alpha2 deficiency promotes vascular smooth muscle cell migration via S-phase kinase-associated protein 2 upregulation and E-cadherin downregulation. *Arterioscler Thromb Vasc Biol* 33 (12):2800-9.

Stone, J. D., A. Narine, P. R. Shaver, J. C. Fox, J. R. Vuncannon, and D. A. Tulis. 2013. AMP-activated protein kinase inhibits vascular smooth muscle cell proliferation and migration and vascular remodeling following injury. *Am J Physiol Heart Circ Physiol* 304 (3):H369-81.

Takagi, T., T. Akasaka, A. Yamamuro, Y. Honda, T. Hozumi, S. Morioka, and K. Yoshida. 2000. Troglitazone reduces neointimal tissue proliferation after coronary stent implantation in patients with non-insulin dependent diabetes mellitus: a serial intravascular ultrasound study. *J Am Coll Cardiol* 36 (5):1529-35.

Takaoka, M., D. Nagata, S. Kihara, I. Shimomura, Y. Kimura, Y. Tabata, Y. Saito, R. Nagai, and M. Sata. 2009. Periadventitial adipose tissue plays a critical role in vascular remodeling. *Circ Res* 105 (9):906-11.

Tanner, F. C., M. Boehm, L. M. Akyurek, H. San, Z. Y. Yang, J. Tashiro, G. J. Nabel, and E. G. Nabel. 2000. Differential effects of the cyclin-dependent kinase inhibitors p27(Kip1), p21(Cip1), and p16(Ink4) on vascular smooth muscle cell proliferation. *Circulation* 101 (17):2022-5.

Uemura, Y., R. Shibata, N. Kanemura, K. Ohashi, T. Kambara, M. Hiramatsu-Ito, T. Enomoto, D. Yuasa, Y. Joki, K. Matsuo, M. Ito, S. Hayakawa, H. Ogawa, T. Murohara, and N. Ouchi. 2015. Adipose-derived protein omentin prevents neointimal formation after arterial injury. *Faseb j* 29 (1):141-51.

Vasamsetti, S. B., S. Karnewar, A. K. Kanugula, A. R. Thatipalli, J. M. Kumar, and S. Kotamraju. 2015. Metformin inhibits monocyte-to-macrophage differentiation via AMPK-mediated inhibition of STAT3 activation: potential role in atherosclerosis. *Diabetes* 64 (6):2028-41.

Wang, H., Q. H. Meng, T. Chang, and L. Wu. 2006. Fructose-induced peroxynitrite production is mediated by methylglyoxal in vascular smooth muscle cells. *Life Sci* 79 (26):2448-54.

Wei, Y., D. Wang, and M. J. Pagliassotti. 2005. Fructose selectively modulates c-jun N-terminal kinase activity and insulin signaling in rat primary hepatocytes. *J Nutr* 135 (7):1642-6.

Woods, A., K. Dickerson, R. Heath, S. P. Hong, M. Momcilovic, S. R. Johnstone, M. Carlson, and D. Carling. 2005. Ca2+/calmodulin-dependent protein kinase kinase-

beta acts upstream of AMP-activated protein kinase in mammalian cells. *Cell Metab* 2 (1):21-33.

Yasunari, K., M. Kohno, H. Kano, K. Yokokawa, T. Horio, and J. Yoshikawa. 1995. Aldose reductase inhibitor prevents hyperproliferation and hypertrophy of cultured rat vascular smooth muscle cells induced by high glucose. *Arterioscler Thromb Vasc Biol* 15 (12):2207-12.

Yoshimoto, T., M. Naruse, H. Shizume, K. Naruse, A. Tanabe, M. Tanaka, K. Tago, K. Irie, T. Muraki, H. Demura, and L. Zardi. 1999. Vasculo-protective effects of insulin sensitizing agent pioglitazone in neointimal thickening and hypertensive vascular hypertrophy. *Atherosclerosis* 145 (2):333-40.

Young, P. W., D. R. Buckle, B. C. Cantello, H. Chapman, J. C. Clapham, P. J. Coyle, D. Haigh, R. M. Hindley, J. C. Holder, H. Kallender, A. J. Latter, K. W. Lawrie, D. Mossakowska, G. J. Murphy, L. Roxbee Cox, and S. A. Smith. 1998. Identification of high-affinity binding sites for the insulin sensitizer rosiglitazone (BRL-49653) in rodent and human adipocytes using a radioiodinated ligand for peroxisomal proliferator-activated receptor gamma. *J Pharmacol Exp Ther* 284 (2):751-9.

Yu, W., R. Liu-Bryan, S. Stevens, J. K. Damanahalli, and R. Terkeltaub. 2012. RAGE signaling mediates post-injury arterial neointima formation by suppression of liver kinase B1 and AMPK activity. *Atherosclerosis* 222 (2):417-25.

Zhang, H., A. Zhang, D. E. Kohan, R. D. Nelson, F. J. Gonzalez, and T. Yang. 2005. Collecting duct-specific deletion of peroxisome proliferator-activated receptor

gamma blocks thiazolidinedione-induced fluid retention. *Proc Natl Acad Sci U S A* 102 (26):9406-11.